



## **ABSTRACT**

1D and 2D basin modelling together with seismic interpretation has been done on four 2D lines in the Northern North Sea. The thesis presents the development of the basin from the structural point of view and the results shows thermal and maturity history by using Petromod software. The structural development of the basin was constructed from seismic and data from two wells to account for tectonic and thermal history. The major source rock is the Upper Jurassic Draupne Formation, which is a marine organic rich shale. The results of the modelling show, that, the source rock reaches a temperature of about 180°C at the present day in the deepest parts of the basin. According to Sweeney and Burnham (1990), the vitrinite reflectance data shows that the source rock is matured and has passed the oil window from main oil to dry gas, and large amount of oil was generated in the late Cretaceous to present. From the transformation ratio it shows that 95% to 100% of the source rock is transformed. At 155 Ma most areas were immature and these areas had been buried at the depth of 1200m, At 151 Ma the source rock was mature enough to initiate the onset of early oil generation, At 149 Ma there was onset of main oil generation. At 140 Ma there was onset of late oil generation, and at 100 Ma the source rock was mature enough for wet gas generation, At 65.50 Ma there was onset of dry gas generation at the depth of 4200 m, and at 50 Ma the source rock started to be overmature at the depth of 6200 m, At present time large parts of the area is still generating gas as well as oil generation. Significant amounts of gas generation in the Upper Jurassic source rock formed when higher formation temperatures were attained during middle-late Tertiary. The source rock and reservoir rock of the study area shows significant prospect of hydrocarbon generation and accumulation. Along the 2D lines, Mass of generated oil from the source rock ranges between 2.25-2.40 Mtons to 2.40-2.60 Mtons. The mass of gas generated from the source rock is between 0.36-0.39Mto0.49-0.52 Mtons.

## **ACKNOWLEDGEMENT**

I wish to express my gratitude to the Norwegian National Oil Company Statoil for sponsoring my studies through Angolan Norwegian Tanzania higher education initiative (ANTHEI) scholarship. Many thanks to my supervisor, Professor Stephen J. Lippard of the Department of Geology and Mineral Resources Engineering for his time, patience and invaluable advice in writing this thesis.

I owe many thanks to Dr. Nelson Boniface, Mr. Emily Kisakwa of the Department of Geology at University of Dar es salaam-Tanzania for their valuable assistance on this work. Many thanks go to Schlumberger for providing the Petromod and Petrel Software and an academic license to Geology Department at the University of Dar es salaam-Tanzania. Many thanks to my fellow ANTHEI students for their cooperation.

I would like to give my appreciation to my family; My lovely husband Mr Makasi Saimon, my lovely daughter Maureen Makasi, my lovely mother Lydia Shelemia and my sisters Dinah Jackson, Norah Jackson, Rosemary Jackson, and Betty Jackson, My brother David Jackson for their endless love, care and prayers throughout the time of this work.

## TABLE OF CONTENTS

ABSTRACT.....	i
ACKNOWLEDGEMENT .....	ii
LIST OF FIGURES.....	v
CHAPTER 1: INTRODUCTION.....	1
1.1 Basin and Petroleum System Modelling.....	1
1.2 The Petromod Software.....	3
1.3 Objectives of the study.....	4
1.4 Previous Basin Modelling Studies in the Northern North Sea.....	5
CHAPTER 2: GEOLOGY OF THE NORTHERN NORTH SEA.....	6
2.1 Geological Setting.....	6
2.2 Stratigraphic development of the Northern North Sea.....	7
2.2.1 Triassic .....	7
2.2.2 Jurassic .....	8
2.2.3 Cretaceous.....	9
2.2.4 Tertiary .....	10
2.3 Structural Evolution.....	14
2.3.1 Late Permian to Early Triassic rifting.....	15
2.3.2 Middle Jurassic to Early Cretaceous Rifting.....	16
2.3.3 Cretaceous to Cenozoic Post-Rift Deformation.....	17
CHAPTER 3: PETROLEUM GEOLOGY OF THE NORTHERN NORTH SEA.....	19
3.1 Petroleum system.....	19
3.2 Source rocks .....	19
3.2.1 Draupne Formation (Kimmeridge Clay).....	19
3.2.2 Heather Formation.....	20
3.3 Reservoirs.....	20
3.3.1 Triassic and Lower Jurassic.....	20
3.3.2 Middle Jurassic.....	21
3.3.3 Upper Jurassic .....	21
3.4 Traps and Seals.....	22
3.5 Migration.....	22
CHAPTER 4: SEISMIC INTERPRETATION .....	24
4.1 Introduction.....	24
CHAPTER 5: METHODOLOGY.....	29
5.1 Background.....	29
5.2 Workflow .....	29
5.3 Input Data .....	31



5.3.1 Fault Properties .....	31
5.3.2 Gridding .....	31
5.3.3. Age Assignment .....	32
5.3.4 Facies Definition.....	33
5.3.5 Boundary conditions .....	33
5.3.6 Simulation .....	37
5.3.7 Calibration .....	37
CHAPTER 6: RESULTS .....	39
6.1 Burial history.....	39
6.2 Maturation and Petroleum generation history .....	51
6.3 Migration,Saturation and accumulation.....	68
CHAPTER 7: DISCUSSION.....	74
CHAPTER 8: CONCLUSIONS .....	75
REFERENCES .....	77
APPENDICES .....	81

## LIST OF FIGURES

Figure 1.1: Major geological processes in basin modelling(Hantschel and Kauerauf, 2009) ...	2
Figure 1.2: Concept of a petroleum system From Magoon and Dow (1994).....	3
Figure 2.1: Map of the North Sea showing the study area (red rectangle) modified after Ternan Ltd (2012).....	7
Figure 2.2: Triassic and Jurassic lithostratigraphic nomenclature Northern North Sea(Vollset and Doré, 1984).....	9
Figure 2.3: Cretaceous lithostratigraphic nomenclature Norwegian North Sea(Isaksen and Tonstad, 1989).....	10
Figure 2.4: Paleocene lithostratigraphic nomenclature Norwegian North Sea(Isaksen and Tonstad, 1989).....	11
Figure 2.5: Chronostratigraphy of the Nordland Group and the uppermost Hordaland Group in the Viking Graben, northern North Sea(Head et al., 2004).....	13
Figure 2.6: lithostratigraphic nomenclature in the Hordaland and Nordland Groups (Tertiary) Norwegian North Sea(Isaksen and Tonstad, 1989).....	14
Figure 2.7: Structural elements of the North Sea showing the Permo-Triassic and Jurassic rift systems(Færseth, 1996).....	15
Figure 2.8: Structure map of the northern North Sea showing the main area of late Jurassic to early Cretaceous rifting(Gabrielsen et al., 1999).....	18
Figure 4.1: Map showing the seismic lines and well locations.....	24
Figure 4.2: Interpreted dip line (NVGTI -92-102).....	25
Figure 4.5: Interpreted dip line NVGTI-92-104.....	28
Figure 5.1: Workflow for building a basic 2D model.....	30
Figure 5.2: Fault properties definition table.....	31
Figure 5.3: A pre-grid view of the profile NVGTI-92-102.....	32
Figure 5.4: Model view after gridding of the profile NVGTI-92-102.....	32
Figure 5.6: Facies definition table showing lithologies, source rock properties and petroleum system elements.....	33
Figure 5.7: Paleo water depth values of the North Sea based on (Kjennerud et al., 2001).....	34
Figure 5.8: Sediment water interface temperature values (based on Wygrala 1989).....	35
Figure 5.9: Heat flow values based on(Schroeder and Sylta, 1993).....	36
Figure 5.10: Model calibration by comparison of measured and modelled temperature for wells 35/11-5 and 35/11-3s.....	38
Figure 5.11: Model calibration by comparison of measured and modelled vitrinite reflectance for wells 35/11-5 and 35/11-3s.....	38
Figure 6.1: Basin development at 160 Ma when the Upper Jurassic (Draupne FM) sediments were deposited for the modelled line NVGTI-92-109.....	40
Figure 6.2: Basin development at 123 Ma when Lower Cretaceous sediments (Cromer Knoll GP) were deposited of the modelled line NVGTI-92-109.....	40
Figure 6.3: Basin development at 98 Ma at the start of deposition of Upper Cretaceous sediments (Shetland Gp) and the end of deposition of Cromer Knoll Gp of the modelled line NVGTI-92-109.....	41
Figure 6.4: Basin development at 65 Ma after Upper Cretaceous sediments (Shetland Gp) were deposited of the modelled line NVGTI-92-109.....	41
Figure 6.5: Basin development at 62 Ma when Lower Paleocene sediments (Sele FM) were deposited of the modelled line NVGTI-92-109.....	42
Figure 6.6: Basin development at 58.70 Ma when Middle Paleocene sediments (Lista FM) were deposited of the modelled line NVGTI-92-109.....	42

Figure 6.7: Basin development at 56 Ma when Upper Paleocene sediments (Balder FM) were deposited of the modelled line NVGTI-92-109. ....	43
Figure 6.8: Basin development at 23 Ma when Lower Miocene sediments (Hordaland GP) were deposited of the modelled line NVGTI-92-109. ....	43
Figure 6.9: Basin development at 16 Ma when Middle Miocene sediments (Utsira FM) were deposited of the modelled line NVGTI-92-109. ....	44
Figure 6.10: Basin development at present day condition of the modelled line NVGTI-92-109. ....	44
Figure 6.11: Basin development at 160 Ma when the Upper Jurassic (Draupne FM) sediments were deposited of the modelled line NVGTI-92-104. ....	46
Figure 6.12: Basin development at 123 Ma when Lower Cretaceous sediments (Cromer Knoll GP) were deposited of the modelled line NVGTI-92-104. ....	46
Figure 6.13: Basin development at 98 Ma when Upper Cretaceous sediments (Shetland GP) were deposited of the modelled line NVGTI-92-104. ....	47
Figure 6.14: Basin development at 65 Ma when Upper Cretaceous sediments (Shetland GP) were deposited of the modelled line NVGTI-92-104. ....	47
Figure 6.15: Basin development at 62 Ma when Lower Paleocene sediments (Sele FM) were deposited of the modelled line NVGTI-92-104. ....	48
Figure 6.16: Basin development at 58.70 Ma when Middle Paleocene sediments (Lista FM) were deposited of the modelled line NVGTI-92-104. ....	48
Figure 6.17: Basin development at 56 Ma when Upper Paleocene sediments (Balder FM) were deposited of the modelled line NVGTI-92-104. ....	49
Figure 6.18: Basin development at 23 Ma when Lower Miocene sediments (Hordaland GP) were deposited of the modelled line NVGTI-92-104. ....	49
Figure 6.19: Basin development at 16 Ma when Middle Miocene sediments (Utsira FM) were deposited of the modelled line NVGTI-92-104. ....	50
Figure 6.20: Basin development at present day condition of the modelled line NVGT 92-104. ....	50
Figure 6.21: Maturity development of the Draupne FM at 155 Ma on the modelled line NVGTI-92-109. ....	52
Figure 6.22: Maturity development of the Draupne FM at 151 Ma on the modelled line NVGTI-92-109. ....	52
Figure 6.23: Maturity development of the Draupne FM at 149 Ma on the modelled line NVGTI-92-109. ....	53
Figure 6.24: Maturity development of the Draupne FM at 145 Ma on the modelled line NVGTI-92-109. ....	53
Figure 6.25: Maturity development of the Draupne FM at 140 Ma on the modelled line NVGTI-92-109. ....	54
Figure 6.26: Maturity development of the Draupne FM at 104 Ma on the modelled line NVGTI-92-109. ....	54
Figure 6.27: Maturity development of the Draupne FM at 100 Ma on the modelled line NVGTI-92-109. ....	55
Figure 6.28: Maturity development on the Draupne FM at 86 Ma on the modelled line NVGTI-92-109. ....	55
Figure 6.29: Maturity development on the Draupne FM at 74 Ma on the modelled line NVGTI-92-109. ....	56
Figure 6.30: Maturity development of the Draupne FM at 65.50 Ma on the modelled line NVGTI-92-109. ....	56
Figure 6.31: Maturity development of the Draupne FM at 58.70 Ma on the modelled line NVGTI-92-109. ....	57

Figure 6.32: Maturity development of the Draupne FM at 50.00 Ma on the modelled line NVGTI-92-109 .....	57
Figure 6.33: Maturity development of the Draupne FM at present time on the modelled line NVGTI-92-109. ....	58
Figure 6.34: Maturity development of the Draupne FM at 155 Ma on the modelled line NVGTI-92-104. ....	58
Figure 6.35: Maturity development of the Draupne FM at 151 Ma on the modelled line NVGTI-92-104. ....	59
Figure 6.36: Maturity development of the Draupne FM at 149 Ma on the modelled line NVGTI-92-104. ....	59
Figure 6.37: Maturity development of the Draupne FM at 145 Ma on the modelled line NVGTI-92-104. ....	60
Figure 6.38: Maturity development on the Draupne FM at 140 Ma of the modelled line NVGTI-92-104 .....	60
Figure 6.39: Maturity development of the Draupne FM at 104 Ma on the modelled line NVGTI-92-104. ....	61
Figure 6.40: Maturity development of the Draupne FM at 100 Ma on the modelled line NVGTI-92-104. ....	61
Figure 6.41: Maturity development of the Draupne FM at 86 Ma on the modelled line NVGTI-92-104. ....	62
Figure 6.42: Maturity development of the Draupne FM at 74 Ma on the modelled line NVGTI-92-104. ....	62
Figure 6.43: Maturity development of the Draupne FM at 65.50 Ma on the modelled line NVGTI-92-104. ....	63
Figure 6.44: Maturity development of the Draupne FM at 58.70 Ma on the modelled line NVGTI-92-104. ....	63
Figure 6.45: Maturity development of the Draupne FM at 50.00 Ma on the modelled line NVGTI-92-104. ....	64
Figure 6.46: Maturity development of the Draupne FM at present time on the modelled line NVGTI-92-104. ....	64
Figure 6.47: Depth converted profile showing temperature overlay of the modeled line NVGTI-92-109 at present day condition. ....	65
Figure 6.48: Vitrinite reflectance overlay for NVGTI-92-109 at present day condition. ....	66
Figure 6.49: Transformation ratio overlay for NVGTI-92-109 at present day condition. ....	67
Figure 6.50: Depth converted profile showing temperature overlay of the modeled line NVGTI-92-104 at present day condition. ....	67
Figure 6.51: Vitrinite reflectance overlay for NVGTI-92-104 at present day condition. ....	68
Figure 6.52: Transformation ratio overlay for NVGTI-92-104 at present day condition. ....	68
Figure 6.53: Hydrocarbon saturation overlay for NVGTI-92-109 at present day condition. ....	69
Figure 6.54: Pore pressure overlay for NVGTI-92-109 at present day condition. ....	70
Figure 6.55: Generated mass overlay of oil for NVGTI-92-109 at present day condition. ....	70
Figure 6.56: Generated mass overlay of gas for NVGTI-92-109 at present day condition. ....	71
Figure 6.57: Hydrocarbon saturation overlay for NVGTI-92-104 at present day condition. ....	71
Figure 6.58: Pore pressure overlay for NVGTI-92-104 at present day condition. ....	72
Figure 6.59: Generated mass overlay of oil for NVGTI-92-104 at present day condition. ....	72
Figure 6.60: Generated mass overlay of gas for NVGTI-92-104 at present day condition. ....	73

## **CHAPTER 1: INTRODUCTION**

### **1.1 Basin and Petroleum System Modelling**

Basin modelling is the temporal reconstruction of basin history and specifically refers to the procedure of establishing the sequential record of changes in controls and products, which have occurred during the long geologic history of a basin. The first step in basin modelling is the acquisition of data from general and regional geological knowledge, from wells, various logging techniques and most of all from seismic(Welte et al., 2012).

Integrated basin modelling is used to understand and reconstruct the geological and thermal evolution of a sedimentary basin, to quantify this information and hence to derive, among other results, the history of generation, migration and accumulation of petroleum. This method enables a logical, quantitative treatment of very complex interrelated geological processes and secondly it permits these processes to be examined on the basis of an absolute geological time scale(Welte and Yalcin, 1988).

Basin modelling is dynamic modelling of geological processes in sedimentary basins over geological time spans. A basin model is simulated forward through geological time starting with the sedimentation of the oldest layer until the entire sequence of layers has been deposited and present day is reached. Several geological processes are calculated and updated at each time step (Fig. 1.1). The most important are deposition, compaction, heat flow analysis, petroleum generation, expulsion, phase dissolution, migration and accumulation.

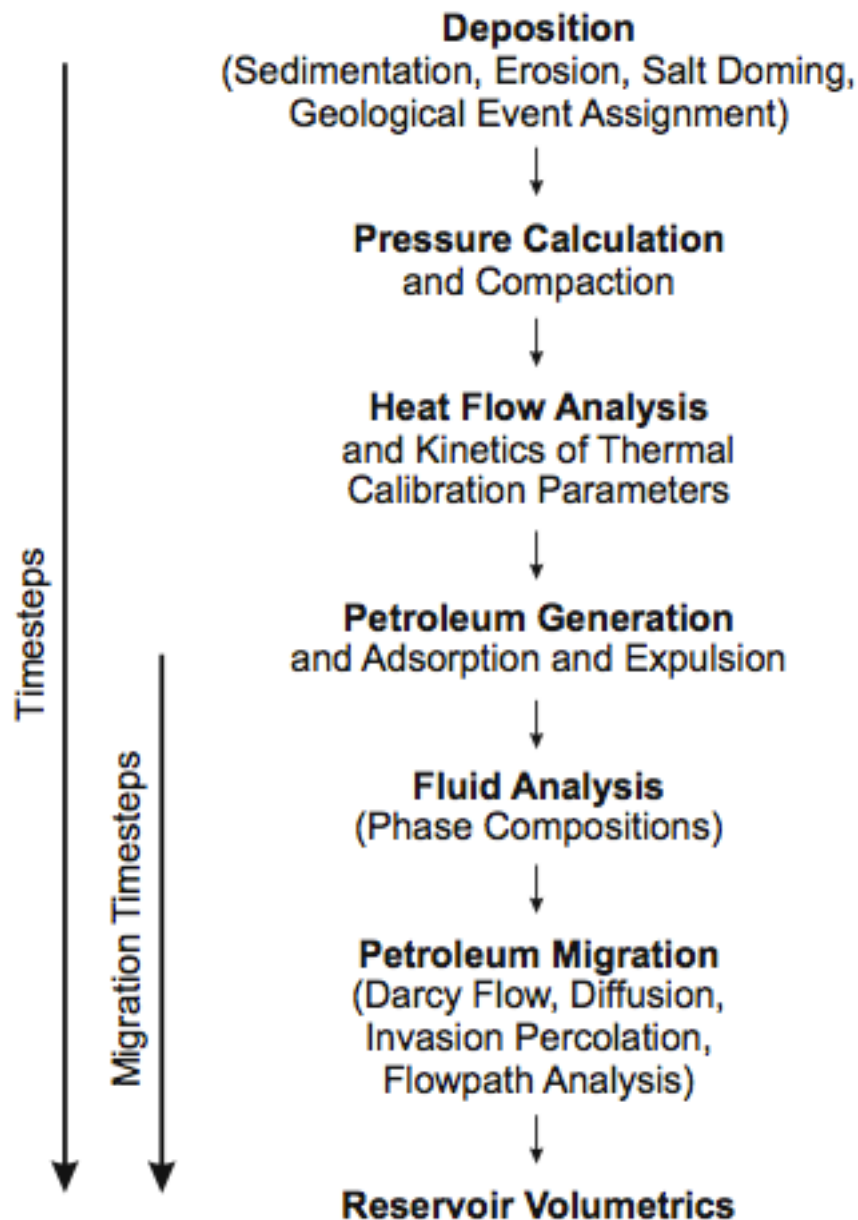


Figure 1.1: Major geological processes in basin modelling(Hantschel and Kauerauf, 2009)

A petroleum system encompasses a pod of active source rock and all related oil and gas accumulations, and includes all the essential elements and processes needed for oil and gas accumulations to exist. The essential elements are the source rock, reservoir rock, seal rock, and overburden rock. The processes include trap formation and the generation-migration-accumulation of petroleum (Fig 1.2). All essential elements must be placed in time and space such that the processes required to form a petroleum accumulation can occur(Magoon and Dow, 1994).

Basin and petroleum system modelling tracks the evolution of a basin through time as it fills with fluids and sediments that may eventually generate or contain hydrocarbons. It allows

geoscientists to examine the dynamics of sedimentary basins and their associated fluids to determine if past conditions were suitable for hydrocarbons to fill potential reservoirs and be preserved there(Al-Hajeri et al., 2009).

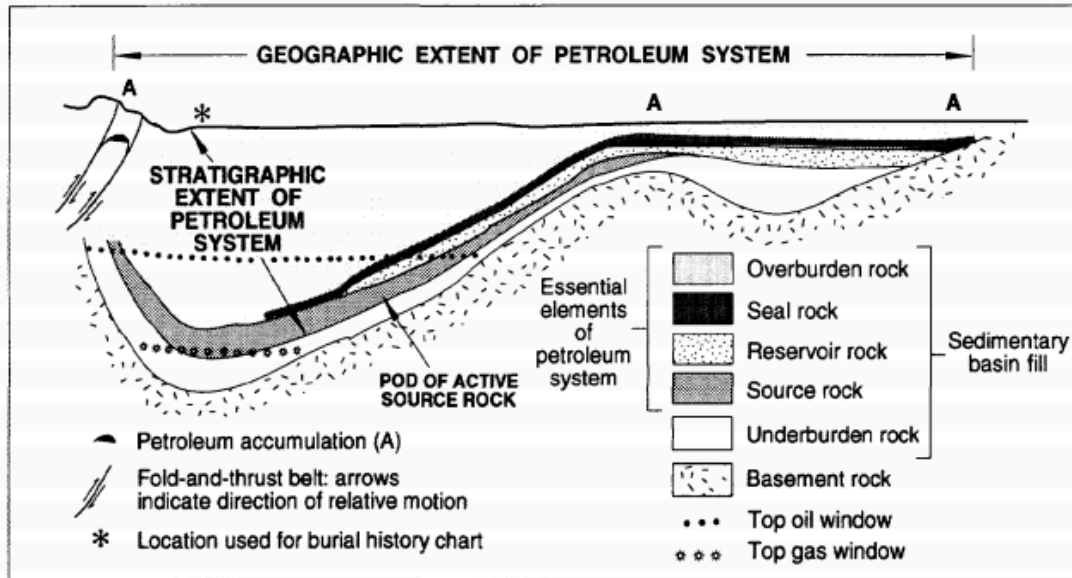


Figure 1.2: Concept of a petroleum system From Magoon and Dow (1994).

## 1.2 The Petromod Software

Petromod simulates the thermogenic generation of multiple hydrocarbon components including oil and gas, their migration through geological strata, and finally predicts the oil and gas accumulations in suitable reservoir formations. Petromod is a software package for the petroleum systems modelling in 1D, 2D and 3D including the thermogenic generation of oil and gas, and the secondary degradation of oil into gas. The software package fully integrates seismic, stratigraphic and geological interpretations into multi-dimensional simulations of thermal, fluid flow and petroleum migration history in sedimentary basins. Petromod is primarily used in hydrocarbon exploration but has also proven to be a valuable tool in research applications(Piñero et al., 2011).

Petromod software uses a database of reaction kinetics to predict the phases and properties of hydrocarbons generated from source rocks of various types. Migration and accumulation can be modelled by invasion percolation in the Petromod Software. A Petromod model helps to quantify the location and timing of petroleum expulsion from source rock, volumes and composition of the products and migration pathways(Al-Hajeri et al., 2009).

Petroleum system modelling can be done in one dimension(1D) at a single point in a basin such as a well or a pseudo-well. Petroleum migration, accumulation and loss cannot be assessed with 1D modelling as petroleum migration always has a lateral component which does not exist in a 1D model.

Petroleum system modelling can be done in two dimensions (2D) along a geologic cross-section. Petroleum migration, accumulation and loss can be assessed with 2D modelling, but only along the cross-section. If the 2D section is positioned appropriately, it can be a useful tool for some basic hydrocarbon risk assessment, for example hydrocarbon column height against seal quality calculations. The most important for 2D modelling is the location within the regional structural framework.

Petroleum system modelling can be done in three dimensions (3D) for a complete 3-dimensional data model which can cover an area ranging from a charge area for a single prospect to an entire basin or region, and which are mostly constructed from 2D seismic lines. Petroleum migration, accumulation and loss can clearly be most accurately assessed with 3D modelling. Constructing a 3D data model is the only way to obtain a comprehensive volume risk assessment, which is always the key question in exploration with respect to charge.

### **1.3 Objectives of the study**

- 2D seismic interpretation as a function of tracing seismic horizon and fault interpretation by using Petrel 2015.
- Determining the burial and petroleum generation history of source rocks in the northern North Sea through subsidence history and thermal maturity modelling.
- Predicting potential petroleum migration mechanisms and pathways for source rock and reservoir rocks.
- 2D Petroleum system modelling of the source rock maturity, and hydrocarbon accumulation in the Northern North Sea using Petromod 2015.



#### **1.4 Previous Basin Modelling Studies in the Northern North Sea**

Different basin and petroleum system modelling studies have been carried out in the northern North Sea.(Goff, 1983) modelled the hydrocarbon generation and migration from Jurassic source rocks in the East Shetland Basin and Viking Graben. 1D and 2D Modelling was used in basin analysis predictions of known hydrocarbon occurrences in the North Sea Viking Graben by (Iliffe et al., 1991).

3D oil migration modelling of the Jurassic petroleum system of the Statfjord area by (Johannesen et al., 2002) led to increased understanding of the migration routes and definition of oil migration fairways in this area. A 2D basin modelling study by (Di Primio and Skeie, 2004)was used for the development of a compositional kinetic model for hydrocarbon generation and phase equilibria modelling of the Snorre Field.(Corver et al., 2011) studied source rock maturation characteristics of symmetric and asymmetric Grabens inferred from intergrated analogue and numerical modelling of the southern Viking Graben in the northern North Sea, where the source rock maturation zones were calculated using 1D-thermal modelling for different graben types.

(Moretti and Deacon, 1995) carried out a complete study of the petroleum system that includes subsidence, maturation, and migration history of the Tampen Spur area by using a two-dimensional TEMISPACK analysis of a seismic line crossing the area where various hypotheses could be tested and later applied in a three-dimensional sense. (Schroeder and Sylta, 1993) developed a three-dimensional model of the hydrocarbon system within the North Viking Graben with the aim of gaining quantitative insights into the local hydrocarbon system and used the results to aid in the risking and ranking of prospects.1D models were used to obtain hydrocarbon generation histories.

## **CHAPTER 2: GEOLOGY OF THE NORTHERN NORTH SEA**

### **2.1 Geological Setting**

The Northern North Sea forms part of the European plate which was deformed during the Mesozoic within the boundaries defined by the Tornquist, Biscay and Rockall –Faeroes fault system(Beach, 1985). The prolonged history of extension that began in the Devonian with the extension of the thickened crust formed during the Caledonian Orogeny characterize the North Sea rift basin(Coward et al., 2003).The Northern North Sea province is dominated by the Viking Graben, which continues into the Sogn Graben towards the north. These Grabens are flanked by the East Shetland Basin and the Tampen Spur to the west, and the Horda Platform to the east (Fig 2.1). These are Jurassic-Cretaceous features, and the main crustal thinning took place in the late Middle to Late Jurassic, followed by thermal subsidence and sediment loading in the Cretaceous. However, the Viking Graben and its margins are underlain by an older major rift basin of assumed Permian-Early Triassic age(Faleide et al., 2015).

The northernmost North Sea rift basin, i.e. the Viking Graben and adjacent platform areas, experienced two episodes of lithospheric stretching, the late Permian-early Triassic and middle Jurassic-earliest Cretaceous. The tectonic extension in the northern Viking Graben during these stretching episodes is known to have varied both spatially and temporarily, leading to considerable variability in architecture and composition of the syn-rift infill. A diagnostic feature of the middle Jurassic-earliest Cretaceous evolution of the northern North Sea, is that the tilted fault block sub-basins appear to have developed through series of distinct tectonic phases (Ravnås et al., 2000).The northern North Sea basin, one arm of the trilete, failed North Sea rift system, experienced approximately 15% extension during the Bathonian-Volgian. The majority of the strain is accommodated on large normal fault arrays with displacement maxima typically in excess of 1 km. The fault systems strike N-S in the southern part of the basin and NNE-SSW in the north (McLeod and Underhill, 2000).

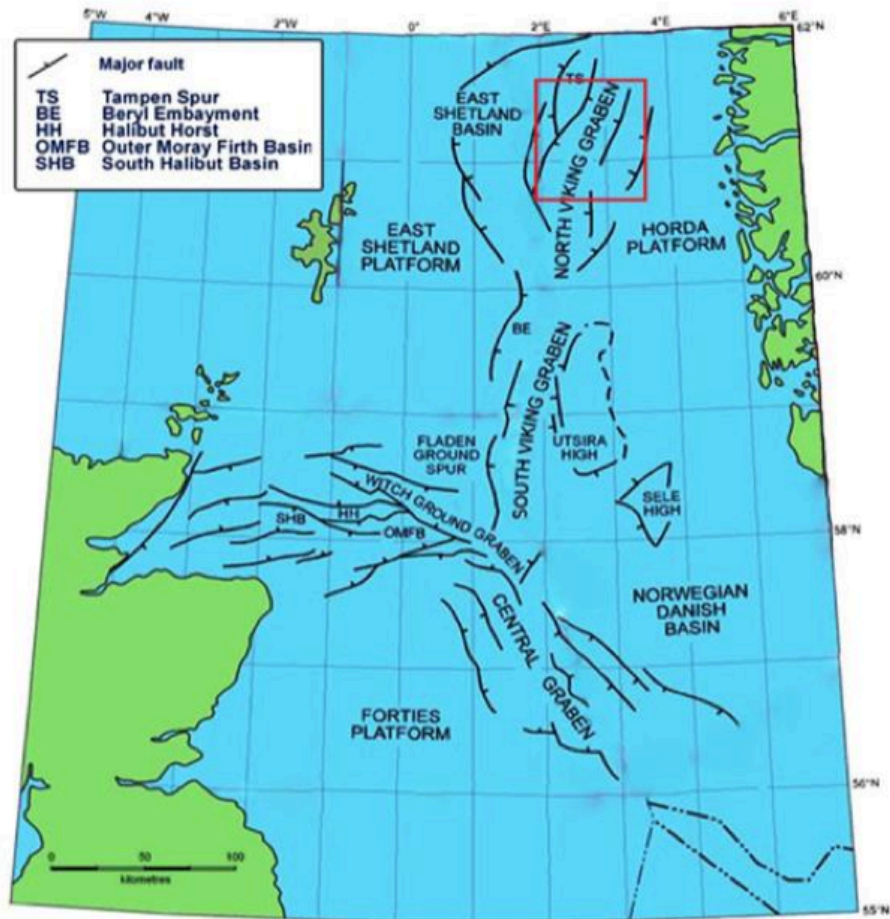


Figure 2.1: Map of the North Sea showing the study area (red rectangle) modified after Ternan Ltd (2012).

## 2.2 Stratigraphic development of the Northern North Sea

### 2.2.1 Triassic

Triassic lithologies typically consist of interbedded, continental, red to variegated claystones, siltstones, shales, and sandstones. Reservoir properties generally are poor due to calcareous cement and a clay matrix. Triassic sediments commonly are identified by their characteristic “red beds” (Kirk, 1980). The Permian-early Triassic syn-rift succession consists of alluvial red beds (alluvial fan, fluvial sandstones, and alluvial plain mudstones) and lacustrine mudstones. On the Horda Platform, underneath the Viking Graben and in the East Shetland Basin syn-rift strata are postulated based on their wedge-shaped stratal geometries. The middle Triassic experienced several subsidence stages which, together with climatic variations, exerted a major control on the periodic outbuilding and retreat of rift marginal, alluvial and shallow marine clastic wedge (Ravnås et al., 2000).

In the late Triassic the continental clastic sedimentation continued right up to the end of the Triassic (Rhaetian) in the Northern North Sea areas(Faleide et al., 2015).

### **2.2.2 Jurassic**

The transition from Triassic to Jurassic approximately coincides with a change from continental to shallow marine environments. A transgression in the early Jurassic led to the accumulation of black shales over large parts of NW Europe and they are exposed in Yorkshire in northeast England and Dorset in southern England. In the northern part of the North Sea fluvial and partly marine sandstones of Lower Jurassic age are important reservoir rocks in the Viking Graben. The Staffjord Group is succeeded by the Dunlin Group, which is dark marine shale, but normally without enough organic content to become a significant source rock. Then follows the Brent Group, a prograding delta sequence which forms the main reservoir rocks in the Northern North Sea(Faleide et al., 2015).

The Middle to Upper Jurassic succession in the Viking Graben area was deposited during an overall transgression. Seven second order transgressive/ regressive (T-R) facies cycles can be identified in the Jurassic from the Lower Toarcian to the base of the Cretaceous. Three cycles occur during a minor rift phase and four during a major rift phase. The regressive phase of the cycles occurs during periods of most active fault rotation, These T-Rfacies cycles are the dominant control on facies distribution. The T-Rfacies correlate throughout the Viking Graben area regardless of the local tectonic setting or the local sediment source and supply, and appear to be synchronous(Sneider et al., 1995).The onset of extension during Middle Jurassic (Bajocian) is marked by the drowning of the Brent delta and subsequent deposition of the shallow, marine Tarbert Formation and overlying Viking Group mudstones. Transgression continued with the deposition of Bathonian-Oxfordian mudstones of the Heather Formation and the subsequent shale-dominated Draupne Formation(Dawers and Underhill, 2000).

The Upper Jurassic Viking Group, to a large extent consists of dark mudstones and shales. The group is subdivided into five formations. The Draupne Formation (Kimmeridge Clay), which is dark brown to black shales, was deposited in a restricted, deep marine environment. The Heather Formation, which is grey silty claystones that was deposited in an open marine environment. The remaining formations within the Viking Group are shallow marine sandstones, which were deposited on the Horda Platform (Fig 2.2).

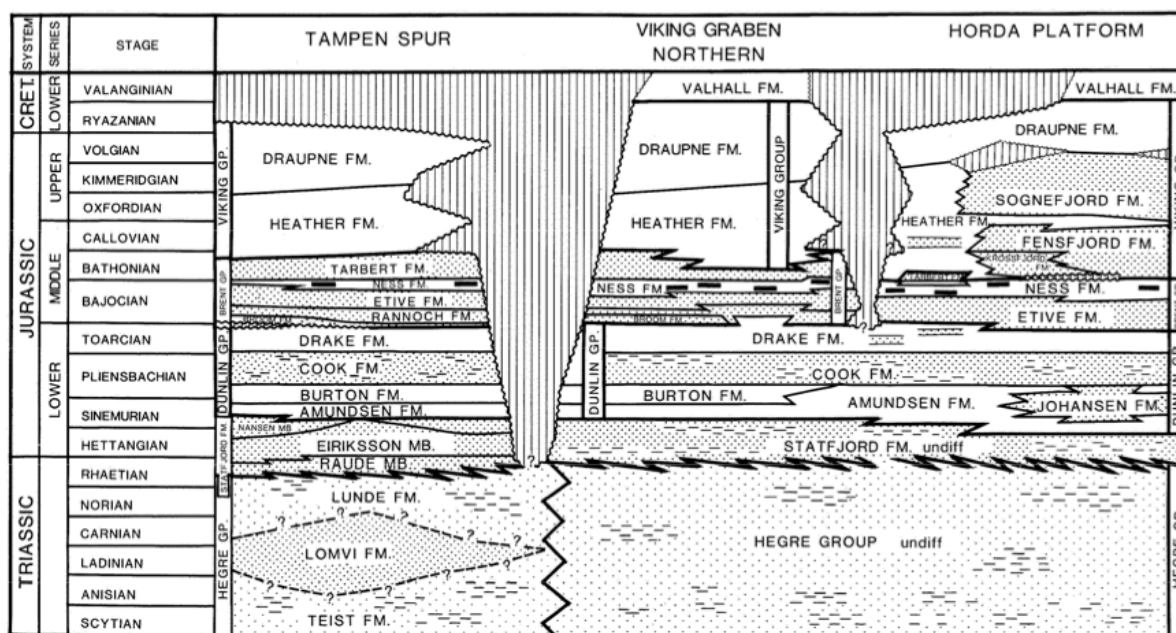


Figure 2.2: Triassic and Jurassic lithostratigraphic nomenclature Northern North Sea (Vollset and Doré, 1984).

### 2.2.3 Cretaceous

At the beginning of the Cretaceous (Fig 2.3) there was a change from restricted marine to more open marine conditions. In the northern North Sea the Lower Cretaceous deposits are thin, fine grained, mainly shales with some limestones (Kirk, 1980). In the Viking Graben the carbonate content diminishes northwards and we do not have pure limestone (chalk) facies like that in the southern and central part of the North Sea. Instead shales predominate (Fig 2.3), though often with a significant carbonate content (Faleide et al., 2015).

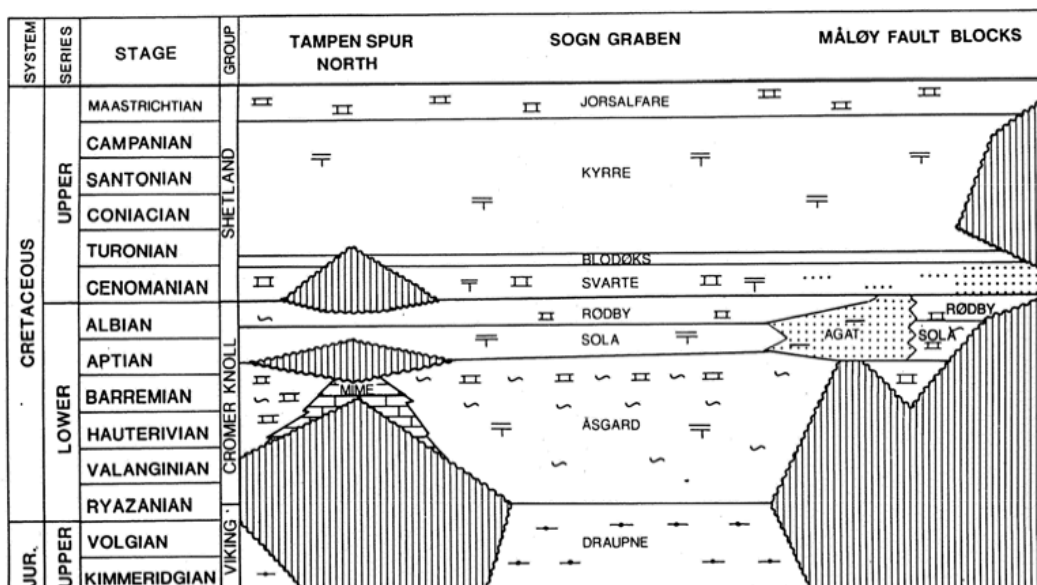
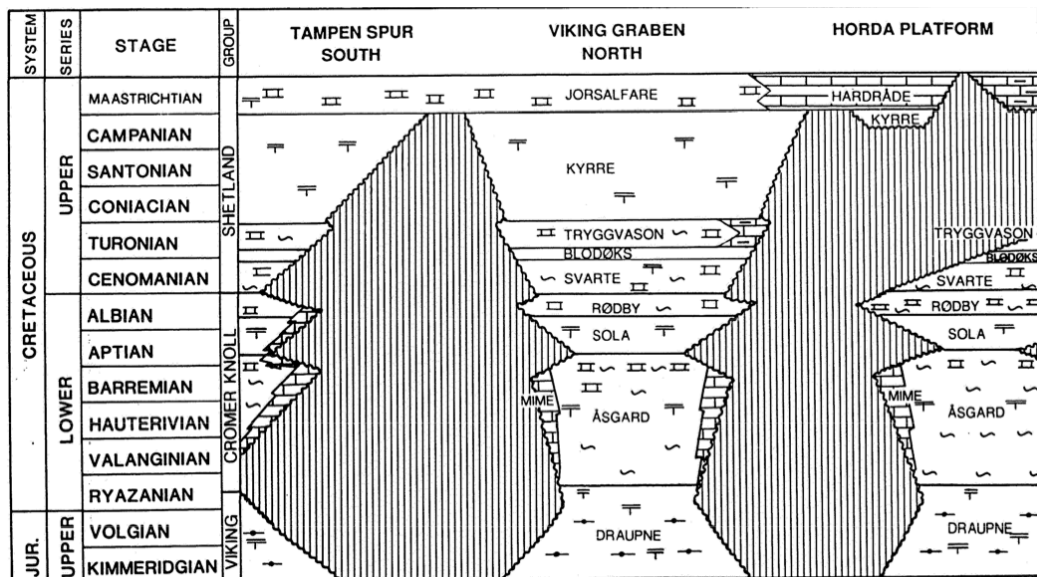


Figure 2.3: Cretaceous lithostratigraphic nomenclature Norwegian North Sea (Isaksen and Tonstad, 1989)

### 2.2.4 Tertiary

The regional tectonic setting, which was dominated by subsidence in the Viking Graben and Witch Ground Graben areas, had an important influence on the thickness and distribution of the Paleocene sands. Following deposition of the Danian, middle Paleocene sedimentation was controlled by uplift and faulting along the flanks of these areas with large quantities of sand being shed off the East Shetland Platform. At this time, the basin becomes increasingly cut off from open marine circulation. The top of the Paleocene is marked by a regional

unconformity representing a late Paleocene-early Eocene transgression which affected much of north-western Europe (Mudge and Bliss, 1983).

The Paleocene Rogaland Group consists primarily of deep water clay stones and mudstones with minor thin siltstones and sandstones of the Lista Formation. A regionally recognized mixed volcanic tuff sequence (ash fall deposits), known as the Balder Formation, is preserved over much of the North Sea basin at the top of the Paleocene (Fig 2.4).

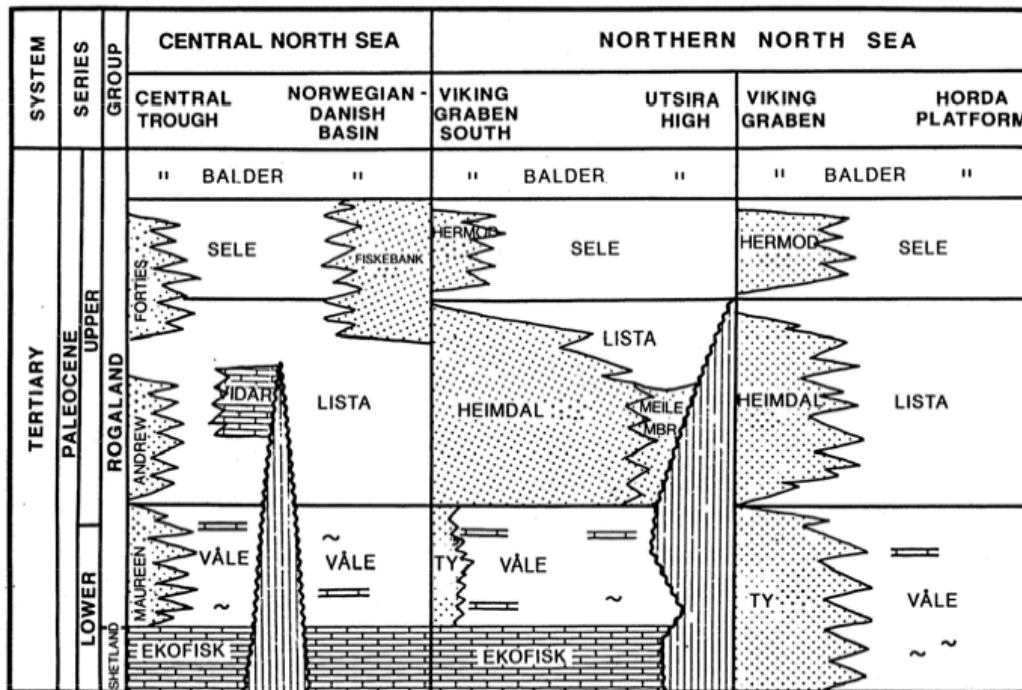


Figure 2.4: Paleocene lithostratigraphic nomenclature Norwegian North Sea (Isaksen and Tonstad, 1989)

The lower Eocene sands have also been interpreted as being of deep-sea submarine-fan origin. As the lower Eocene sands in many places overlie the shallow-water shelf-deltaic deposits with only the Balder Formation separating the two, it would be necessary to postulate extremely rapid differential subsidence to account for their deep-sea origin (Morton, 1982). At the Eocene-Oligocene transition, southern Norway became uplifted. This uplift, in combination with prograding units from both the east and west, gave rise to a shallow threshold in the northern North Sea, separating deeper waters to the south and north. The uplift and shallowing continued into Miocene time when a widespread hiatus formed in the northern North Sea (Faleide et al., 2015).

During the Neogene, the northern North Sea connected the deeper central North Sea and the Norwegian–Greenland basins. Deposition during the early Miocene was dominated by slow argillaceous sedimentation. A break occurred during the early to mid-Miocene with erosion of underlying Oligocene and Miocene deposits. Denudation of the margins of the central to northern North Sea basin resulted in deposition of mainly quartz-rich fine-to-medium grained sands with thin interbedded clay layers, comprising the sandy part of the Utsira Formation. The eastern and western limits of the Utsira Sand are mainly defined by stratigraphic lapout. The southern and the northern limits are defined by a lateral transition into shaly sediments. Deposition of the upper part of the Utsira Sand seems to have continued into Pliocene times (Fig 2.6). The lowermost part of Upper Pliocene is probably missing throughout most of the Norwegian Viking Graben area (Gregersen and Johannessen, 2007).

The Nordland Group is an important stratigraphical unit within the Upper Cenozoic of the northern North Sea. At its base lies the Utsira sand, the upper part of which is dated as early Late Pliocene. The Nordland Group overlies the Hordaland Group and comprises the basal, dominantly sandy Utsira sand, and overlying dominantly argillaceous units. It is locally over 1500m thick with strata ranging in age from late Middle Miocene through Holocene (Fig 2.5). Major paleoclimatic fluctuations also affected Late Cenozoic sedimentation in the northern North Sea, with most notably, glacial sediment transport westwards from Norway during the latest Pliocene and Quaternary (Head et al., 2004).



NEOGENE				PERIOD
MIOCENE		PLIOCENE		EPOCH
EARLY	MIDDLE	EARLY	LATE	AGE
BURDIGALIAN (PARS)	SERRAVALLIAN	ZANCLLEAN	PIA-CEN-ASIAN	GEOCHRONOLOGY (Berggren et al., 1995a,b)
16.4	14.8	5.32	3.58	0.00
				1.77
				2.60
				7.12
				11.2
				14.8
				16.4
HORDALAND GROUP		NORDLAND GROUP		LITHO-STRATIGRAPHY
SKADE FORMATION (PARS)		UNNAMED FORMATIONS		
HORDALAND GROUP SHALES		NORDLAND GROUP mudstones		PRINCIPAL CALIBRATION POINTS
SAND		UTSIRA		
HORDALAND GROUP SHALES		UTSIRA		Well 15/9-A-11 (marine palynomorphs and foraminifera: late Late Pliocene, 1.8-2.4 Ma, this study)
HORDALAND GROUP SHALES		UTSIRA		Well 15/9-A-23 (marine palynomorphs: Early Pliocene, Pflaeger et al., 2002; ca. 4.5 Ma, this study)
HORDALAND GROUP SHALES		UTSIRA		Well 24/12-1 (calcareous algae: 11.7-10.3 Ma, T. Eldvin, unpublished)
HORDALAND GROUP SHALES		UTSIRA		Well 24/12-1 (calcareous algae: 12-14 Ma, Eldvin et al., 2002)
HORDALAND GROUP SHALES		UTSIRA		Well 24/12-1 (strontium isotope age: 15.4 Ma, Eldvin et al., 2002)

Figure 2.5: Chronostratigraphy of the Nordland Group and the uppermost Hordaland Group in the Viking Graben, northern North Sea (Head et al., 2004)

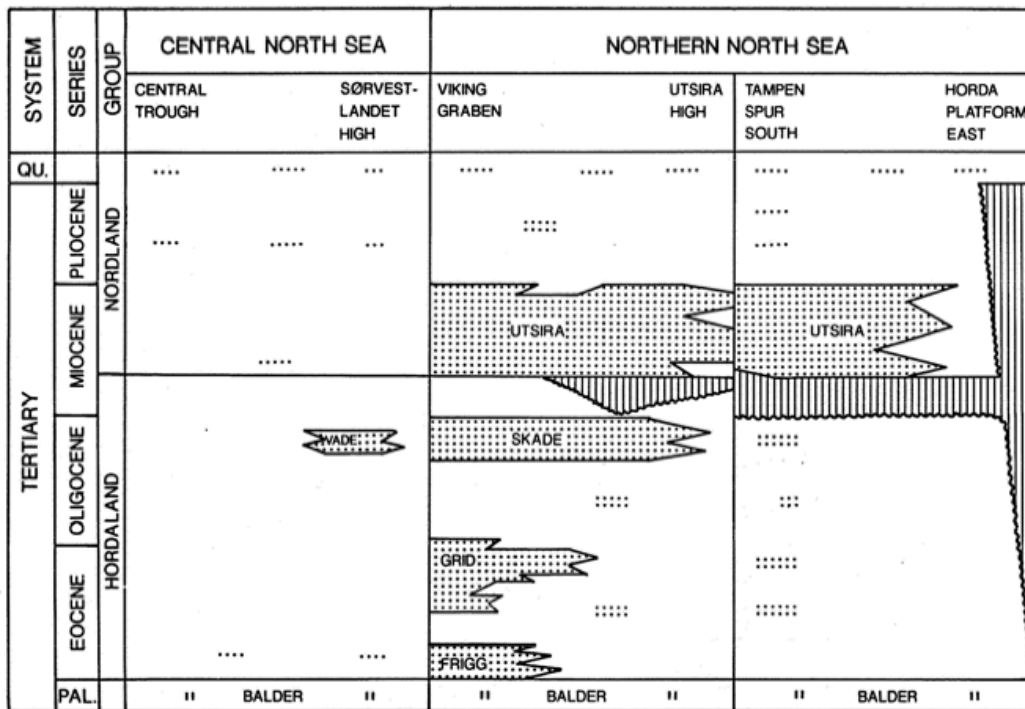


Figure 2.6: Lithostratigraphic nomenclature in the Hordaland and Nordland Groups (Tertiary) Norwegian North Sea(Isaksen and Tonstad, 1989)

### 2.3 Structural Evolution

The northern North Sea sedimentary basin is 170-200 km wide, and is a N-trending zone of extended crust, flanked by the west Norwegian mainland to the east and the Shetland Platform to the west (Fig 2.7). The reason why this part of the basin had a complex structural development is because it was subjected to multiple stretching with the interference of two major extensional phases, and extension affected a heterogeneous basin substrate both as regards composition and inherited grain. The overall structure and the composite fault pattern seen now in the northern North Sea resulted from major extensional phases in Permo-Triassic and Middle-Late Jurassic. Upper crustal extension resulted in variably tilted fault-block and basins bounded by planar or listric faults (Færseth, 1996).

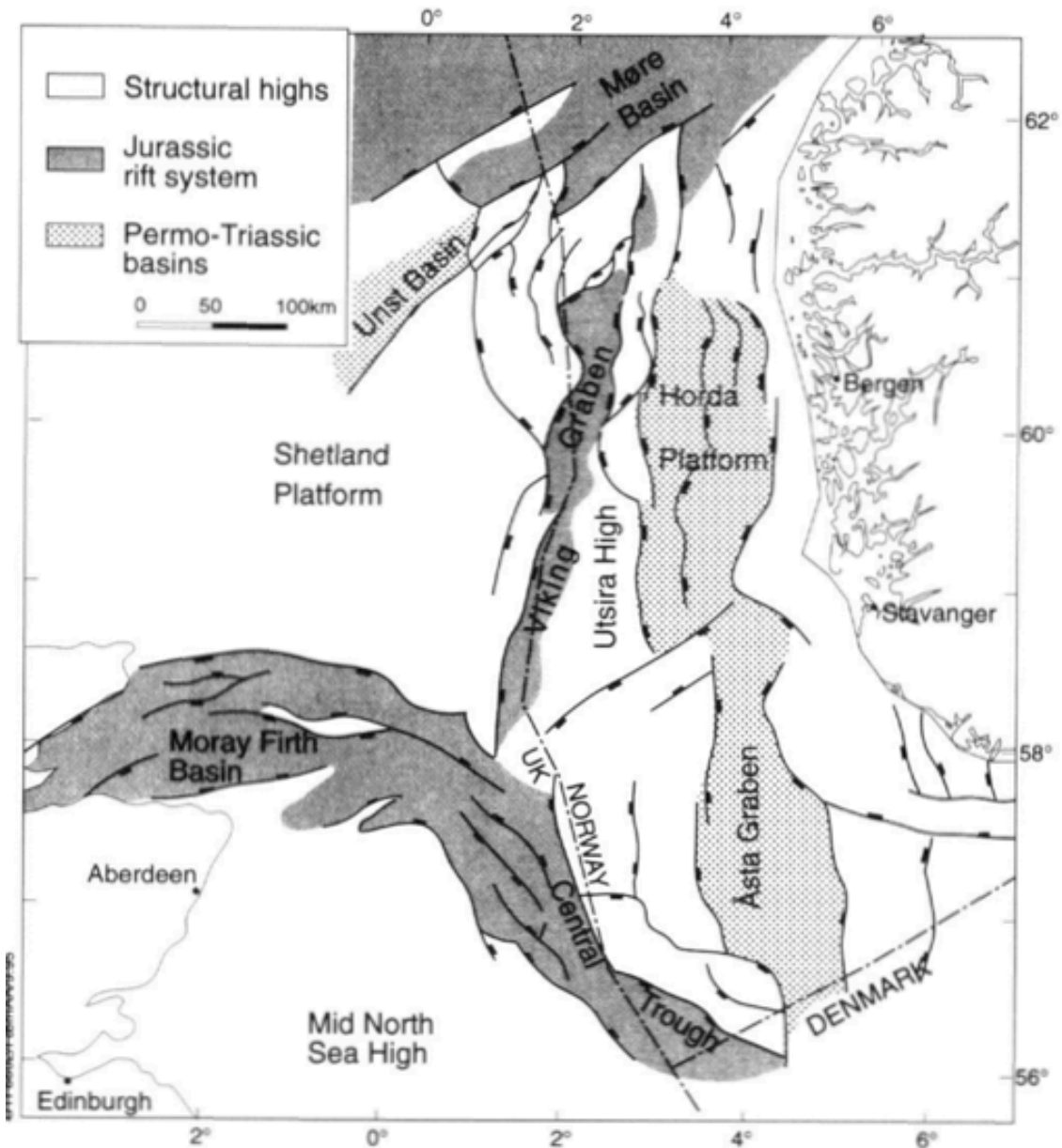


Figure 2.7: Structural elements of the North Sea showing the Permo-Triassic and Jurassic rift systems(Færseth, 1996)

### 2.3.1 Late Permian to Early Triassic rifting

Late Permian to early Triassic rifting in the northern North Sea is characterized by largely north-south trending faults that form easterly or westerly tilted half-grabens. In the central part of the Viking Graben this rifting phase is strongly overprinted by middle Jurassic to Early Cretaceous extension, Triassic fault blocks can be readily identified in the east and west of this zone(Færseth, 1996). Different structures have been formed during the late Permian to early Triassic rifting, but in the east of the Viking Graben, the major Triassic structures are

found in the Sogn Graben, the Horda Platform and in the Stord Basin. The Øygarden Fault Zone marks the eastern limit of the Triassic basin where north-trending faults offset the basement by up to 8km. The fault blocks are 15-20 km wide and the stretching factor is estimated to be 1.38 and 1.40(Odinsen et al., 2000).

The north-trending, easterly dipping bounding fault of the Sogn Graben has a throw of about 4.5km, of which around 2 km can be attributed to Triassic extension. Basement on the eastern side of the fault block was uplifted and eroded during the Triassic and was progressively overlapped in an easterly direction by younger Mesozoic sediments(Færseth, 1996).The north-westerly dipping North Tern Fault formed a Triassic basin-bounding fault, as its continuation northwards into the West Penguin Fault. Other Faults, such as the Cormorant Fault, show slight to moderate thickness changes between the footwall and the hanging wall. Westerly rotated half-grabens are bounded by the (north-south) orientated, easterly dipping Snorre and Hutton Faults(Færseth, 1996).The late Permian-early Triassic master faults were partly reactivated in the late Jurassic rifting, influencing the general structural pattern of the entire basin and promoting segmentation and subsidence with opposing polarities in some areas.

### **2.3.2 Middle Jurassic to Early Cretaceous Rifting**

The major structures in the North Sea are due to the Middle Jurassic to Early Cretaceous rifting, and the Viking Graben is the major structural element of the northern North Sea. The North, Central and South Viking Grabens segments are north to north-easterly trending structures(Thomas and Coward, 1996).The middle Jurassic –early Cretaceous rifting phase resulted in characteristic wedge-shaped packages which only partially infill the fault block topography. The sediments infill of the middle Jurassic-earliest Cretaceous rift basins was essentially deep marine(Ravnås et al., 2000).

In the East Shetland Basin, the fault blocks are characterized by pronounced footwall uplift and hanging wall subsidence. The tilted fault blocks represent the basic unit of the structure, but may be complicated by a secondary fault network. The fault blocks may show simple tilting away from the north or north –easterly trending master fault, or may show uplift of one corner, suggesting that there has been a slight rotation of the fault block about a vertical axis during latest Jurassic to earliest Cretaceous extension(Thomas and Coward, 1995).

### **2.3.3 Cretaceous to Cenozoic Post-Rift Deformation**

The Cretaceous to Cenozoic post-rift period was dominated by regional thermal subsidence, with superimposed pulses of uplift along the western and eastern flanks of the basin. On the western margin of the northern North Sea, deposition of large submarine fans in the basin during the Paleogene resulted from the tectonic uplift and eastward tilting of the Scottish Mainland, the East Shetland Platform, and the Inner Moray Firth Basin (Thomson and Underhill, 1993).

A late Eocene to early Oligocene uplift of a deeply weathered erosional peneplain surface across Fennoscandia, led to sediment outbuilding and an increase in the rate of sediment accumulation in the northern North Sea (Riis, 1996). The Pliocene sequence in the northern North Sea is characterised by outbuilding from Norway and the deposition of a major late Pliocene clastic wedge.

During the thermal subsidence that followed the Permo-Triassic rifting, faulting occurred on both margins as a consequence of the interaction of lateral variations in the thermal subsidence, sediment loading, compaction and flexure. Thermal subsidence still continued when the mid-Jurassic rifting started. Rotation of major fault blocks shows that the middle Jurassic to early Cretaceous rifting was initiated in Late Bajocian-early Bathonian time, and terminated in early Ryazanian time (Ravnås et al., 2000).

There were multiple pulses of faulting separated by intervening stages of relative tectonic quiescence; this pattern was a major influence on the nature and architecture of the sediments in the basin (Ravnås et al., 2000). (Roberts et al., 1990) suggested that an east-west extension direction explains the pattern of faulting in the Viking Graben during the late Jurassic. Extension of 15% is considered to be a reasonable estimate for the stretching in the East Shetland Basin. On the Horda Platform, the Late Jurassic stretching was only 5%, whereas in the axis of the Viking Graben the stretching reached 30-40% (Roberts et al., 1993).

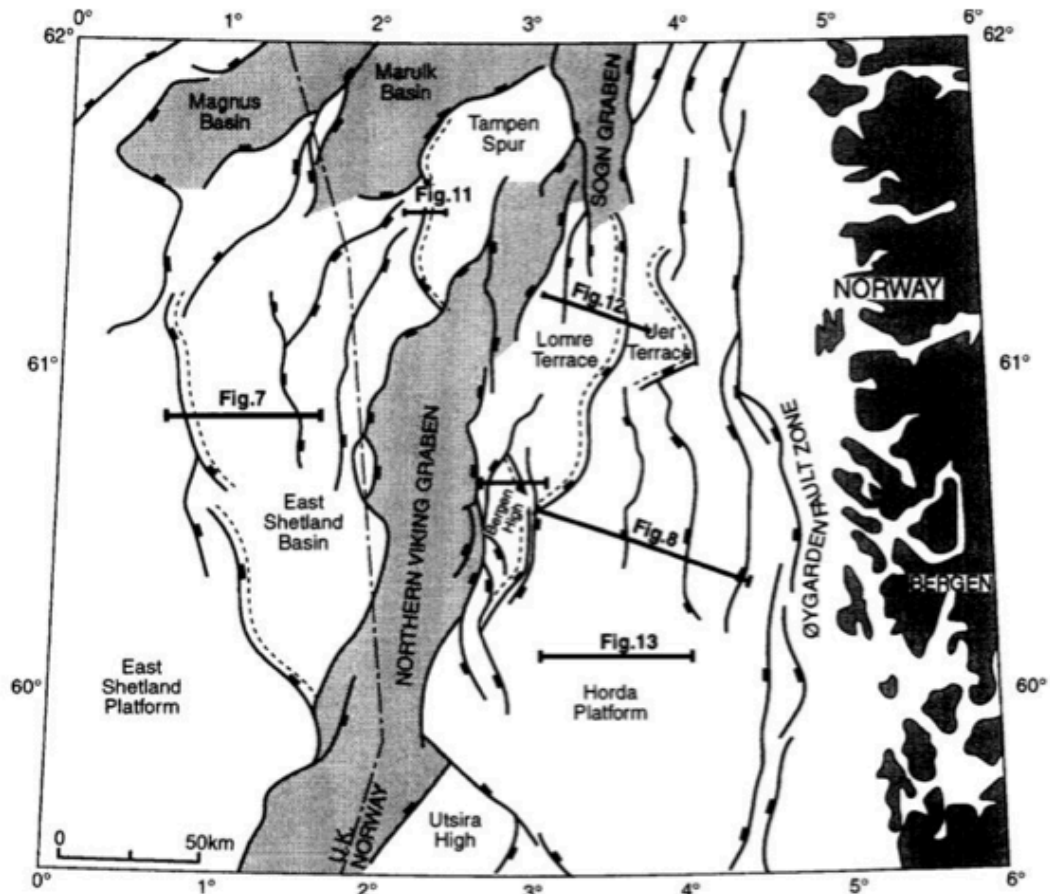


Figure 2.8: Structure map of the northern North Sea showing the main area of late Jurassic to early Cretaceous rifting (Gabrielsen et al., 1999).

## **CHAPTER 3: PETROLEUM GEOLOGY OF THE NORTHERN NORTH SEA**

### **3.1 Petroleum system**

The key to all the plays is the presence of organic-rich Upper Jurassic shales (source rocks) and a rift system of the same age. The rifting provided the structures (the traps) and post-rift cooling caused the subsidence necessary for hydrocarbon generation. The Lower-Middle Jurassic play results from pre-rift uplift in the south providing clastic input for a delta system in the north, the thick sandstone reservoir of which were preserved during the subsequent rifting (Pegrum and Spencer, 1990).

### **3.2 Source rocks**

In the northern North Sea the main source rocks is the Upper Jurassic Draupne Formation, which is an excellent oil source rock, but can also generate gas at high maturity, and the Heather Formation, which is lean dry gas source rock. Both Draupne and Heather Formations belong to the Viking Group.

#### **3.2.1 Draupne Formation (Kimmeridge Clay)**

The Draupne Formation represents the most important source rock unit in the northern North Sea. It was deposited during the Oxfordian-Ryazanian in a marine environment with restricted bottom water circulation and thus under anaerobic conditions (Cooper and Barnard, 1984). The formation is typically made up of brownish black, medium to dark olive grey and grey black, non-calcareous mudstones. It is locally silty and micaceous and may also include nodular carbonates. Its thickness ranges from 50-500m, In the East Shetland Basin the Kimmeridge Clay unit is up to 500m thick. In terms of its kerogen type the formation is commonly classified as type II (marine sapropelic) oil prone source rock (Goff, 1983).

Uranium contents within the Draupne Formation are high, corresponding to high organo – carbon contents (Telnaes et al., 1991). The oil source potential of the Kimmeridge Clay unit is directly related to kerogen facies, which may vary according to the depositional environment and type of organic matter (Cornford, 1998).

Organically rich mudstones within the Kimmeridge Clay unit have TOC contents of around 6%, locally reaching in excess of 10% or as low as 2%. The Hydrogen Indices (HI) values range between 200 to 400 mg/gTOC (Kubala et al., 2003).

### **3.2.2 Heather Formation**

The Heather Formation comprises dark grey, commonly silty mudstones with abundant interbedded carbonates bands; the mudstones tend to be more calcareous than the overlying Kimmeridge Clay unit. The thickness of this formation varies from place to place, it reaches 350 m in the East Shetland Basin, 600 m in the south Viking Graben and 700 m in the central North Sea, and can be more than 1000 m in the Viking Graben(Kubala et al., 2003). The age of Heather Formation ranges from Bathonian-Kimmeridgian.

TOC contents within the Heather unit are lower than in the Kimmeridge Clay unit at around 2-2.5%(Goff, 1983). The hydrogen indices (HI) are in the range 100-200 mg/gTOC, but can be above 200 mg/gTOC in some areas and can rarely exceed 300 mg/gTOC. Along the axial regions of the North Viking and Central Grabens where the Heather unit is at a late-to post-mature stage for oil generation the hydrogen indices may be less than 100 mg/ gTOC(Kubala et al., 2003).

## **3.3 Reservoirs**

### **3.3.1 Triassic and Lower Jurassic**

The Snorre field is located on the Tampen Spur, which is a platform high on the western flank of the Viking Graben. The main reservoir horizons are the fluvial sandstones in the upper member of the Upper Triassic Lunde Formation and the Upper Triassic to Lower Jurassic Statfjord Formation. The Lunde Formation is the uppermost formation of the Triassic Hegre Group, it was deposited during the thermal subsidence phase following a late Permian to Early Triassic rifting episode (Morad et al., 1990).

The Lunde Formation is the principal oil reservoir in the Snorre Field and is an important gas reservoir in the Gullfaks, Sør and Visund fields. The Triassic-Lower Jurassic reservoir rocks are heterogeneous; permeability and porosity reflect sedimentary facies and textural variations modified by diagenesis (Nystuen and Fält, 1995).

The Triassic reservoirs generally occur in tilted faults blocks with varying levels of late Jurassic to early Cretaceous erosion, and varying degrees of late Jurassic and Cretaceous



onlap. With the exception of the Snorre Field, the northern North Sea fields with Triassic hydrocarbon accumulations have most of their hydrocarbons in overlying Lower and Middle Jurassic reservoirs. In Triassic sandstones, the reservoir-quality porosity is mainly a function of initial depositional facies; the more distal, cleaner and mature the sands, the higher the initial and ultimate porosity (Goldsmith et al., 2003).

In the northern North Sea the Lower Jurassic reservoirs are commonly found within sandstones of the Rhaetian-Sinemurian Statfjord Group, and locally in the Pliensbachian-Toarcian Cook Formation of the Dunlin Group. Many oil fields in the northern part of the North Sea also have Statfjord Group sandstones as reservoir rocks. The reservoir properties are a function of depositional conditions, both on account of primary sorting and because diagenetic changes are usually determined by the primary mineralogical composition and sorting (Faleide et al., 2015).

### **3.3.2 Middle Jurassic**

The Aalenian-Bathonian Brent Group forms most of the Middle Jurassic reservoirs in the Northern North Sea. The formations within the Brent Group are Tarbert (youngest), Ness, Etive, Rannoch and Broom (Vollset and Doré, 1984). Most of the Middle Jurassic reservoir sandstones are arkoses or subarkoses. They consist mainly of quartz, which together with kaolinite, albite and illite comprise more than 95%. The main mineral cement in these sandstones is quartz overgrowths, Authigenic kaolinite is a common pore –filling mineral at burial depths of 2500-3500m, and illite is found in increasing amount below 3500m (Walderhaug and Bjørkum, 1992).

### **3.3.3 Upper Jurassic**

Upper Jurassic (Bathonian-Kimmeridgian) sandstones provide good reservoirs particularly in the platform areas, where fault block rotation is moderate (e.g. the Troll Field) and in mixed structural-stratigraphic traps along fault block crests. In the Troll Field the reservoirs are of Upper Jurassic age and contain mostly gas formed in the deepest part of the basin (> 4500m) (Faleide et al., 2015)

In the northern North Sea, Upper Jurassic shallow marine reservoirs are rare, although localised, shallow marine sandstones occur along the Tampen Spur in the Snorre-Statfjord

area as a result of footwall uplift and erosion during the early phase of rifting in the North Viking Graben (Dawers et al., 1999).

### **3.4 Traps and Seals**

The geometry of the rotated fault- block traps was created initially during active rifting. In the northern North Sea, the earliest Jurassic extension is of latest Bajocian to mid-Callovian age and was succeeded by a major phase of faulting during the mid-Oxfordian to early Kimmeridgian (Rathey and Hayward, 1993). The most important traps are clustered on the Tampen Spur on the eastern flank of the Viking Graben where the three largest oilfields, Statfjord, Brent and Gullfaks, are located. The traps are mainly structural and are located in the crests of the footwalls of rotated fault blocks.

The typical trap in the northern North Sea is a tilted fault block with at least one fault sealing the hydrocarbon column (Knott et al., 1993; Knott, 1993). The Cretaceous shales/mudstones provide a regional seal which often coincides with the development of overpressure above deep graben centres reflecting restricted pore water escape (Burley, 1993).

### **3.5 Migration**

Migration is the process by which petroleum fluids move from the low porosity, fine-grained source rocks, where they are generated, to higher porosity reservoir rocks, where they may (under suitable circumstances) form a highly concentrated hydrocarbon accumulation. Primary migration is defined as the movement of the newly generated petroleum from the low permeability source rock to its first encounter with higher permeability beds usually a sandstone or fractured limestone body. Secondary migration is the subsequent transfer of petroleum through higher permeability strata known as carrier beds. If suitable reservoir structure is encountered within the range of secondary migration, a petroleum accumulation may be formed. In the northern North Sea primary migration is through pressure driven flow of a discrete hydrocarbon phase through pores and micro fractures (England et al., 1987).

The main driving force during secondary migration is buoyancy (the difference in density of the hydrocarbon phase compared to that of the formation water). In the northern North Sea vertical migration of hydrocarbon has occurred along the major half graben-bounding faults

with some leakage of hydrocarbons along the faults where sandstones within the Mesozoic section terminate against them. However, the bulk of the hydrocarbons follow the structural contours towards structural culminations(Kubala et al., 2003). The main conduits for the migration of hydrocarbon within the study area are sandstones of the Brent Group(Miles, 1990).

The main modes of migration from source rock to reservoir are intercalation of source rock and reservoir, juxtaposition of source and reservoir across faults, and vertical migration through micro-fracture systems(Curtin and Ballestad, 1986). In the northern North Sea the main mechanism of migration is short distance migration due to juxtaposition of reservoir and source rocks, and migration in the rotated fault blocks. In the northern North Sea the timing of oil generation and migration ranges from the late Cretaceous through to the present(Barnard and Bastow, 1991). Oil migrates through a three dimensional, oil wet, kerogene network (McAuliffe, 1979). Oil expulsion is a direct consequence of maturation, and that oil migrates through microfractures created by abnormal pore pressure resulting from generation(Momper, 1978).

# CHAPTER 4: SEISMIC INTERPRETATION

## 4.1 Introduction

Seismic Interpretation is the extraction of subsurface geologic information from seismic data. Interpreting seismic data requires an understanding of the subsurface formations and how they may affect wave reception. Seismic interpretation can be used to delineate both structural and stratigraphic traps.

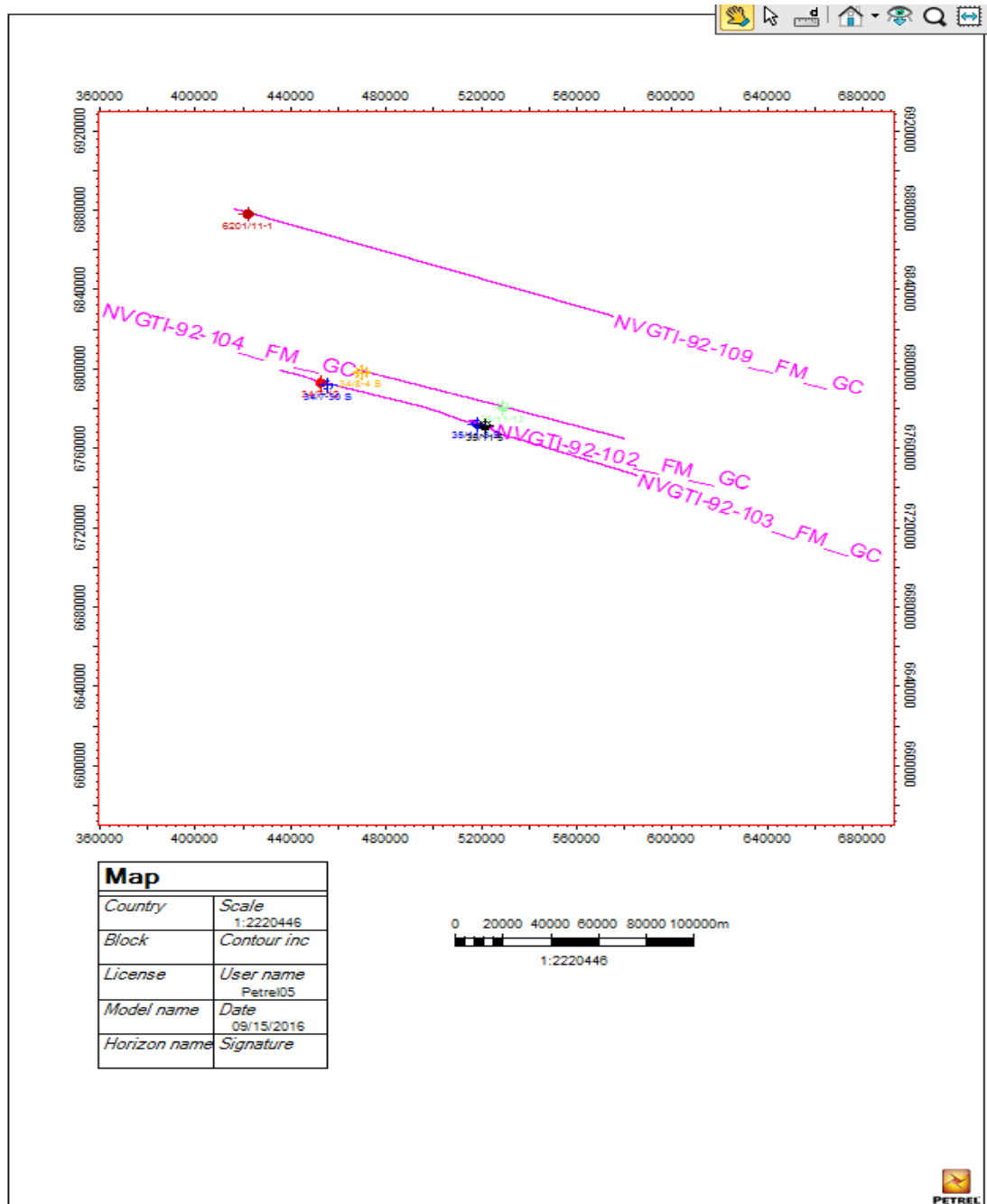


Figure 4.1: Map showing the seismic lines and well locations.

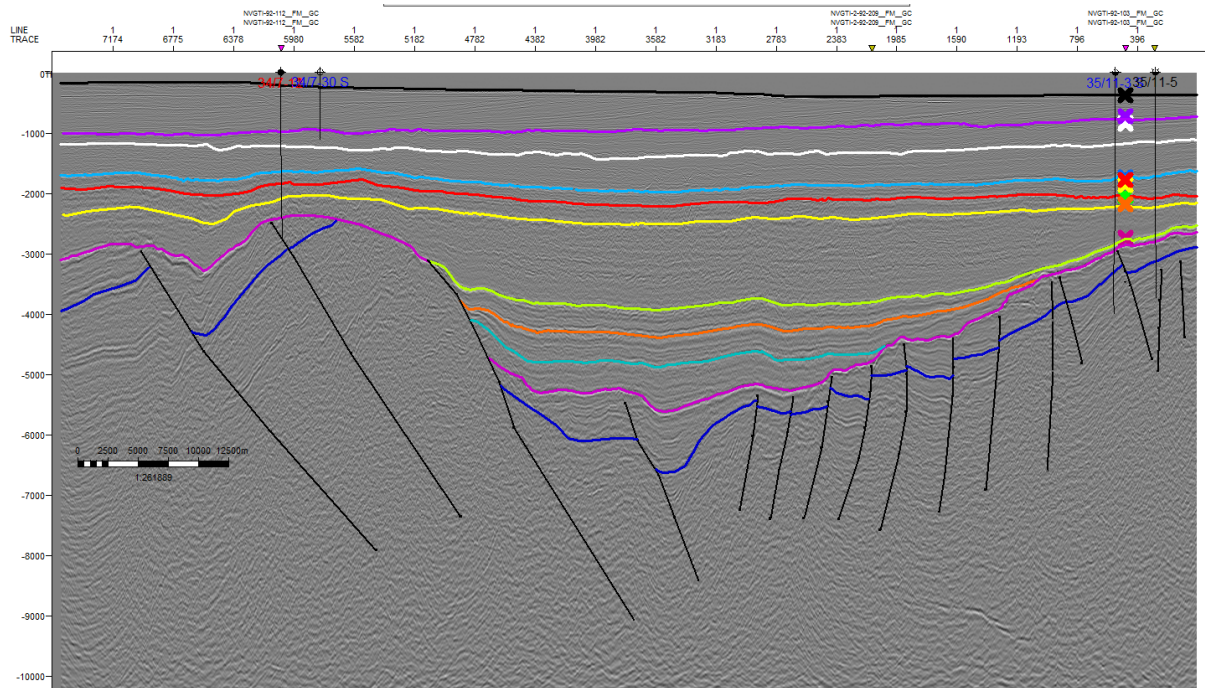


Figure 4.2: Interpreted dip line (NVGTI -92-102)

Fig 4.2 is the dip line (NVGTI-92-102), which contains four drilled wells (35/11-5, 35/11-3s, 34/7-12, 34/7-30s) (Fig 4.1). The dark blue reflector in the east of the main graben boundary fault is the Top Middle Jurassic (Top Brent Group), which is Bajocian to early Bathonian in age, and marks the base of the syn-rift Upper Jurassic sequence. The pink reflector is the Top Draupne Formation, that represents the Base Cretaceous Unconformity (BCU) which east of the main fault marks the boundary between syn-rift Upper Jurassic and post-rift Lower Cretaceous. The BCU is interpreted to the west of the main fault over the fault blocks.

The next two overlying reflectors (turquoise, orange) are intra-Cretaceous, and represent the Top Cromer Knoll Group, which is Late Ryazanian to Albian/Early Cenomanian in age, the green reflector is the Top Shetland Group. These sequences onlap the BCU. Above the intra-Cretaceous reflectors is the Sele Formation (yellow reflector), Lista Formation (red reflector), Top Balder Formation (blue reflector), Top Hordaland Group (white reflector), The Utsira Formation (purple reflector) and the Top Nordland Group (Sea bed) (black reflector).

Tilted fault blocks are observed (Fig 4.2), which indicate that the area has experienced tectonic extension and that subsidence was caused partly by major extensional phases. The half-graben structures with wedge shaped packages indicate syn-rift sedimentation, which shows that the sediments were deposited during the rifting. The transition from syn rift

development phase to post rift development phase is observed by termination of the syn rift faulting and the subsidence will be controlled dominantly by thermal contraction and sediment loading. The BCU is the prominent unconformity of the North Sea and marks the boundary between the syn and post-rift sequences for the late Jurassic rifting phase.

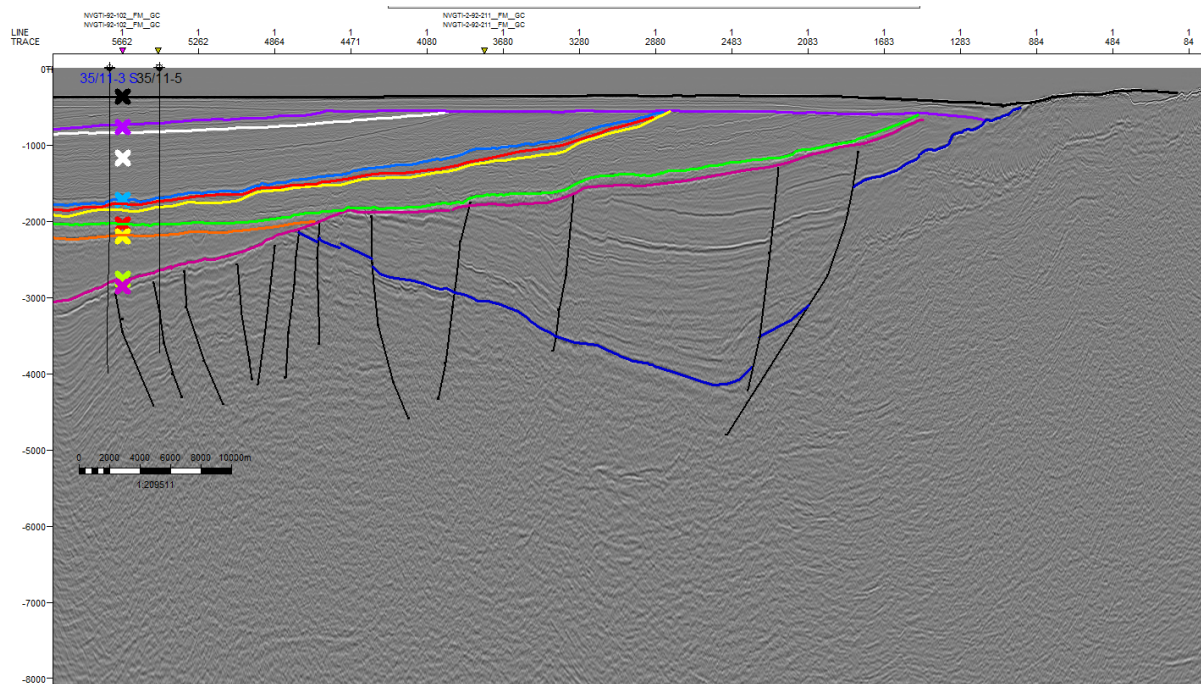


Figure 4.3: Interpreted dip line (NVGTI-92-103)

Fig 4.3 is the dip line (NVGTI-92-103), which has two drilled wells (35/11-3s, 35/11-5) (Fig 4.1). This line shows only the eastern part of the area, and the main eastern boundary fault (Øy garden Fault) to the northern North Sea basin. The lowermost reflector (dark blue) is Top Basement, which extends up to the sea floor at the eastern end. West of the main fault, the basement defines the base of the eastward tilted fault block that was formed during the Permo-Triassic (P-T) rifting phase.

The parallel sequences between the two reflectors (yellow and purple) is the Lower-Middle Jurassic and represents the post-rift sequence to the Permian-Triassic rifting. Above the purple reflector is the Upper Jurassic syn-rift representing the second rift phase, which extends up to the BCU (pink reflector).

This line indicates that the area has experienced two rift episodes, the first rift phase and the second rift phase, both of which form wedge-shaped packages. There is clear evidence that these rift phases took place during active rifting because in the wedge shaped packages the



sediments increase in thickness toward the faults. These wedge shaped packages are related to the Permo-Triassic and late Jurassic rifting phases on the Horda Platform.

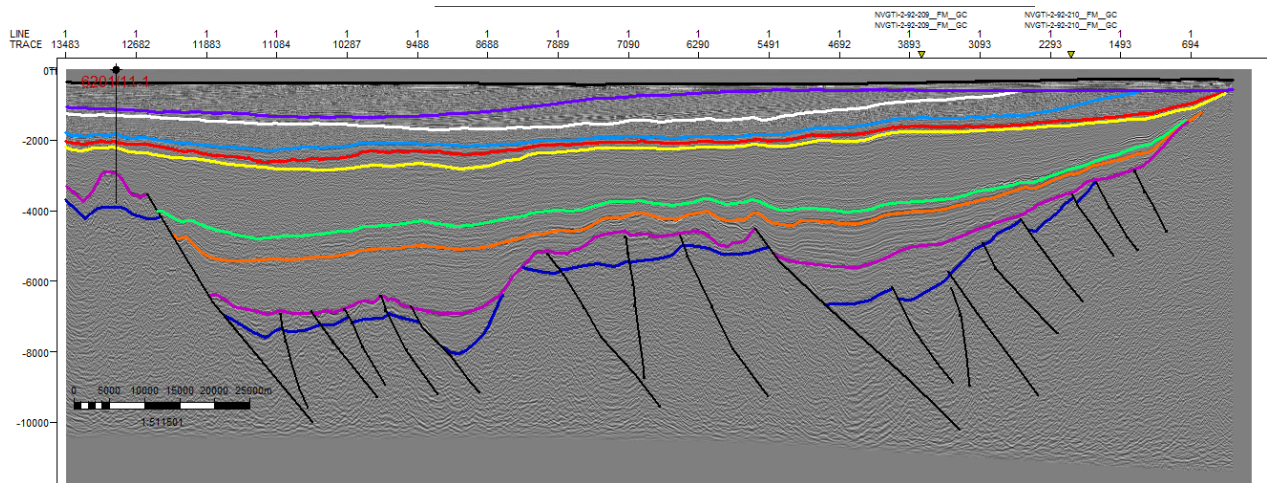


Figure 4.4: Interpreted dip line (NVGTI-92-109)

Fig 4.4 is the dip line (NVGTI-92-109), which has one drilled well (6201/11-1) (Fig 4.1). This line crosses two Grabens with a high between them. They are the southern end of the Sogn Graben in the east and northern end of the Viking Graben in the west. The dark blue reflector is the Top Middle Jurassic (Top Brent Group). The syn-rift sequence is between the BCU, which is the Draupne Formation (pink reflector) and the Top Middle Jurassic, (dark blue reflector), Above the BCU is the overlying Cretaceous sequence Top Cromer Knoll Group (orange reflector) and the Top Shetland Group (green reflector) representing the post rift phase. Above the Cretaceous sequences are the Sele Formation (yellow reflector), Lista Formation (red reflector), Top Balder Formation (blue reflector), Top Hordland Group (white reflector), Utsira Formation (purple reflector) and Top Nordaland Group (Sea bed) (black reflector).

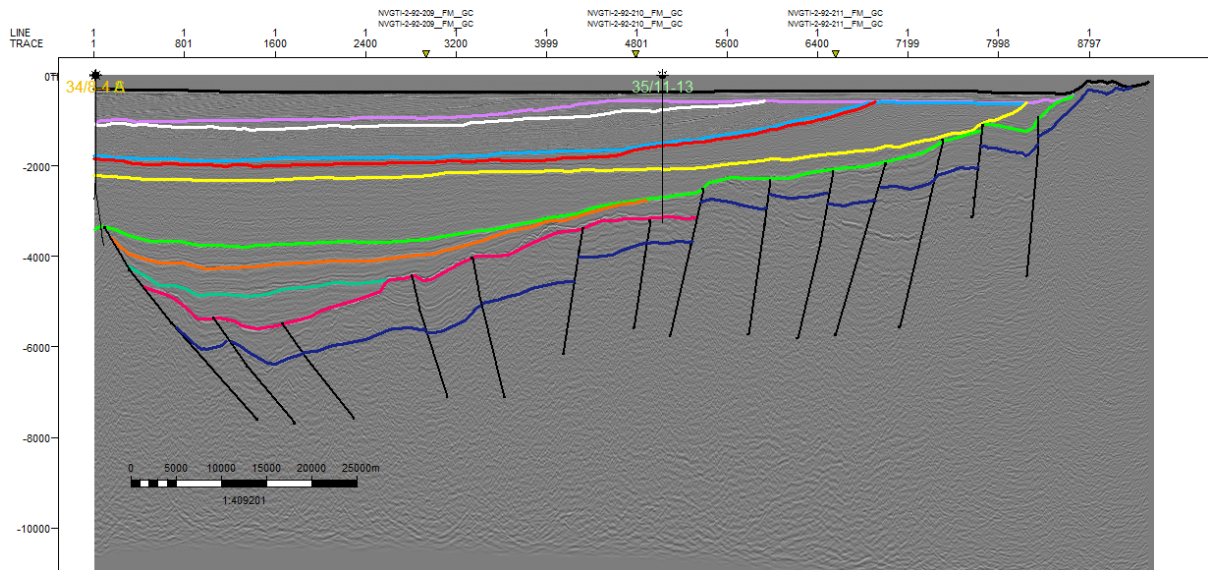


Figure 4.5: Interpreted dip line NVGTI-92-104.

Fig 4.5) is the dip line (NVGTI-92-104), which has two drilled wells (35/11-13 and 34/8-4S) (Fig 4.1). This line covers only the western part of the area. Top Middle Jurassic (Top Brent Group) is indicated by the dark blue reflector. Above the Brent Group is the BCU, which is the Top Draupne Formation (pink reflector). Above the BCU is the overlying Cretaceous sequence Mime Formation (turquoise reflector) which onlaps the BCU, Top Cromer Knoll Group (orange reflector) and the Top Shetland Group (green reflector) representing the post rift phase. Above the Cretaceous sequences are the Sele Formation (yellow reflector), Lista Formation (red reflector), Top Balder Formation (blue reflector), Top Hordaland Group (white reflector), Utsira Formation (purple reflector) and the Top Nordaland Group (Sea bed) (black reflector), the Sele Formation, Lista Formation, Top Balder Formation, Top Hordland Group toplaps the Utsira Formation.



## **CHAPTER 5: METHODOLOGY**

### **5.1 Background**

A good way to reduce investment risk in oil and gas exploration is to ascertain the presence, types and volumes of hydrocarbons in a prospective structure before drilling. The basic objective of Basin and Petroleum System Modelling is to examine the dynamics of sedimentary basins and their associated fluids to determine if past conditions were suitable for hydrocarbons to fill potential reservoirs and be preserved there (Al-Hajeri et al 2009).

Basin and Petroleum System Modelling facilitates visualization of geologic processes by developing predictive exploration and reservoir models, integrating sequence stratigraphy and assessment units, predicting the extent and timing of petroleum generation in source rocks, structural deformation that influences basin architecture, migration pathways, and location of potential traps and accumulations (Martinelli, 2010). Basin modelling can be done in 1D, 2D or 3D depending on the type of the data available and the aim of the study.

The aim of this study is to build a 2D model for predicting potential petroleum migration mechanism and pathways for source rock and reservoir rocks. Also to model the source rock maturity and hydrocarbon accumulation of the study area.

### **5.2 Workflow**

There are various steps involved in the Basic Model Building Workflow for PetroMod 2D (Fig 5.1). Petro Builder 2D distinguishes between pre-grid and gridded data. Pre-grid data are the initial horizons and faults that constitute the geometric input for the model. Faults are important for petroleum systems analysis because they can have a considerable impact on migration pathways. Once faults have been implemented in a model, properties relevant for migration can be assigned to the faults and the simulation will take this special feature into account.

To simulate the evolution of a petroleum system, pre-grid horizons and faults need to be gridded. The gridding algorithm ensures that each node of a horizon or fault lies on a grid point. In contrast to pre-grid horizons, gridded horizons consist of nodes at each grid intersection and extend to the model boundaries. It is recommended to perform age

assignment after gridding; this is because the gridding algorithm automatically generates horizons, layers and gridded horizons as well as default facies maps. The ages are manually entered. Horizons define the layers in a model. PetroBuilder 2D defines the thickness of a layer according to the vertical distance between the horizons.

In PetroMod facies show a range of petrophysical properties and reservoir or source characteristics are assigned to the different strata of the model. By assigning a facies to a layer you specify the petrophysical properties for that layer are specified, which is essential for a realistic simulation. Facies include the lithology and source rock property information on TOC content and distribution, kerogen type and petroleum kinetics.

In the simulation run to include the paleo water depth (PWD), the water depth or paleo depth table is used. Boundary conditions define the basic energetic conditions for the temperature and burial history of the source rock and, consequently, for the maturation of organic matter through time. Boundary conditions prepare the model for simulation.

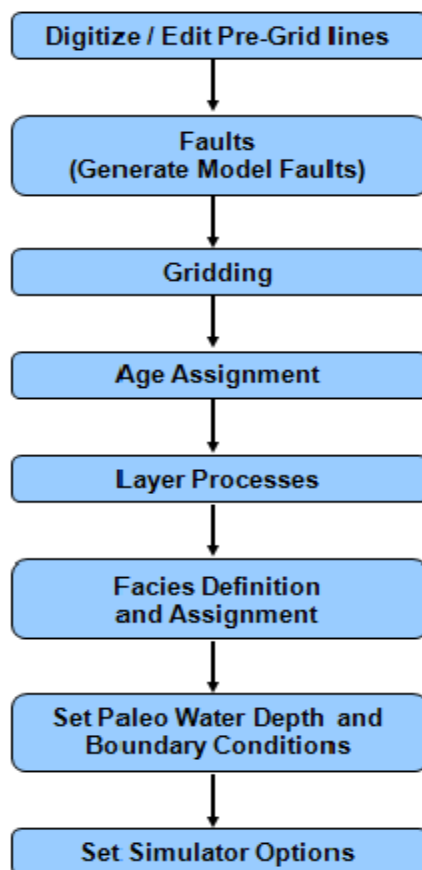


Figure 5.1: Workflow for building a basic 2D model.

## 5.3 Input Data

### 5.3.1 Fault Properties

Fault properties are defined in the fault property definition table (Fig 5.2). The fault properties tell the simulator how to handle faults. In PetroMod, fault activities do not mean tectonic events, i.e. geometric activities. Instead, fault activities summarize the characteristics (properties) of a fault which are relevant for migration. The ages of the faults have been assigned based on (Færseth, 1996) (Fig 5.2).

Fault Property Definition														
Insert <input type="text" value="fault properties"/> <input checked="" type="checkbox"/>														
Name	-	Period	Age from [Ma]	Age to [Ma]	Type	SGR Mode	SGR [%]	SGR Map	FCP Mode	FCP [MPa]	FCP Map	Perm. Mode	Permeability [log(mD)]	Perm. Map
Fault_16		1	251.00	145.50	Open	Value		→	Value		→	Value		→
Fault_15		1	251.00	145.50	Open	Value		→	Value		→	Value		→
Fault_14		1	251.00	145.50	Open	Value		→	Value		→	Value		→
Fault_13		1	251.00	145.50	Open	Value		→	Value		→	Value		→
Fault_12		1	251.00	145.50	Open	Value		→	Value		→	Value		→
Fault_11		1	251.00	145.50	Open	Value		→	Value		→	Value		→
Fault_10		1	251.00	145.50	Open	Value		→	Value		→	Value		→
Fault_9		1	251.00	145.50	Open	Value		→	Value		→	Value		→
Fault_8		1	251.00	145.50	Open	Value		→	Value		→	Value		→
Fault_7		1	251.00	145.50	Open	Value		→	Value		→	Value		→
Fault_6		1	251.00	145.50	Open	Value		→	Value		→	Value		→
Fault_5		1	251.00	145.50	Open	Value		→	Value		→	Value		→
Fault_4		1	251.00	145.50	Open	Value		→	Value		→	Value		→
Fault_3		1	251.00	145.50	Open	Value		→	Value		→	Value		→
Fault_3		2	145.50	65.50	Closed	Value		→	Value		→	Value		→
Fault_2		1	251.00	145.50	Open	Value		→	Value		→	Value		→
Fault_1		1	251.00	145.50	Open	Value		→	Value		→	Value		→

Figure 5.2: Fault properties definition table.

### 5.3.2 Gridding

In order to simulate the evolution of a petroleum system, pre-grid horizons and faults need to be gridded. The gridding algorithm ensures that each node of a horizon or fault lies on a grid point ( Figs 5.3 and 5.4).

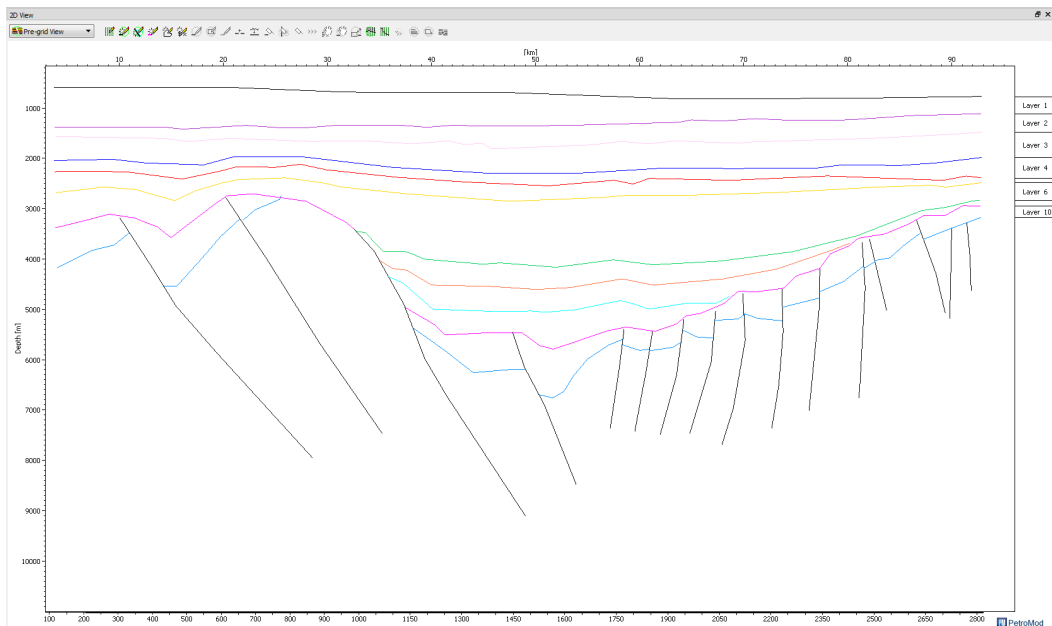


Figure 5.3: A pre-grid view of the profile NVGTI-92-102.

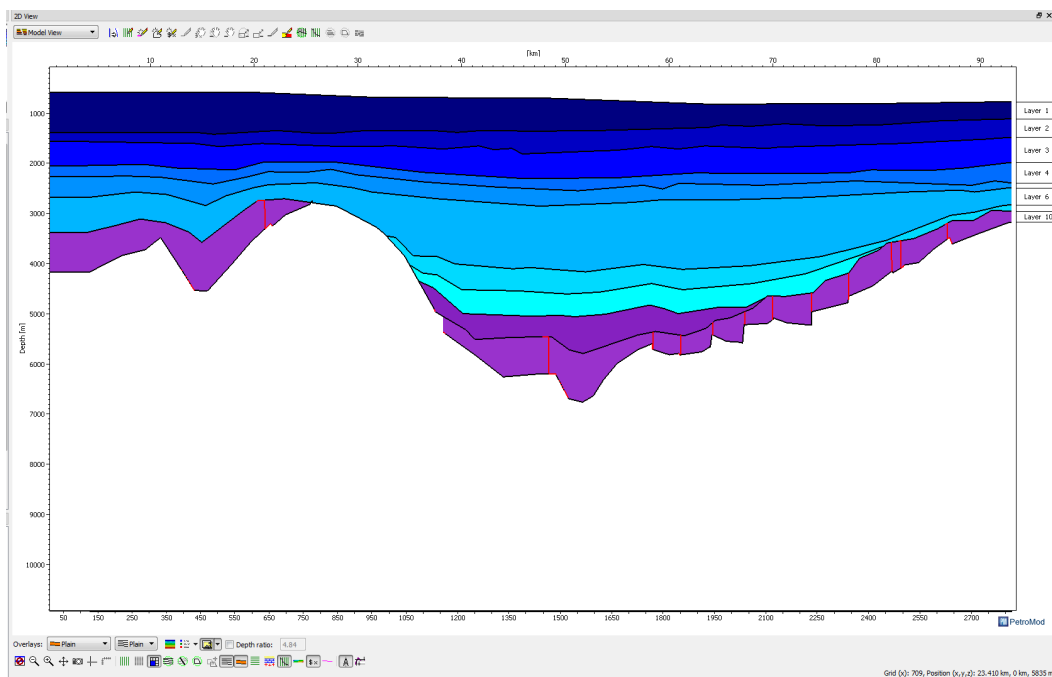


Figure 5.4: Model view after gridding of the profile NVGTI-92-102.

### 5.3.3. Age Assignment

Different ages have been assigned to different layers/units by using the lithostratigraphic sections of well 35/11-3 S from the Norwegian Petroleum Directorate's (NPD) well database/factpages. The geological time scale published by the Geological Society of America (2009) is used for the age boundaries (Fig 5.5).

Age [Ma]	Horizon	Pre-grid Horizon	Gridded Horizon	Erosion Map	Layer	Event Type	Facies Map	No. of Sublayers	Max. Time Step [Ma]
0.00	NORDALAND GROUP	Horizon_1	Horizon_1_Map						
16.00	UTSIRA FORMATION	Horizon_2	Horizon_2_Map		Layer_1	Deposition	Map_Layer_1_Facies	1	10.00
23.00	HORDALAND GROUP	Horizon_3	Horizon_3_Map		Layer_2	Deposition	Map_Layer_2_Facies	1	10.00
55.80	BALDER FORMATION	Horizon_4	Horizon_4_Map		Layer_3	Deposition	Map_Layer_3_Facies	1	10.00
58.70	LISTA FORMATION	Horizon_5	Horizon_5_Map		Layer_4	Deposition	Map_Layer_4_Facies	1	10.00
59.00	SELE FORMATION	Horizon_6	Horizon_6_Map		Layer_5	Deposition	Map_Layer_5_Facies	1	10.00
65.50	SHETLAND GROUP	Horizon_7	Horizon_7_Map		Layer_6	Deposition	Map_Layer_6_Facies	1	10.00
99.60	CROMER KNOLL GROUP	Horizon_8	Horizon_8_Map		Layer_7	Deposition	Map_Layer_7_Facies	1	10.00
125.00	MIME FORMATION	Horizon_9	Horizon_9_Map		Layer_8	Deposition	Map_Layer_8_Facies	1	10.00
130.00	Erosion_31_Top								
145.00	DRALPNE FORMATION	Horizon_10	Horizon_10_Map	ErosionMapID2_145	Erosion_31	Erosion			10.00
168.00	BRENT GROUP	Horizon_11	Horizon_11_Map		Layer_10	Deposition	Map_Layer_10_Facies	1	10.00

Figure 5.5: Age assignment table.

### 5.3.4 Facies Definition

The Draupne Formation is the main source rock for oil and gas with Type II kerogen. The kinetic model used is the Burnham (1989) \_TII. A TOC value of 6% and HI value of 600 [mg HC/g TOC] were used (Fig 5.6).

Name	Color	Lithology Value	Kinetics	TOC Mode	TOC Value [%]	TOC Map	HI Mode	HI Value [mgHC/gTOC]	HI Map	Petroleum System Elements
Nordaland GP		Sandstone (clay rich)								Overburden Rock
Utsira FM		Sandstone (clay poor)								Overburden Rock
Hordaland GP		Sandstone (clay rich)								Overburden Rock
Balder FM		Shale (organic lean, typical)								Overburden Rock
Lista FM		Shale (typical)								Seal Rock
Sele FM		Shale (organic lean, typical)								Seal Rock
Shetland GP		Limestone (chalk, typical)								Reservoir Rock
Cromer Knoll GP		Siltstone (organic rich, typical)								Seal Rock
Mime FM		Limestone (shaly)								Reservoir Rock
Draupne FM		Shale (organic rich, typical)	Burnham(1989)_TII	Value	6.00		Value	600.00		Source Rock
Brent GP		Sandstone (clay rich)								Reservoir Rock

Figure 5.6: Facies definition table showing lithologies, source rock properties and petroleum system elements.

### 5.3.5 Boundary conditions

Boundary conditions define the basic energetic conditions for the temperature and burial history of the source rock and, consequently, for the maturation of organic matter through

time. Boundary conditions prepare the model for simulation. The boundary conditions used in this study are Paleo Water Depth, Sediment Water Interface Temperature (SWIT), and Heat Flow (HF). The heat flow trend of Schroeder and Sylta (1993) has been used for the modelling. The highest heat flow, is 83 mW/m<sup>2</sup> of the late Jurassic rifting period (Figure 5.10). In the North Sea Paleo heat flow values are varied through time that reflects varying tectonic regimes. The sediment water interface temperature values are based on the global mean surface temperatures of Wygrala, (1989). The sediment water interface temperature was automatically assigned in Petromod by defining the continent (Northern Europe) hemisphere and latitude 62 N (Figure 5.8). The paleo water depth trend of Kjennerud et al. (2001) has been used (Figure 5.7).

Water Depth / Paleo Depth					
<input checked="" type="checkbox"/> Enable					
<input type="checkbox"/> <input checked="" type="checkbox"/>					
Age from [Ma]	Reference	Layer	Mode	Depth [m]	Depth map
0.00	Water depth		Value	181	
25.00	Water depth		Value	110	
35.00	Water depth		Value	130	
55.00	Water depth		Value	180	
100.00	Water depth		Value	190	
120.00	Water depth		Value	200	
140.00	Water depth		Value	200	
160.00	Water depth		Value	0	

Figure 5.7: Paleo water depth values of the North Sea based on (Kjennerud et al., 2001)

SWIT			
<input checked="" type="checkbox"/> Enable			
<input type="checkbox"/>	<input checked="" type="checkbox"/>		
Age from [Ma]	Mode	Value [°C]	Map
0.00	Value	5.00	<input type="button" value="→"/>
25.00	Value	15.47	<input type="button" value="→"/>
35.00	Value	17.00	<input type="button" value="→"/>
55.00	Value	17.44	<input type="button" value="→"/>
100.00	Value	22.00	<input type="button" value="→"/>
120.00	Value	22.00	<input type="button" value="→"/>
140.00	Value	20.38	<input type="button" value="→"/>
160.00	Value	21.41	<input type="button" value="→"/>
			<input type="button" value="→"/>

Figure 5.8: Sediment water interface temperature values (based on Wygrala 1989)

Heatflow			
<input checked="" type="checkbox"/> Enable			
<input type="checkbox"/> <input checked="" type="checkbox"/>			
Age from [Ma]	Mode	Value [mW/m <sup>2</sup> ]	Map
0.00	Value	65.49	
32.00	Value	65.50	
38.00	Value	65.51	
44.00	Value	65.52	
50.00	Value	65.54	
56.00	Value	65.57	
62.00	Value	65.62	
68.00	Value	65.69	
74.00	Value	65.79	
80.00	Value	65.96	
86.00	Value	66.20	
92.00	Value	66.56	
98.00	Value	67.10	
104.00	Value	67.92	
110.00	Value	69.15	
116.00	Value	63.00	
123.00	Value	66.00	
130.00	Value	70.00	
137.00	Value	76.00	
145.00	Value	83.00	
147.00	Value	81.00	
149.00	Value	80.00	
151.00	Value	78.00	
153.00	Value	76.00	
155.00	Value	74.00	
157.00	Value	71.00	
159.00	Value	69.00	
161.00	Value	67.00	
163.00	Value	65.00	
165.00	Value	63.00	

Figure 5.9: Heat flow values based on(Schroeder and Sylta, 1993)



### **5.3.6 Simulation**

Simulation is the last step in building a 2D model in the PetroBuilder. 2D simulation has various options, which include output ages, Petro Charge Layer, and thickness uncertainties. The simulator uses only the output ages and overlay classes that have been set in the output ages table. An overlay class comprises all related overlays. The user can decide whether to calculate individual overlays in the overlay classes. It is advisable to add output ages because expulsion and migration of petroleum may be restricted to a limited and comparably short period of time. By defining additional output ages, events can be further subdivided to display the expulsion or migration histories in more detail. Simulating a model by using flow path migration, the simulator assumes 100% upward expulsion of hydrocarbons. The Petro Charge Layer enables downward expulsion for source rocks. In this model the hybrid migration method, which combines both Darcy flow and flow path methods, has been used. Structural depth uncertainties are important in petroleum system modelling, I.e. seismic interpretation is often ambiguous due to velocity uncertainties, the layer thickness is often uncertain.

### **5.3.7 Calibration**

For the model to be accurate calibration has to be performed. In this study calibration has been performed using vitrinite reflectance and the bottom hole temperature from two selected wells (35/11-5 and 35/11-3S). The vitrinite reflectance data were taken from the geochemical information of each well from the NPD factpages website. As seen below there is a good correlation between the modelled and measured vitrinite reflectance values from the wells (Figure 5.12). There is a good match between measured and modelled bottom hole and surface temperatures for both modelled wells (Figure 5.11). The modelled bottom hole temperatures of wells 35/11-5 and 35/11-3s are 130°C and 140°C respectively. There is a good agreement with the measured values of 134°C and 144°C respectively.

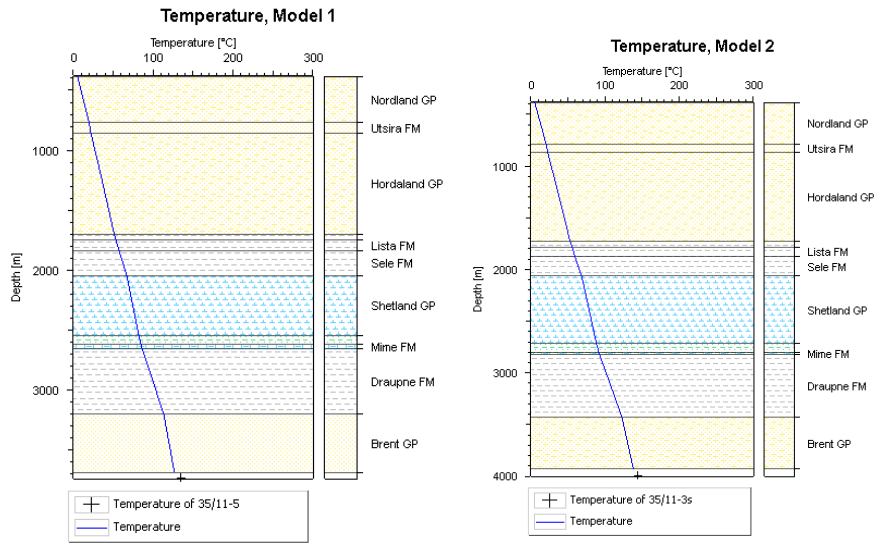


Figure 5.10: Model calibration by comparison of measured and modelled temperature for wells 35/11-5 and 35/11-3s.

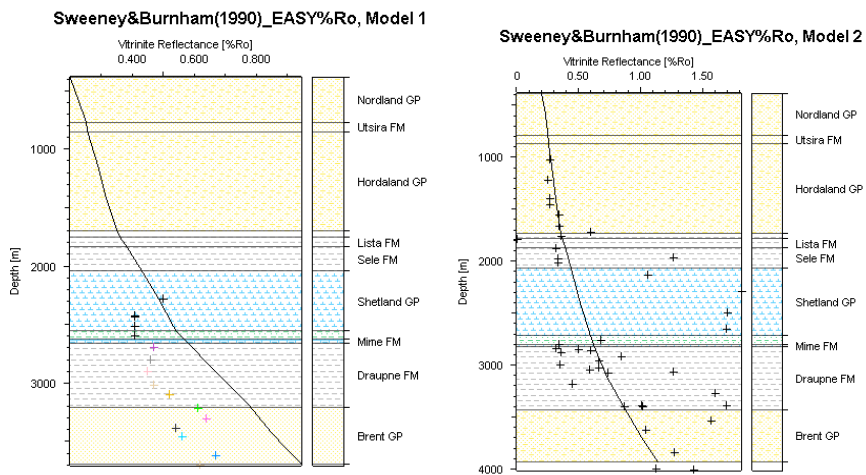


Figure 5.11: Model calibration by comparison of measured and modelled vitrinite reflectance for wells 35/11-5 and 35/11-3s.

## **CHAPTER 6: RESULTS**

### **6.1 Burial history**

Burial history is the subsidence of the basin through geological time. In the northern North Sea the basin started to form during the Permo-Triassic rifting event at about 250 Ma. At the time of rifting the basin experienced variations in subsidence and sediment supply. In the mid Jurassic to late Jurassic, the northern North Sea was characterised by subsidence due to rifting associated with rotational faulting (Fig 6.1). Rapid subsidence of large rotational fault blocks, local uplift of the footwall blocks above the erosional base level, development of submarine relief in the Viking Graben are due to accelerated crustal stretching, as its shown by Lower Cretaceous post-rift sequence and the earlier syn-rift Upper Jurassic(Fig 6.2). During the early Cretaceous the rifting activities ended and the basin was affected by thermal subsidence and sediment loading. The accommodation space required for Tertiary sedimentation was provided by paleo bathymetries at the end of Cretaceous and post rift thermal subsidence following Jurassic rifting. The supply of sediment from the hinterland and continued thermal subsidence from the hinterland played an important role for the deposition of thick sediments during this time (Figs 6.3,6.4,6.5,6.6). During the Tertiary deposition was controlled by several phases of uplift affecting the source areas combined with relative sea level changes and thermal subsidence of the basin. At the end of the Paleocene the sedimentation was interrupted by the deposition of volcanic tuffs comprising the Balder Formation (Fig 6.7). Further subsidence led to a dominance of marine clays in the Eocene and Oligocene periods. The Miocene is represented by a thin sequence of shallow marine sandstones, which indicate a regression and falling sea levels. The western source areas dominated the sediment influx from late Paleocene until the early Miocene. The basin shallowed from relatively deep marine conditions during the late Paleocene to shallow marine and locally fluvial conditions in the early Miocene (Fig 6.8). The sediment influx from west ceased in the early Miocene and most of the mid and late Miocene was characterised by non-deposition (Fig 6.8 and 6.9). The eastern margin continued to uplift and the basement is exposed at the seabed at the present day (Fig 6.9 and 6.10).

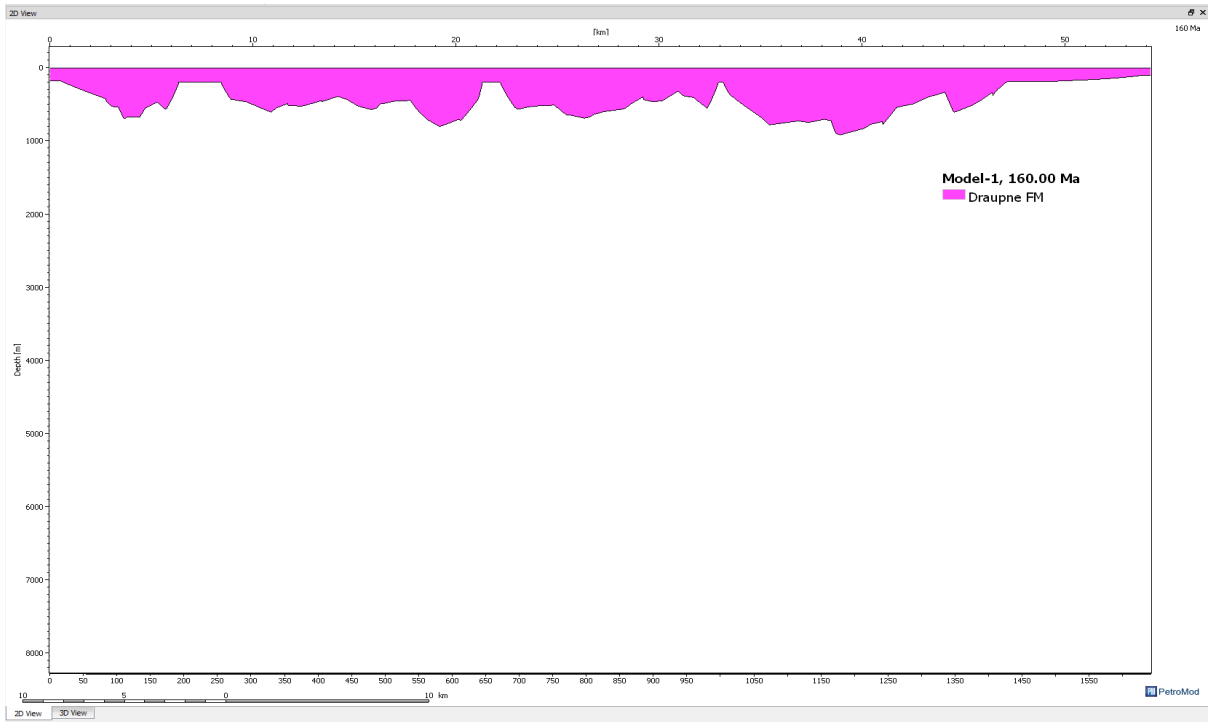


Figure 6.1: Basin development at 160 Ma when the Upper Jurassic (Draupne FM) sediments were deposited for the modelled line NVGTI-92-109.

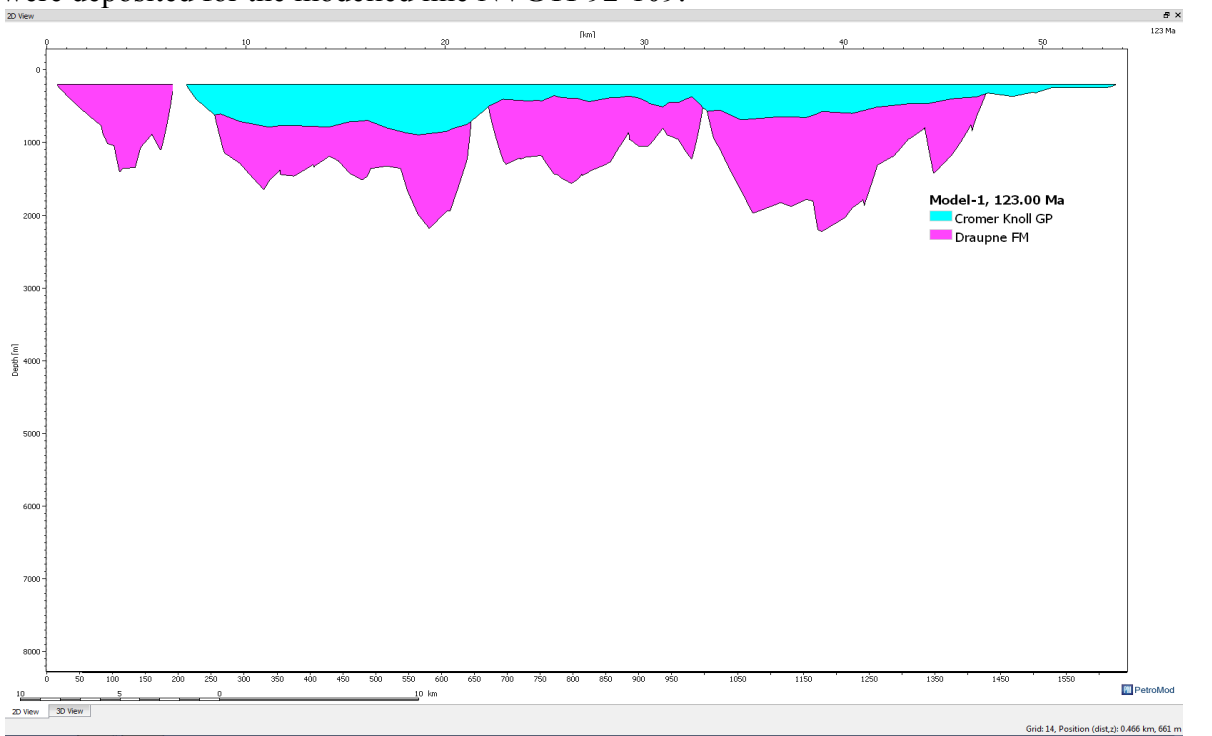


Figure 6.2: Basin development at 123 Ma when Lower Cretaceous sediments (Cromer Knoll GP) were deposited of the modelled line NVGTI-92-109.

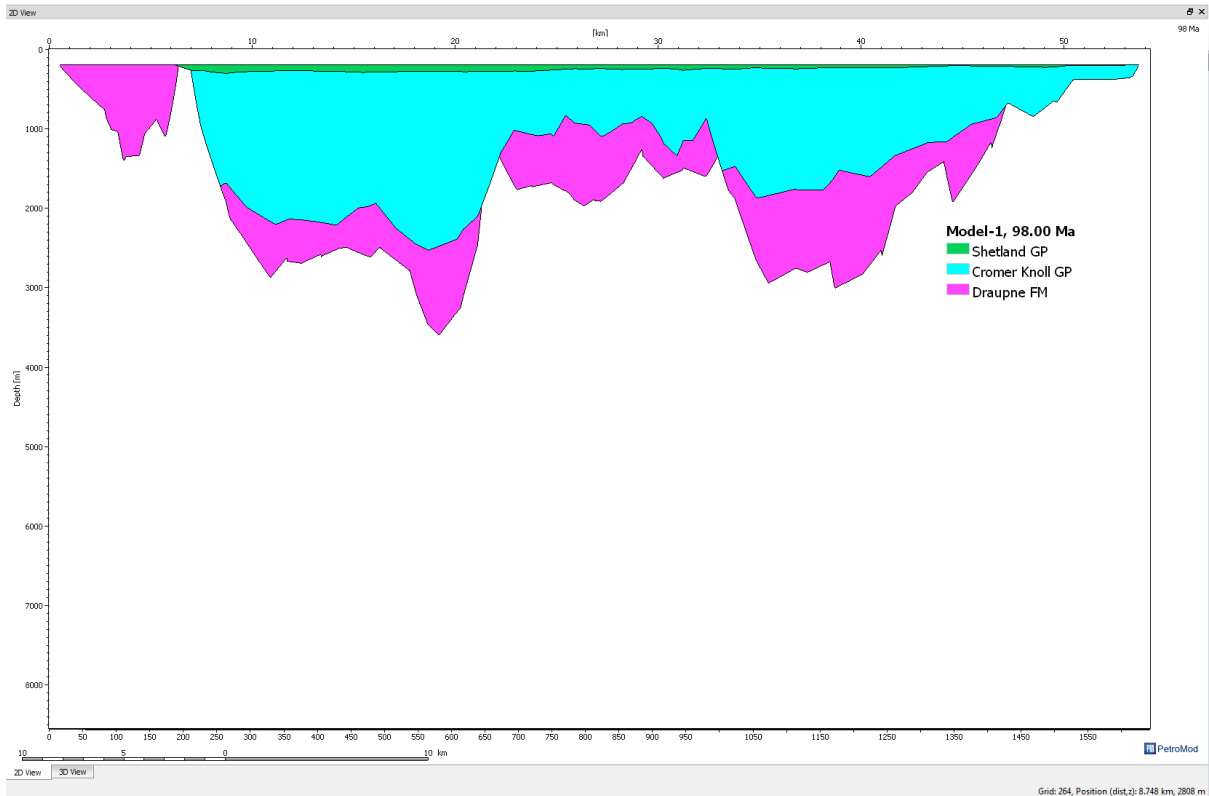


Figure 6.3: Basin development at 98 Ma at the start of deposition of Upper Cretaceous sediments (Shetland Gp) and the end of deposition of Cromer Knoll Gp of the modelled line NVGTI-92-109.

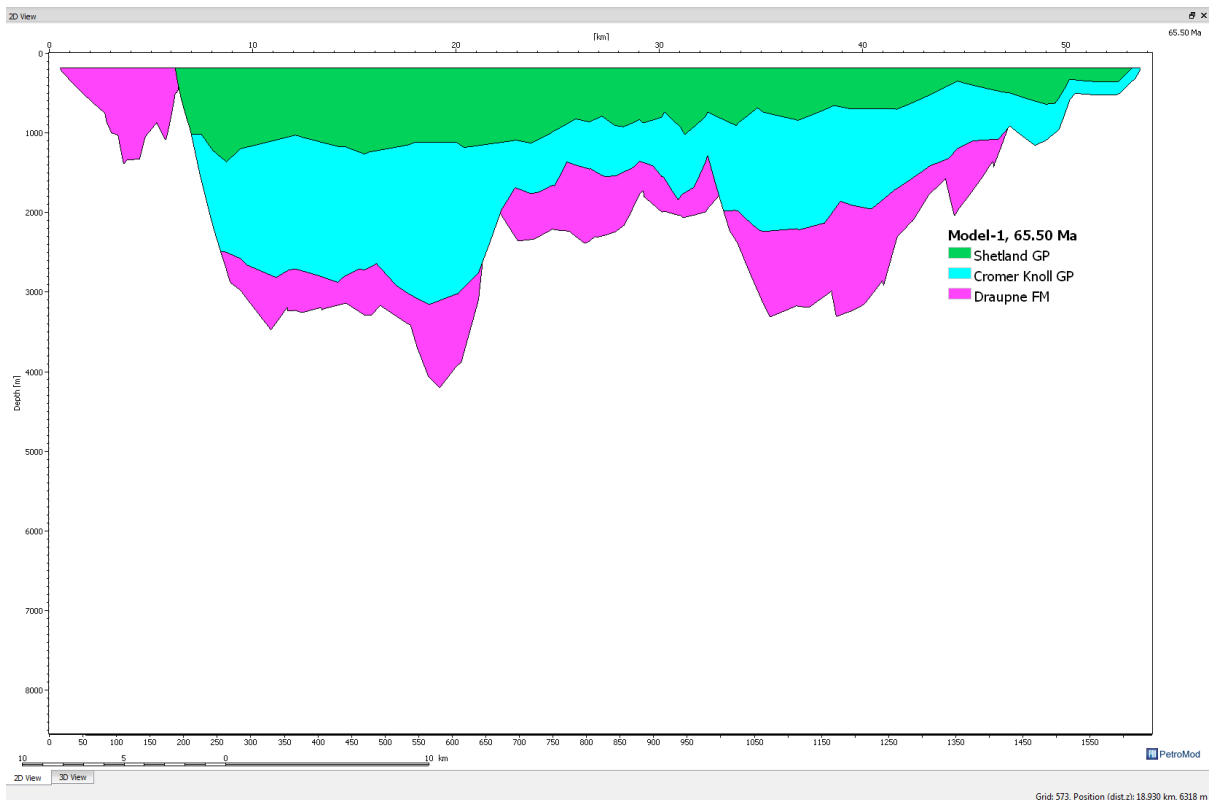


Figure 6.4: Basin development at 65 Ma after Upper Cretaceous sediments (Shetland Gp) were deposited of the modelled line NVGTI-92-109.

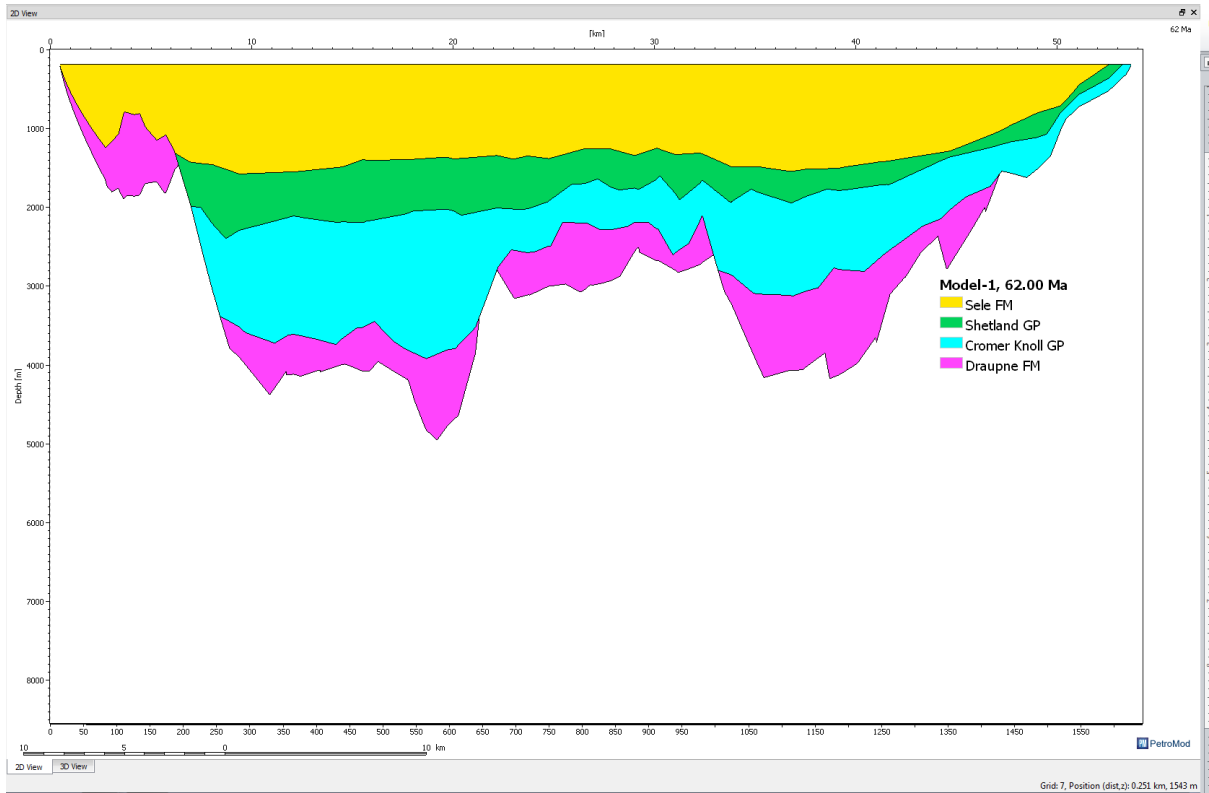


Figure 6.5: Basin development at 62 Ma when Lower Paleocene sediments (Sele FM) were deposited of the modelled line NVGTI-92-109.

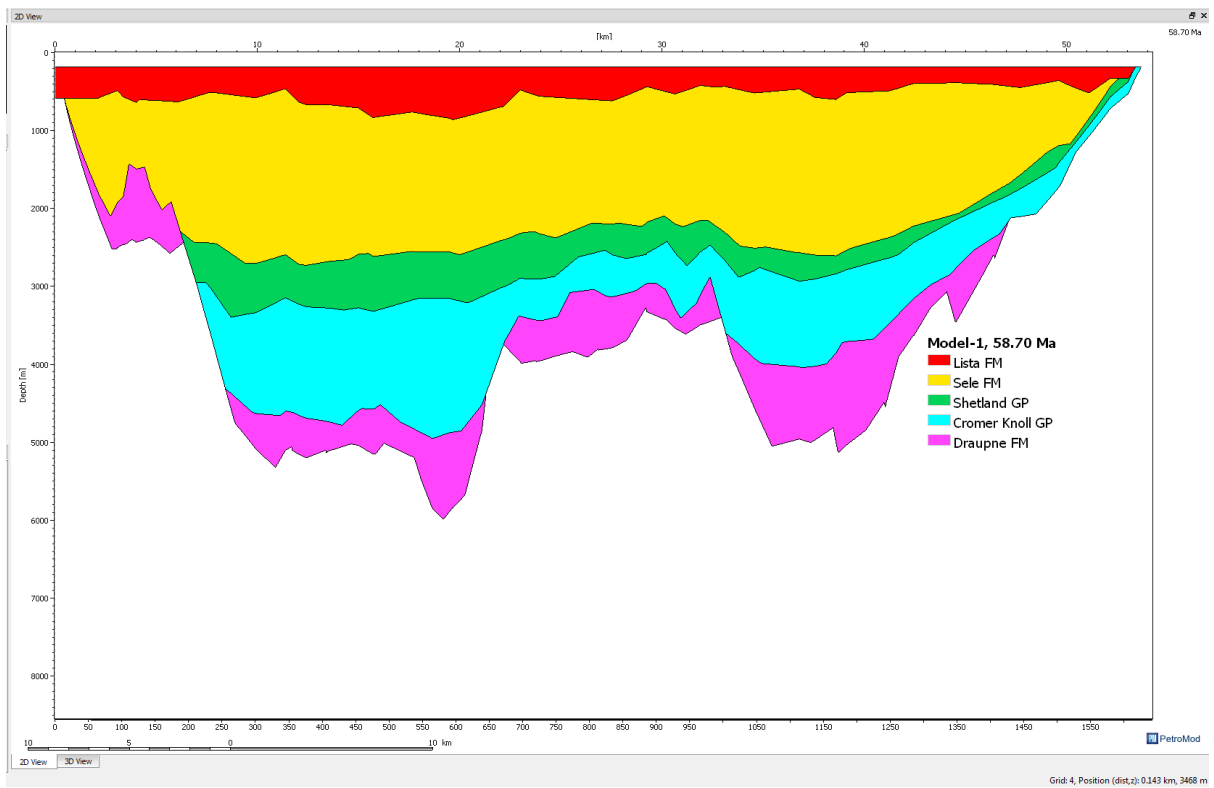


Figure 6.6: Basin development at 58.70 Ma when Middle Paleocene sediments (Lista FM) were deposited of the modelled line NVGTI-92-109.

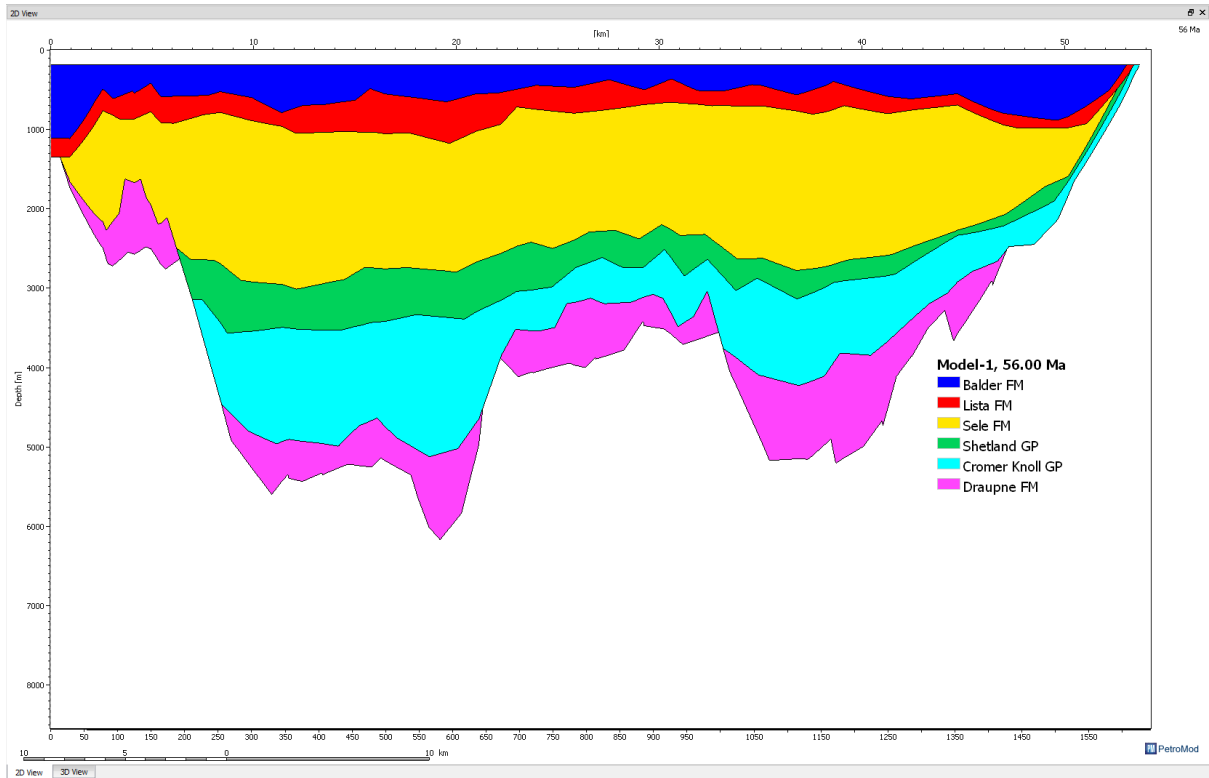


Figure 6.7: Basin development at 56 Ma when Upper Paleocene sediments (Balder FM) were deposited of the modelled line NVGTI-92-109.

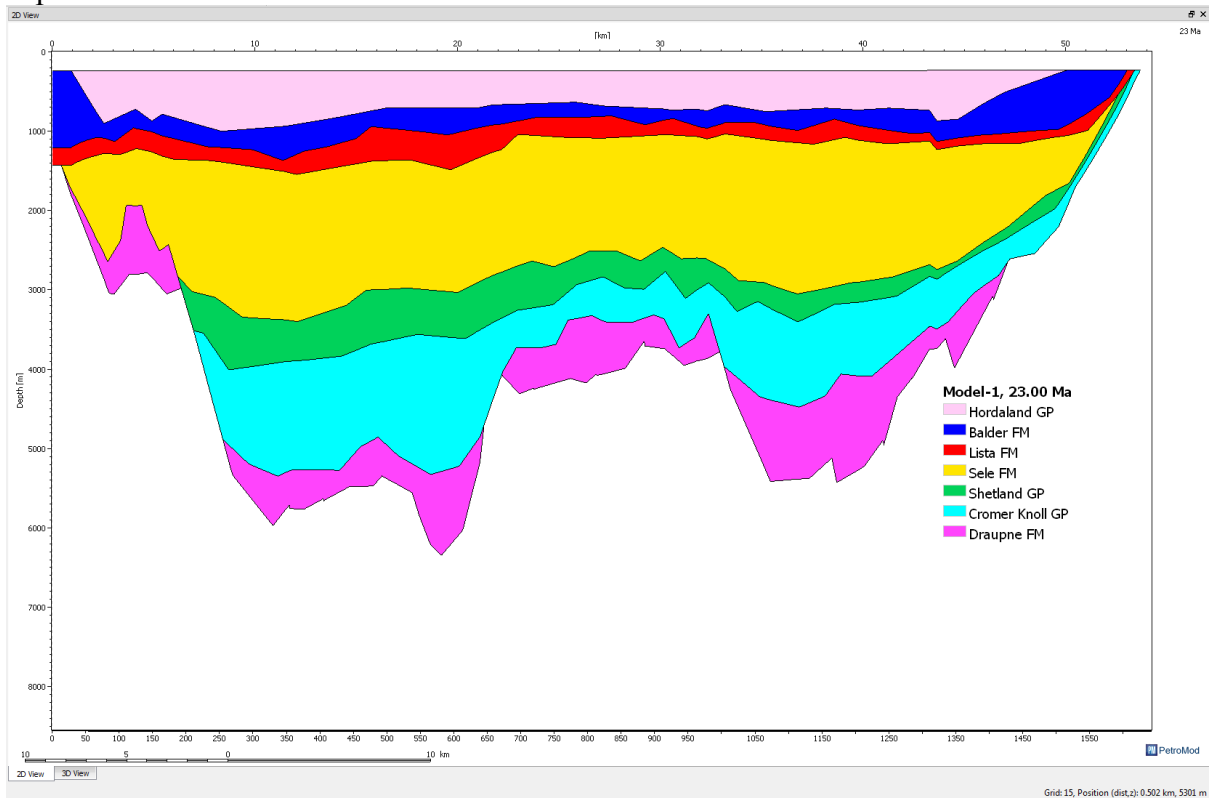


Figure 6.8: Basin development at 23 Ma when Lower Miocene sediments (Hordaland GP) were deposited of the modelled line NVGTI-92-109.

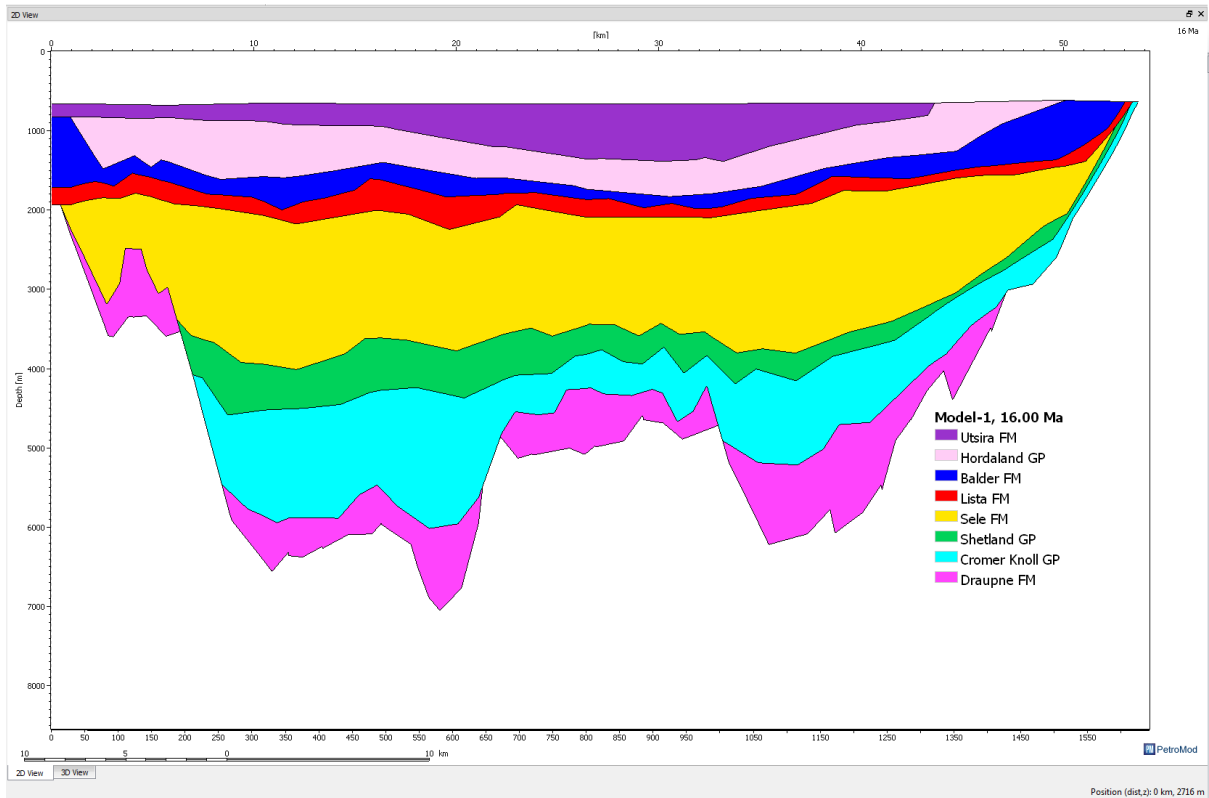


Figure 6.9: Basin development at 16 Ma when Middle Miocene sediments (Utsira FM) were deposited of the modelled line NVGTI-92-109.

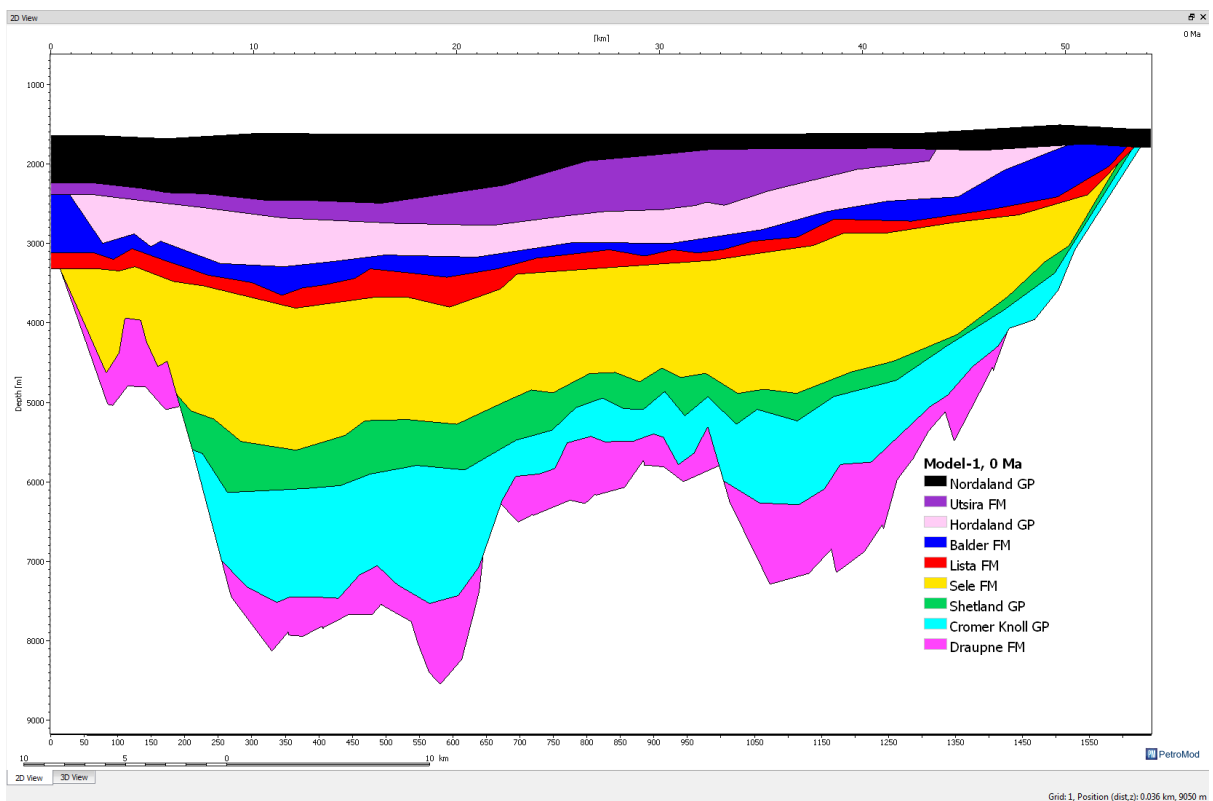


Figure 6.10: Basin development at present day condition of the modelled line NVGTI-92-109.



The burial history of the line NVGTI-92-104 shows the western part of the basin, the most important Jurassic rifting phase took place during the late Jurassic and lasted into the early Cretaceous. During this tectonic episode, major block faulting caused uplift and tilting. At the Sea level the surface is flat (Figs 6.11), and the sea level reached a depth of 200m(6.12). Subsidence rates were comparatively higher between late Jurassic to late Cretaceous (Figs 6.11,6.13). During Cretaceous rifting ceased and was followed by thermal subsidence, the late Cretaceous is dominated by contrasting lithologies. Sedimentation rates were higher between early and late Cretaceous this is shown by the thicknesses of the Cromer Knoll Group (Figs 6.12, 6.13). The basin was buried to a depth of 2800 m98 Ma (Fig. 6.13). During the Paleocene it was the locus of deposition of thick clastic sequences, which now act as the reservoir rocks for several major hydrocarbon accumulations. These deposits, which consist mainly of sandstones interbedded with claystones and siltstones, present deposition at the edge of a large base-of-slope to proximal basin floor fan system, which was sourced from the eastern basin margin (Figs 6.14, 6.15, 6.16, 6.17). The rate of sedimentation increases and the basin was buried to a burial depth of 4900 m (Fig 6.17). In Miocene a deltaic system had developed from the Shetland Platform towards the Norwegian sector of the North Sea, and is represented by the Hordaland Group and Utsira Formation (Figs 6.18, 6.19). Due to major uplift and Quaternary glacial erosion of the Norwegian mainland, thick sequences were deposited into the North Sea during the Neogene. This led to burial of the Jurassic source rocks to depths where hydrocarbons could be generated and the seals were effective, to present day condition (Fig 6.20).



Figure 6.11: Basin development at 160 Ma when the Upper Jurassic (Draupne FM) sediments were deposited of the modelled line NVGTI-92-104.

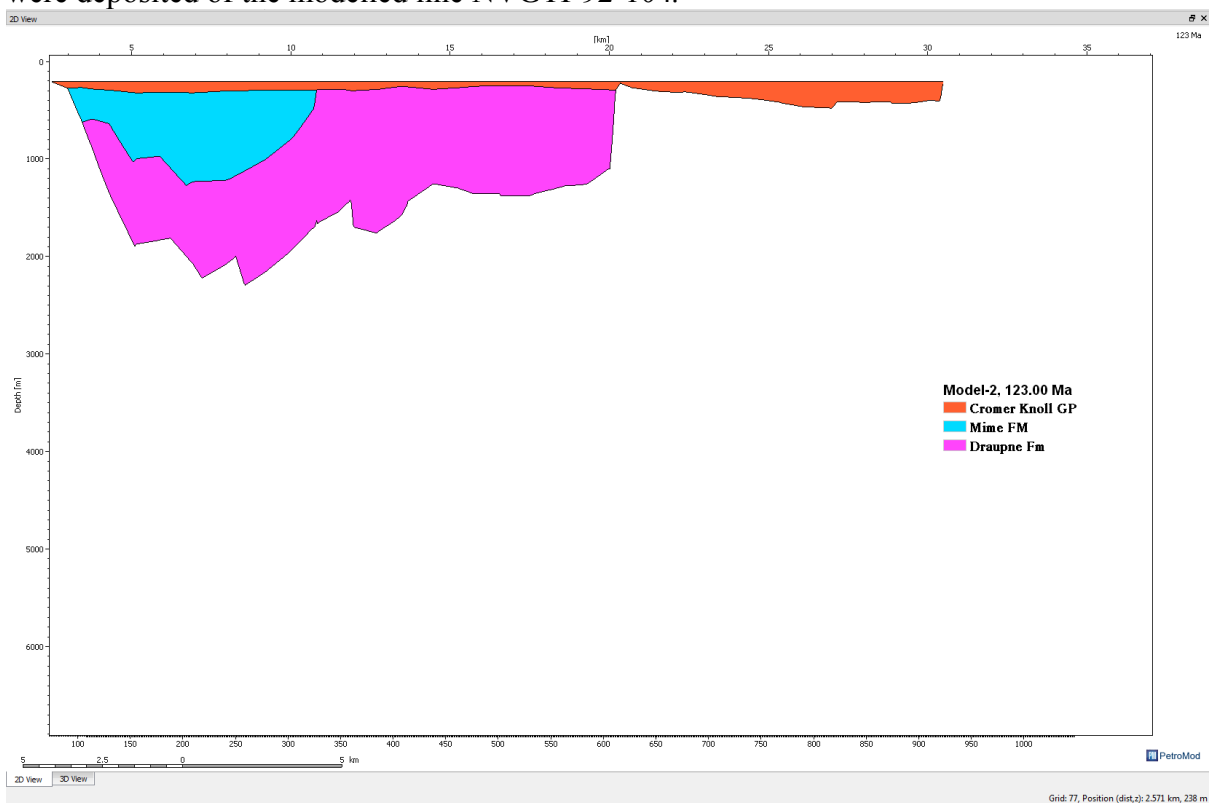


Figure 6.12: Basin development at 123 Ma when Lower Cretaceous sediments (Craumer Knoll GP) were deposited of the modelled line NVGTI-92-104.

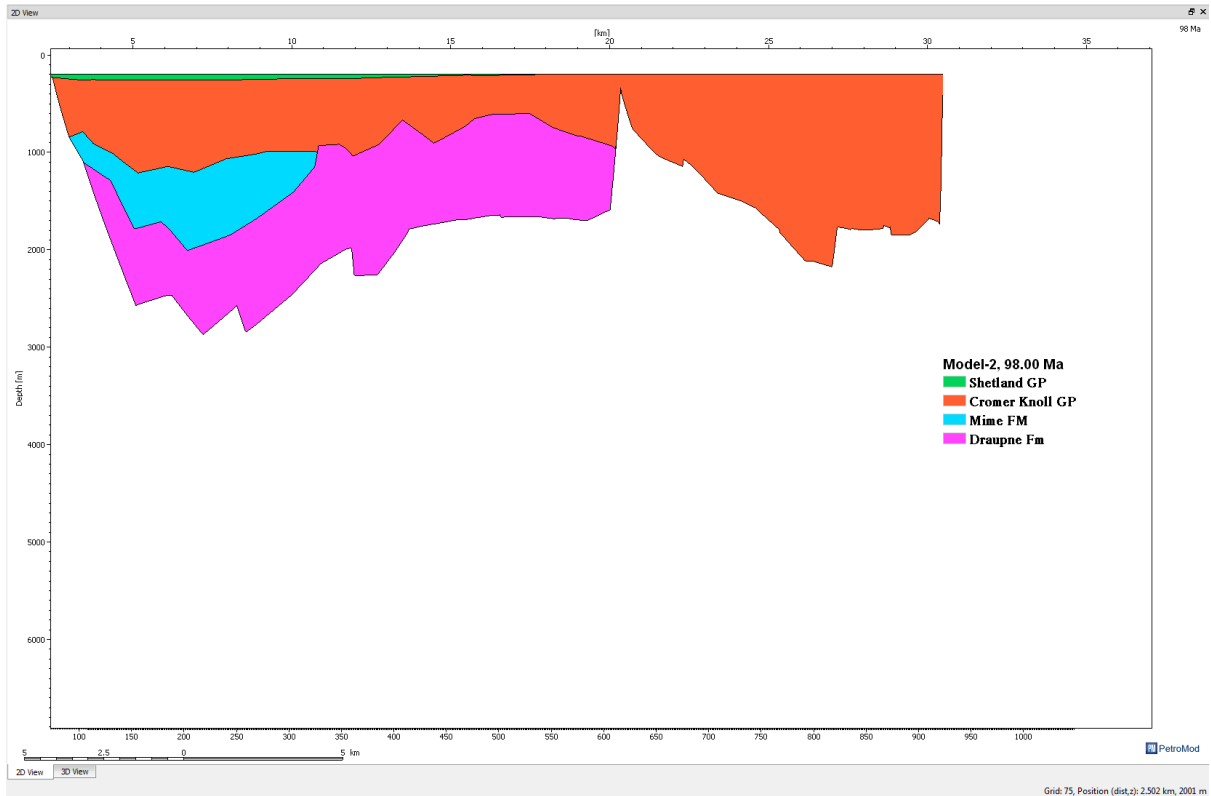


Figure 6.13: Basin development at 98 Ma when Upper Cretaceous sediments (Shetland GP) were deposited of the modelled line NVGTI-92-104.

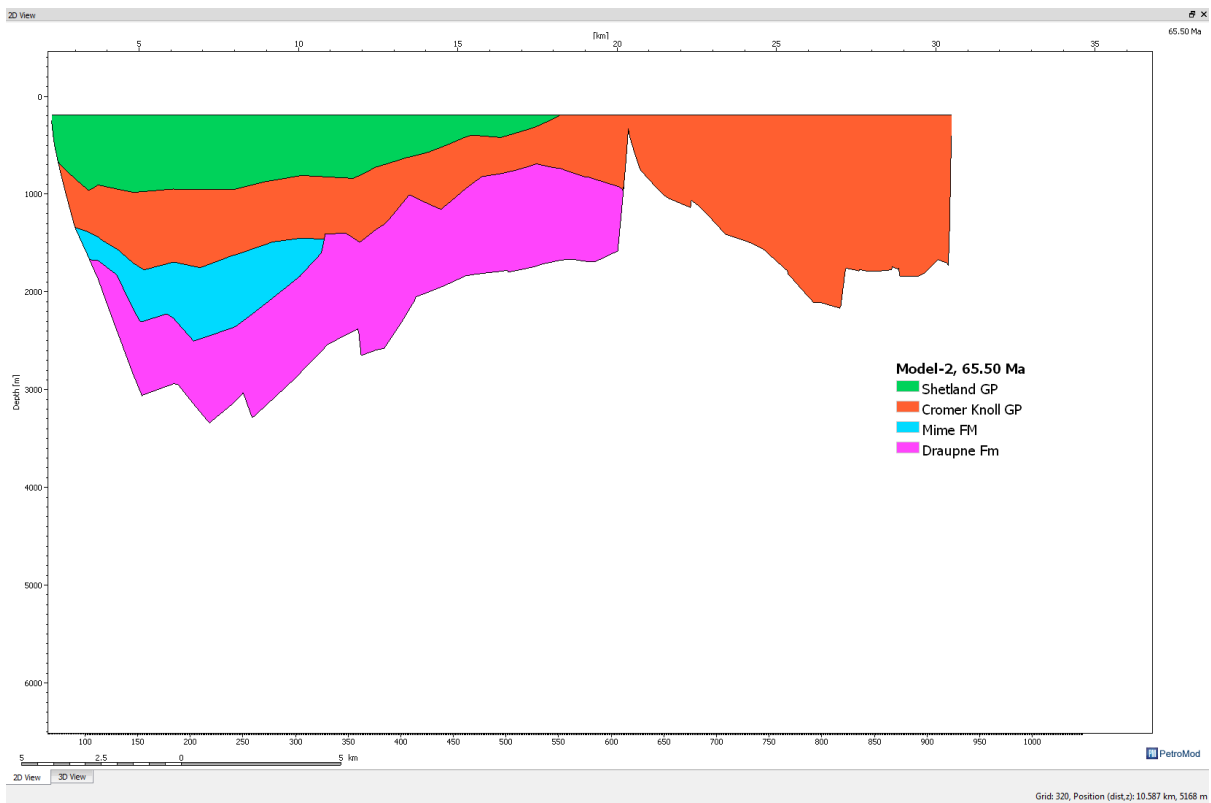


Figure 6.14: Basin development at 65 Ma when Upper Cretaceous sediments (Shetland GP) were deposited of the modelled line NVGTI-92-104.

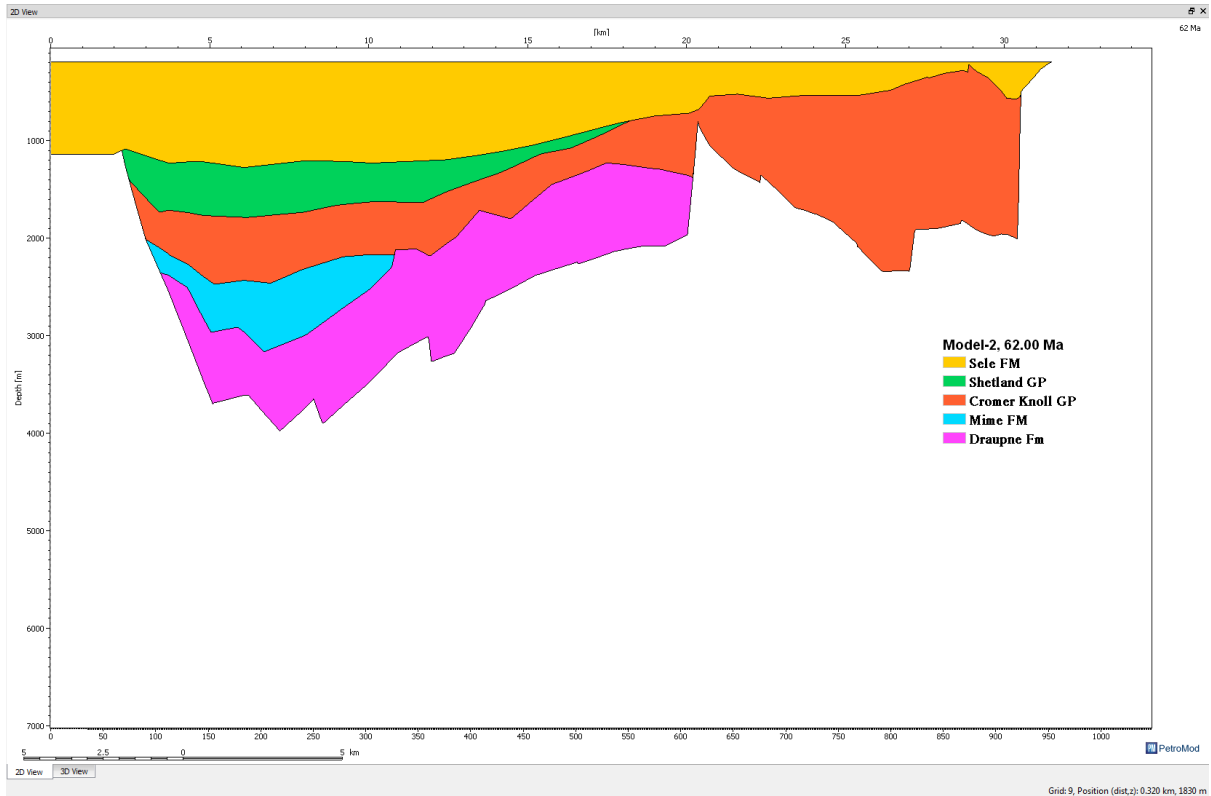


Figure 6.15: Basin development at 62 Ma when Lower Paleocene sediments (Sele FM) were deposited of the modelled line NVGTI-92-104.

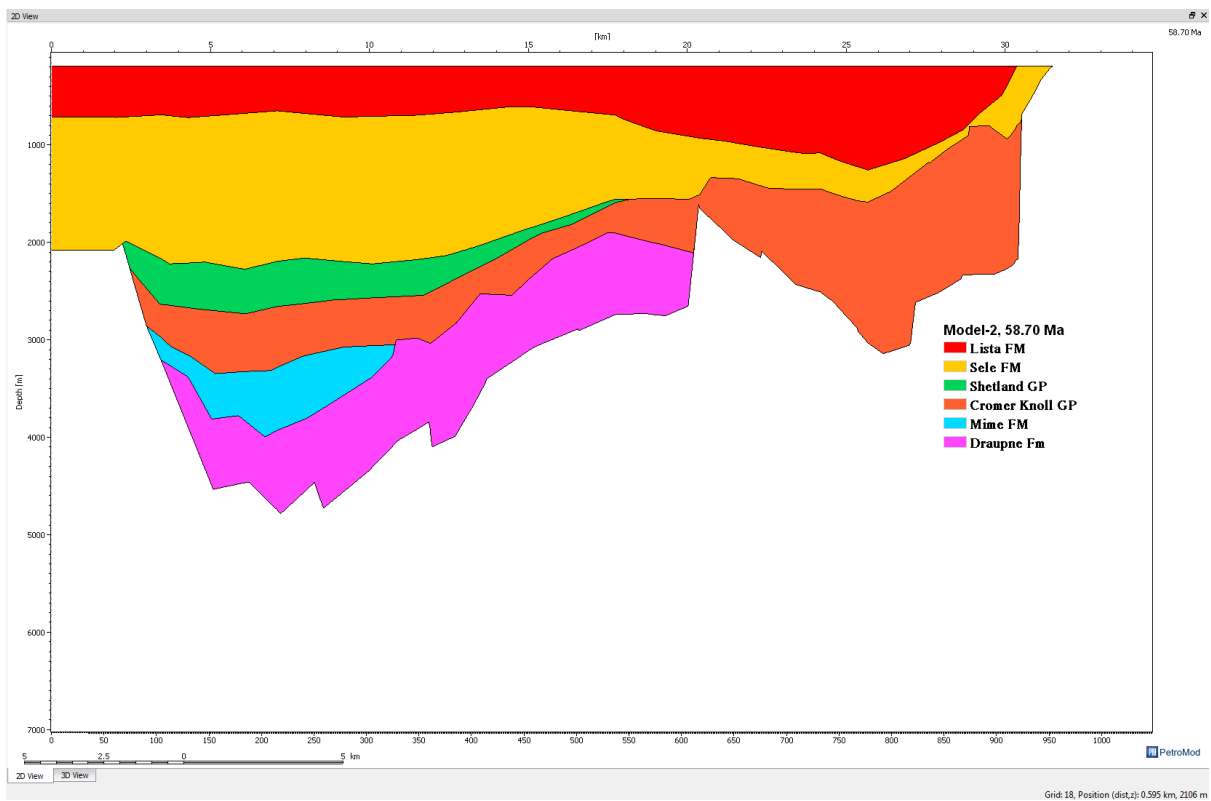


Figure 6.16: Basin development at 58.70 Ma when Middle Paleocene sediments (Lista FM) were deposited of the modelled line NVGTI-92-104.

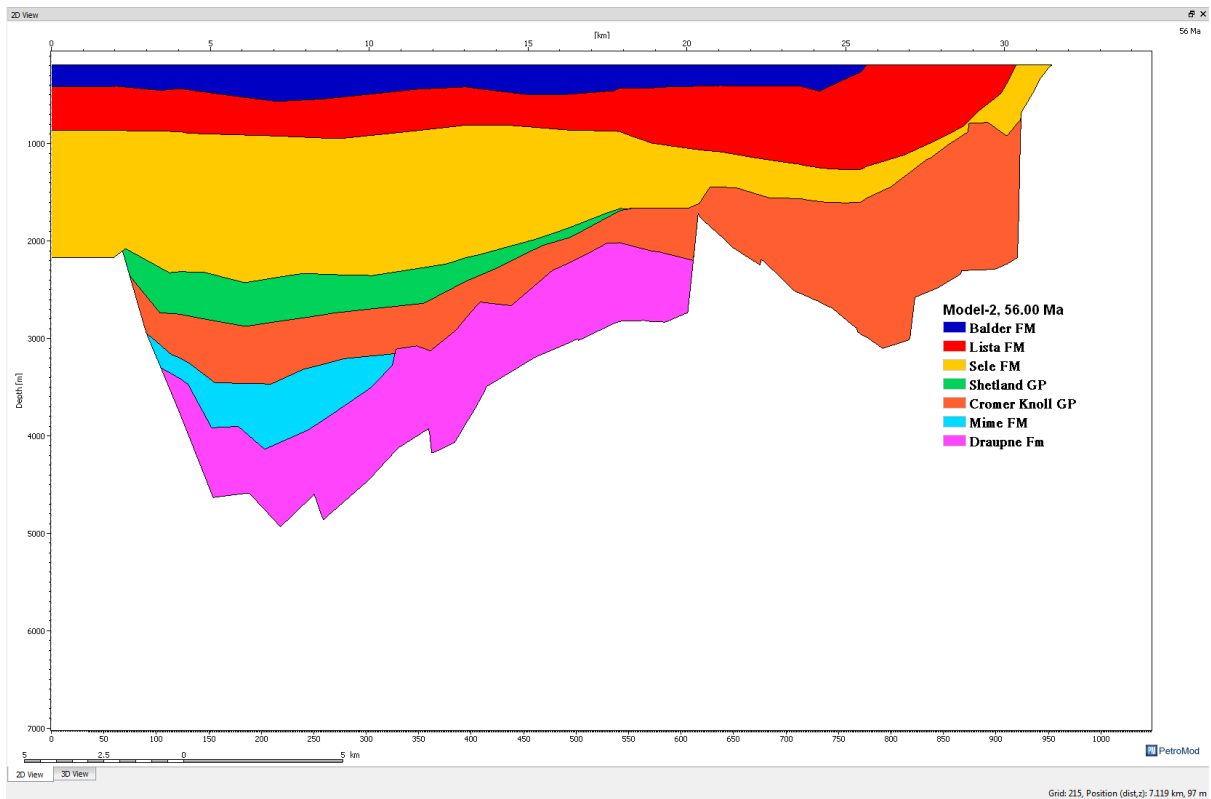


Figure 6.17: Basin development at 56 Ma when Upper Paleocene sediments (Balder FM) were deposited of the modelled line NVGTI-92-104.

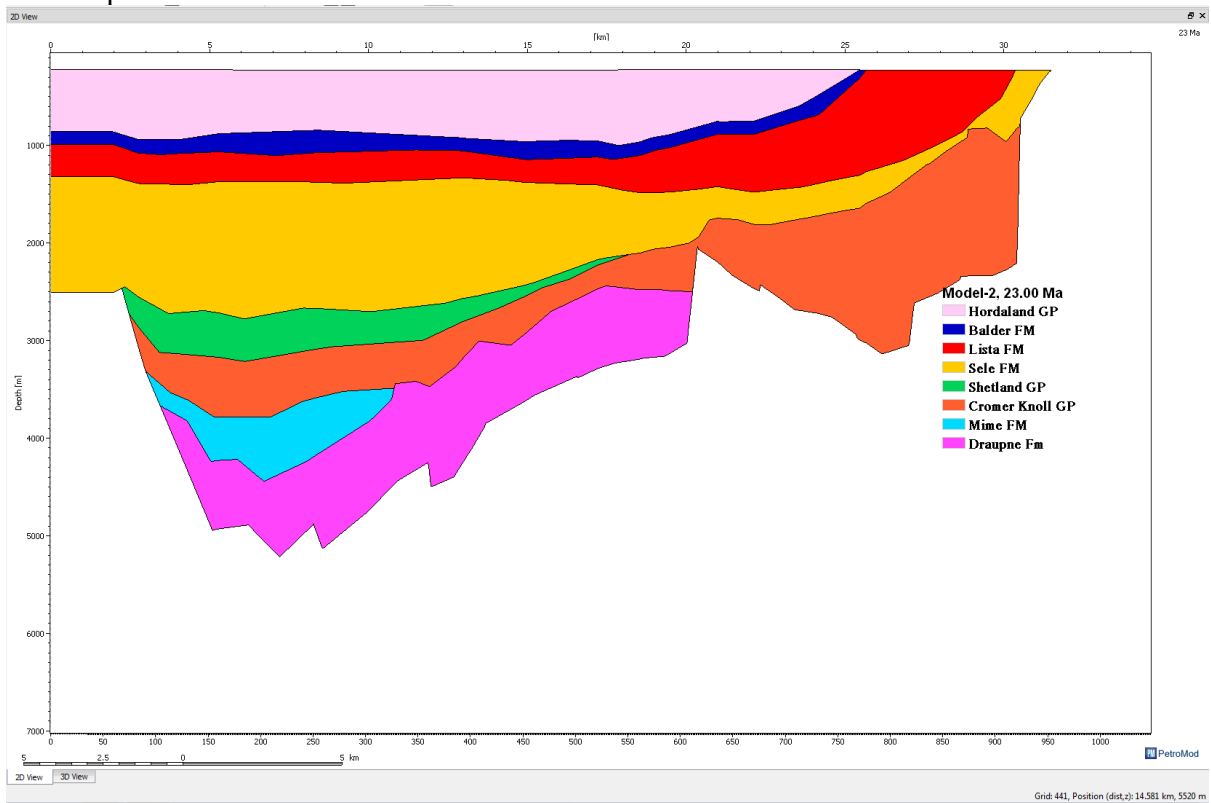


Figure 6.18: Basin development at 23 Ma when Lower Miocene sediments (Hordaland GP) were deposited of the modelled line NVGTI-92-104.

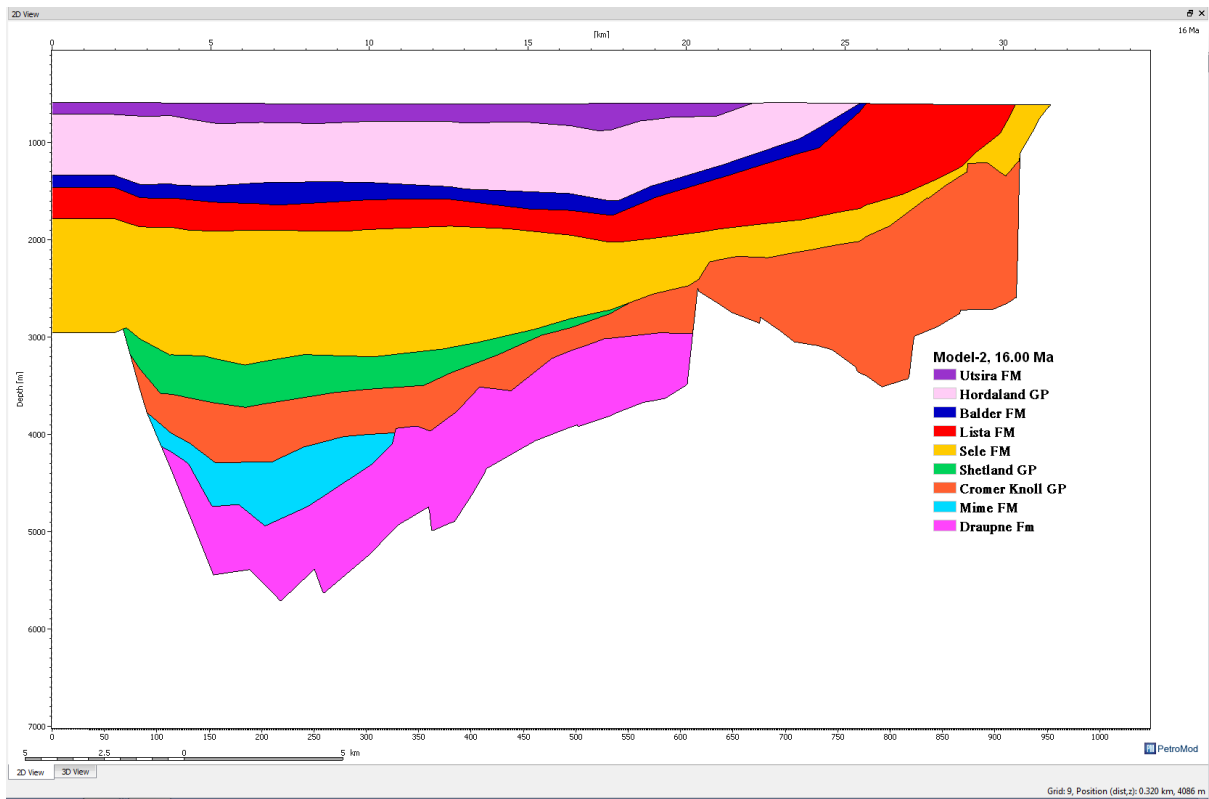


Figure 6.19: Basin development at 16 Ma when Middle Miocene sediments (Utsira FM) were deposited of the modelled line NVGTI-92-104.

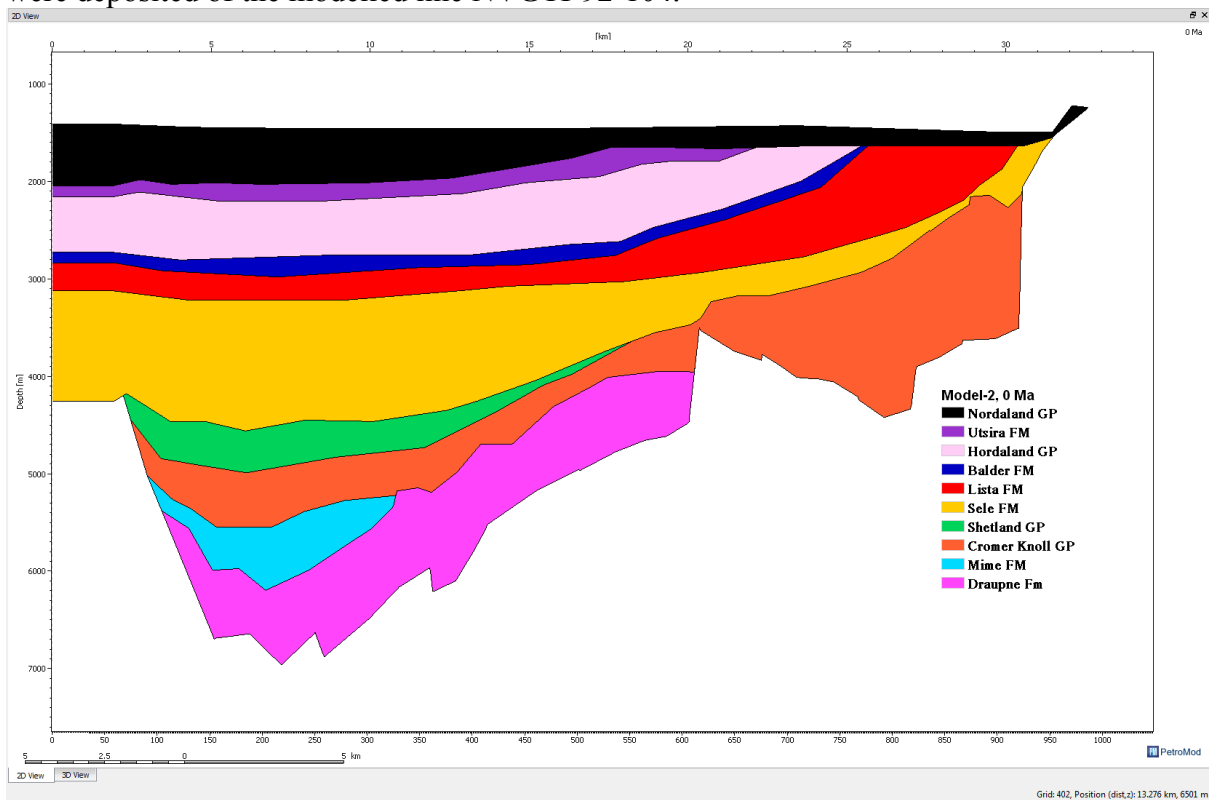


Figure 6.20: Basin development at present day condition of the modelled line NVGT 92-104.

## 6.2 Maturation and Petroleum generation history

The figures in this section show the distribution of maturity and petroleum generation in the Draupne Fm at different time steps of the modelled lines NVGTI-92-109 and NVGTI-92-104. At 155 Ma most areas were immature and these areas had been buried at the depth of 1200m (Fig 6.21 and 6.34). At 151 Ma the deepest buried parts of the source rock were mature enough to initiate the onset of early oil generation (Fig 6.22 and 6.35). At 149 Ma there was onset of main oil generation on the western part of the cross section NVGTI-92-109 when this part was buried at a depth of 2000m (Fig 6.23), while there was no main oil generation in the cross-section NVGTI-92-104 which covers the eastern part of the study area (Fig 6.36). At 145 Ma the main oil generation occurred in both the eastern and western parts of the line NVGTI-92-109 (Fig 6.24) and in the western part of the line NVGTI-92-104 (Fig 6.37). At 140 Ma there was onset of late oil generation of the line NVGTI-92-109 (Fig 6.25), but without onset of late oil generation in the cross-section NVGTI-92-104 (Fig 6.38). At 104 Ma more late oil had been generated in the line NVGTI-92-109 and the basin was buried at a depth of 3400m (Fig 6.26) but still there was no late oil generation in NVGTI-92-104 (Fig 6.39). At 100 Ma the source rock was mature enough for wet gas generation in the western part of the line NVGTI-92-109 and the basin was buried to a depth of 3800m (Fig 6.27), there was no wet gas generation, but only the onset of late oil generation at the burial depth of 2800m of the line NVGTI-92-104 (Fig 6.40). At 86 Ma more wet gas was generated at a burial depth of 4000m of the line NVGTI-92-109 (Fig 6.28), and more late oil generation at a depth of 3000m of the line NVGTI-92-104 (Fig 6.41). At 74 Ma, with increasing burial depth there was more generation of wet gas at the depth of 4200 m of the line NVGTI-92-109 (Fig 6.29), and late oil generation at the depth of 3200 m of the line NVGTI-92-104 (Fig 6.42). At 65.50 Ma there was onset of dry gas generation at the depth of 4200 m of the line NVGTI-92-109 (Fig 6.30), and the onset of wet gas generation at the depth of 3200 m of the line NVGTI-92-104 (Fig 6.43). At 58.70 Ma more dry gas was formed with increasing depth of 5800 m of the line NVGTI-92-109 (Fig 6.31), and more wet gas at the depth of 4800 m of the line NVGTI-92-104 (Fig 6.44). At 50 Ma the source rock started to be overmature at the depth of 6200 m online NVGTI-92-109 (Fig 6.32), and increase of dry and wet gas generation at the depth of 5000 m of the line NVGTI-92-104 (Fig 6.45). At present time large part of the area is still generating gas as well as oil generation (Fig 6.33 and 6.46).

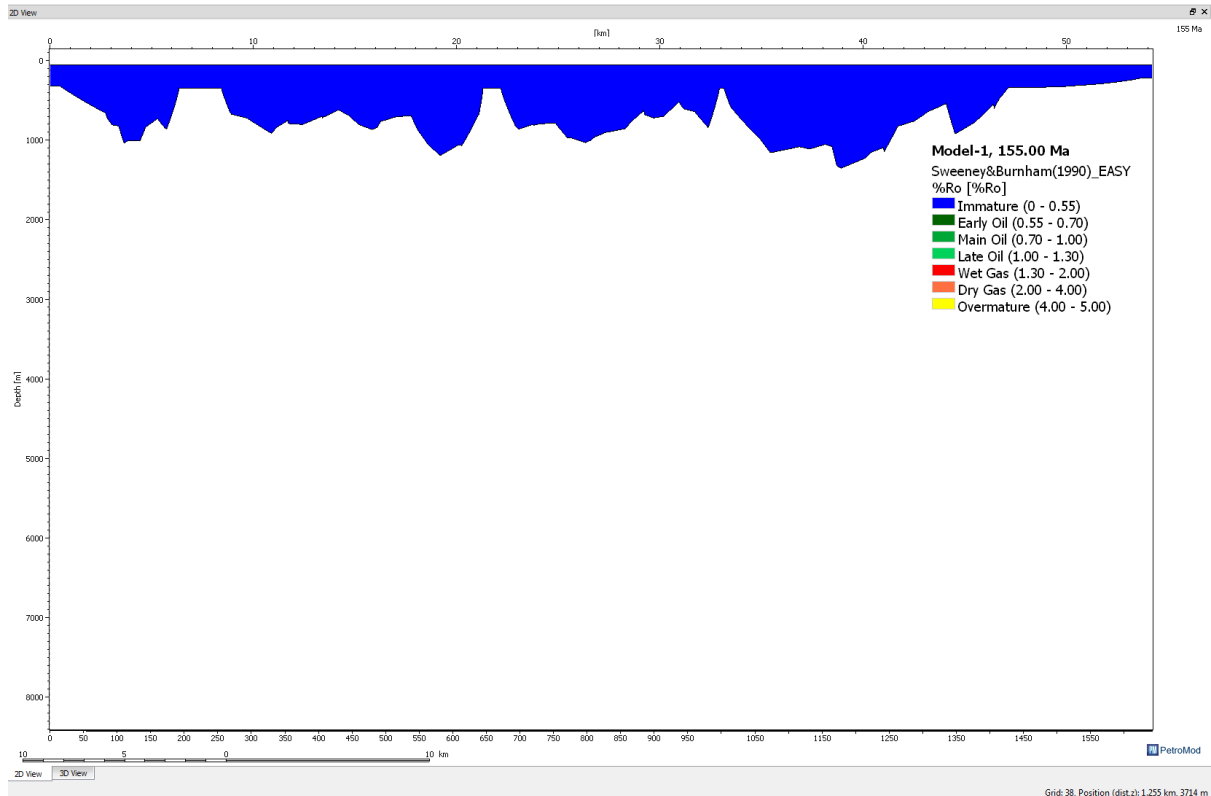


Figure 6.21: Maturity development of the Draupne FM at 155 Ma on the modelled line NVGTI-92-109.

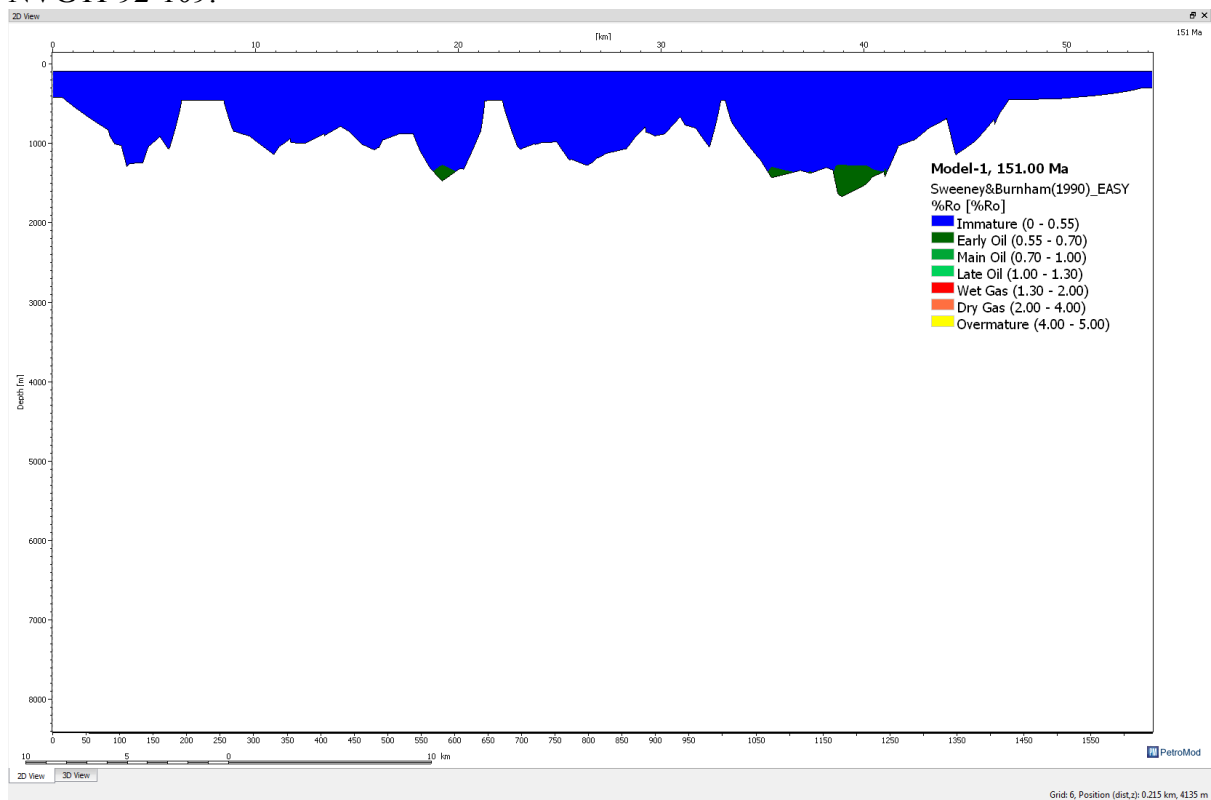


Figure 6.22: Maturity development of the Draupne FM at 151 Ma on the modelled line NVGTI-92-109.



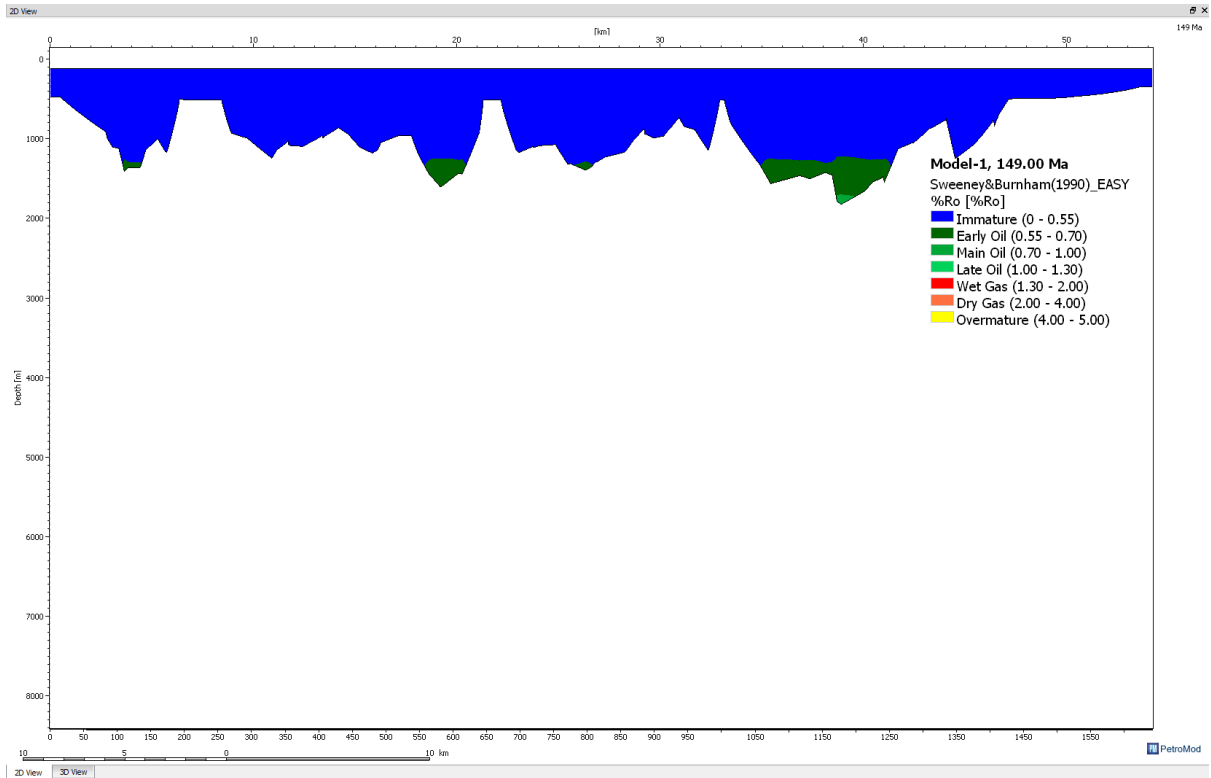


Figure 6.23: Maturity development of the Draupne FM at 149 Ma on the modelled line NVGTI-92-109.

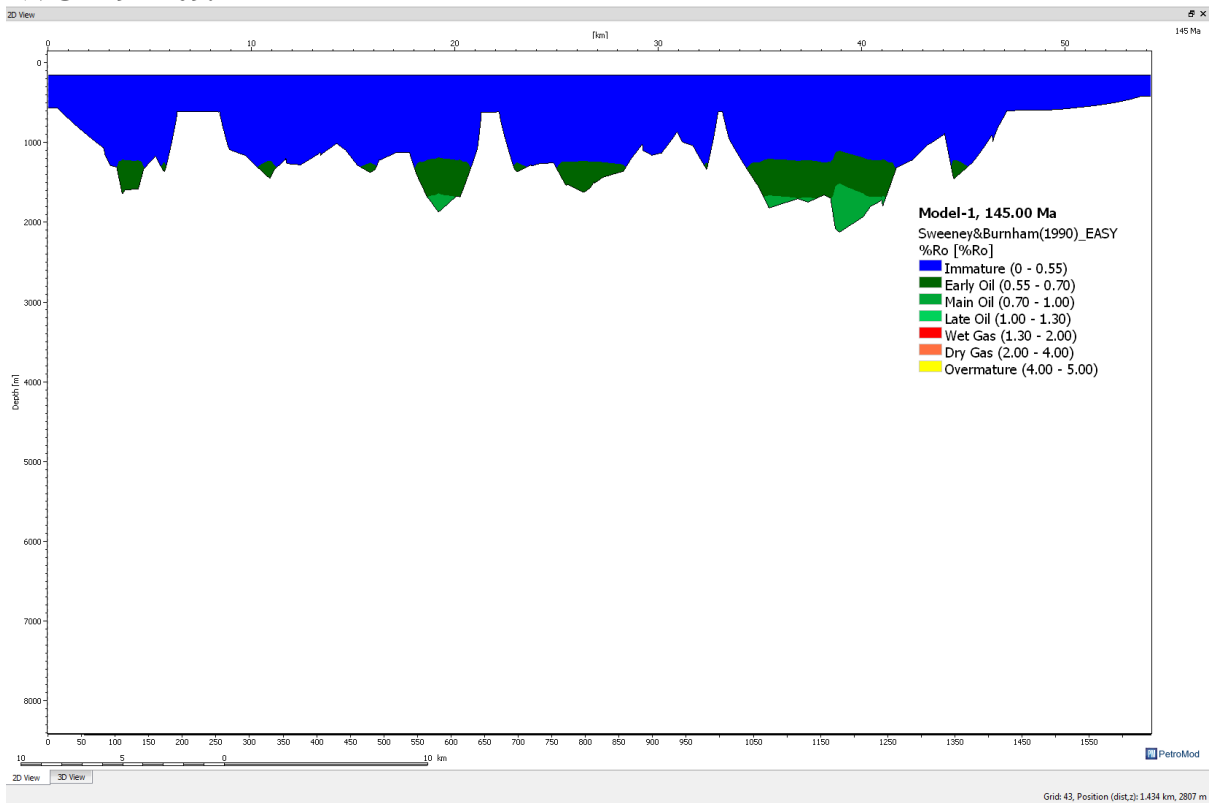


Figure 6.24: Maturity development of the Draupne FM at 145 Ma on the modelled line NVGTI-92-109.

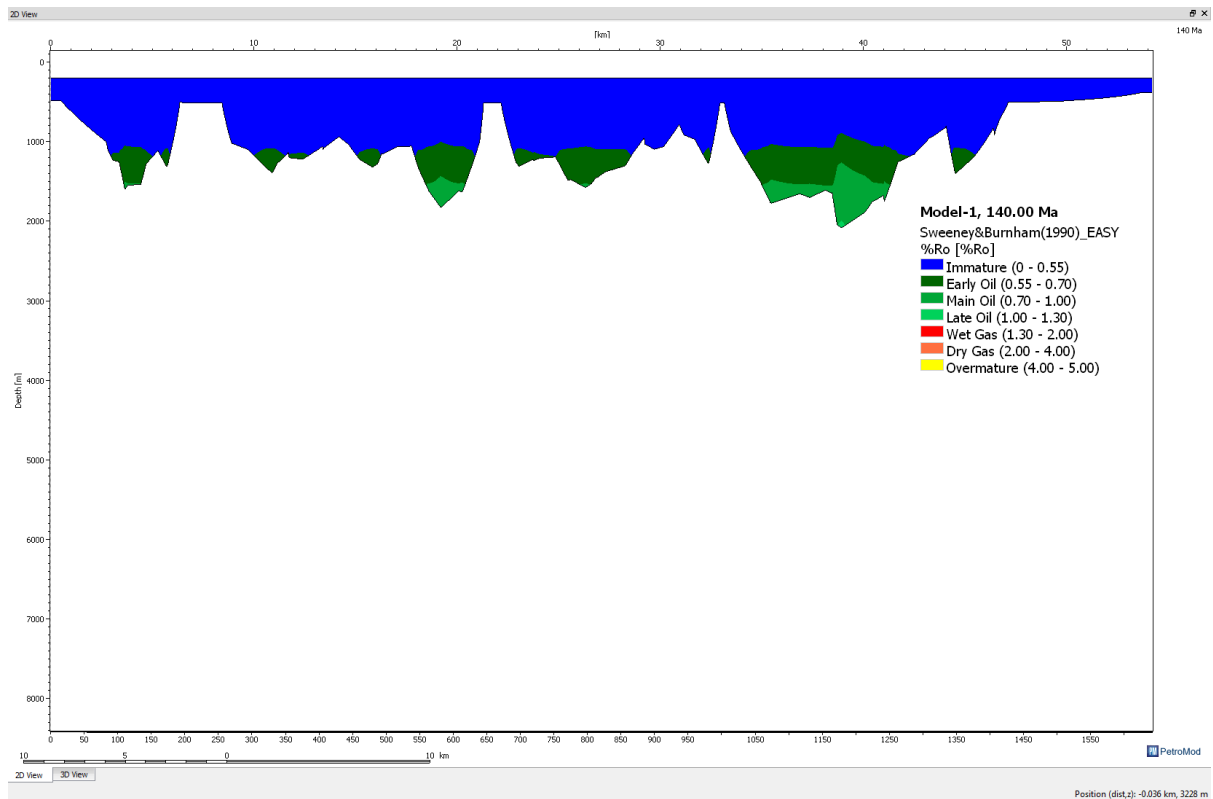


Figure 6.25: Maturity development of the Draupne FM at 140 Ma on the modelled line NVGTI-92-109.

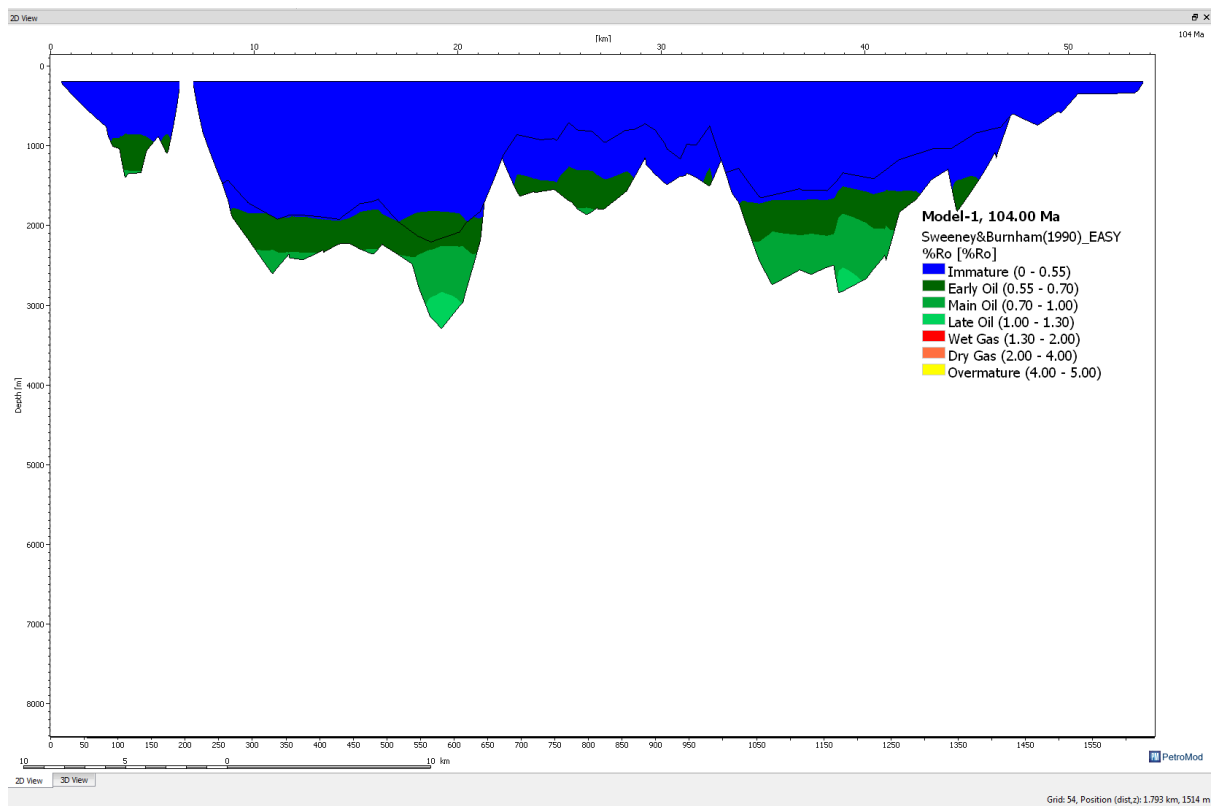


Figure 6.26: Maturity development of the Draupne FM at 104 Ma on the modelled line NVGTI-92-109.

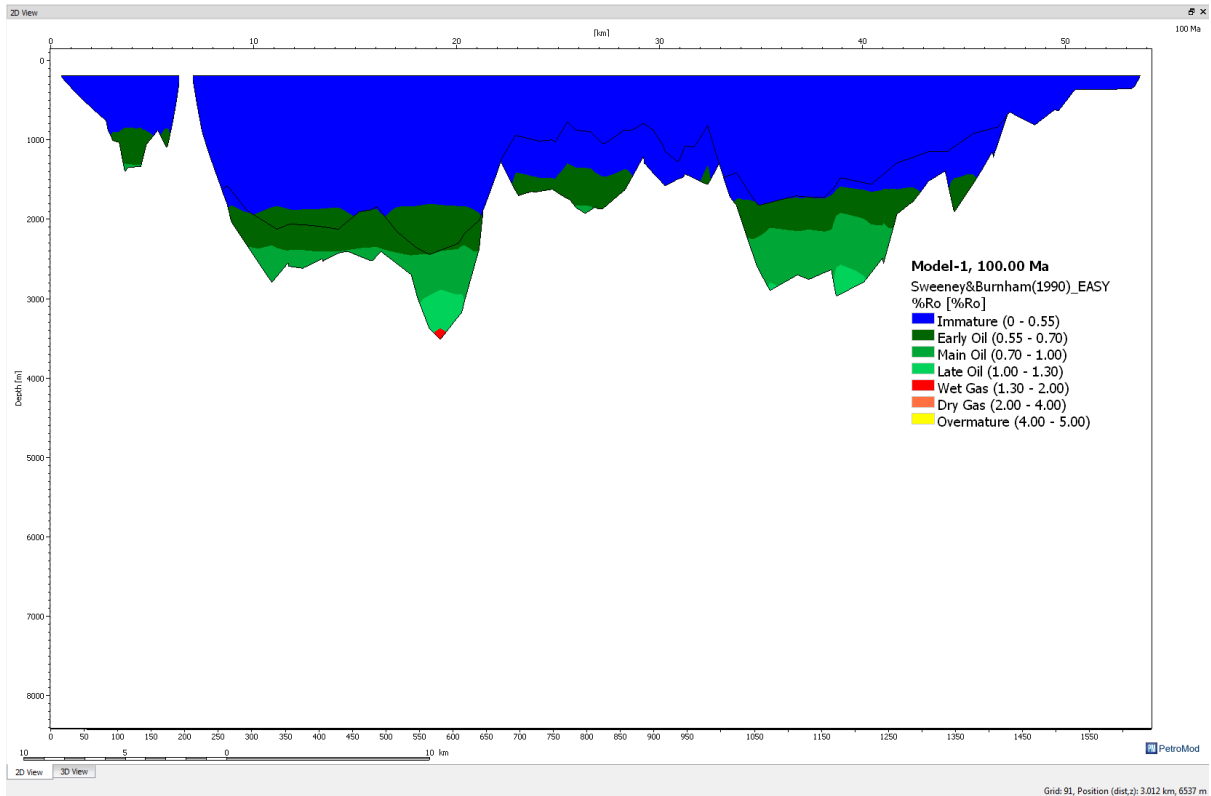


Figure 6.27: Maturity development of the Draupne FM at 100 Ma on the modelled line NVGTI-92-109.

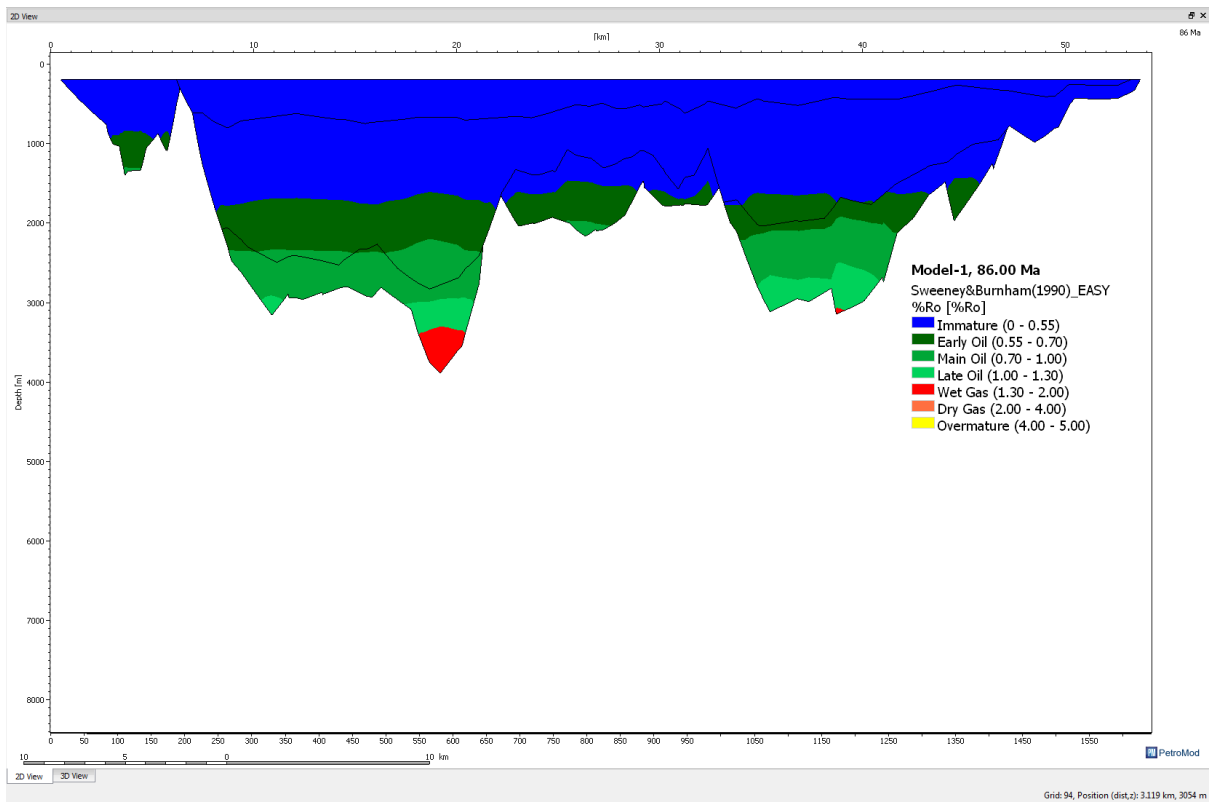


Figure 6.28: Maturity development on the Draupne FM at 86 Ma on the modelled line NVGTI-92-109.

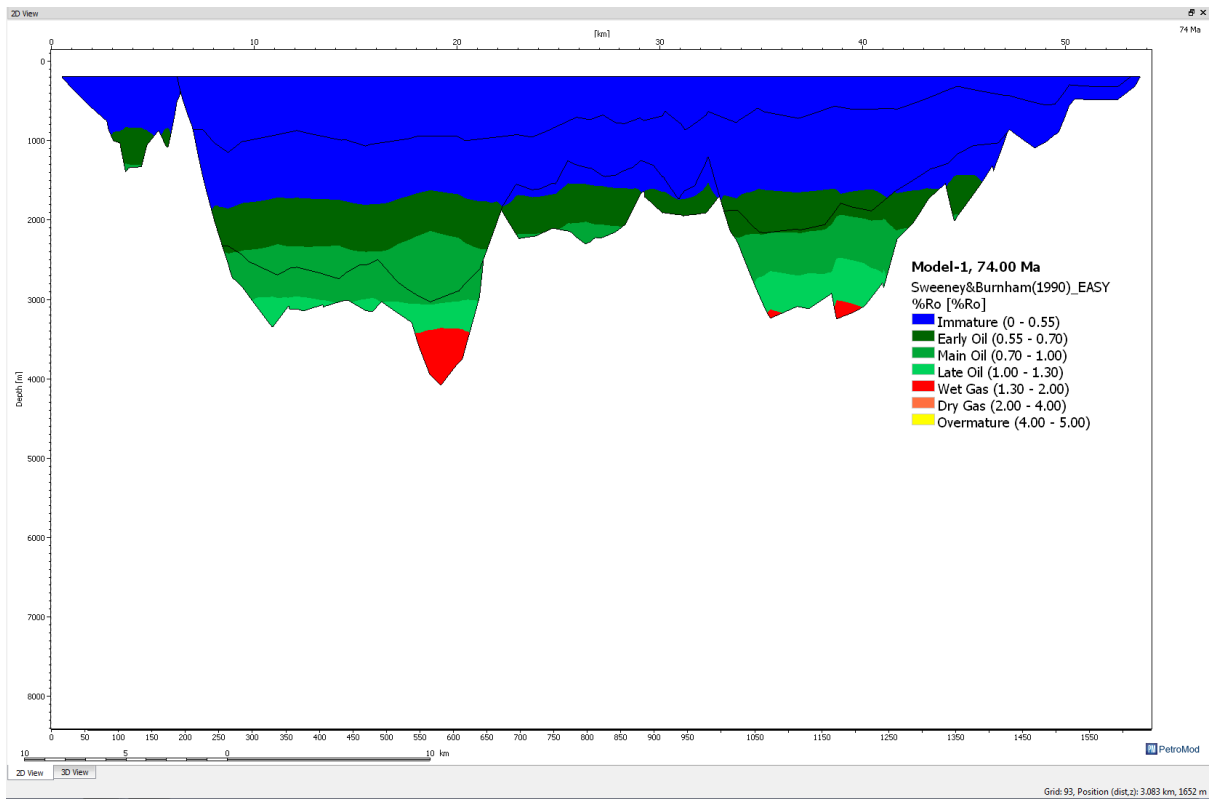


Figure 6.29: Maturity development on the Draupne FM at 74 Ma on the modelled line NVGTI-92-109.

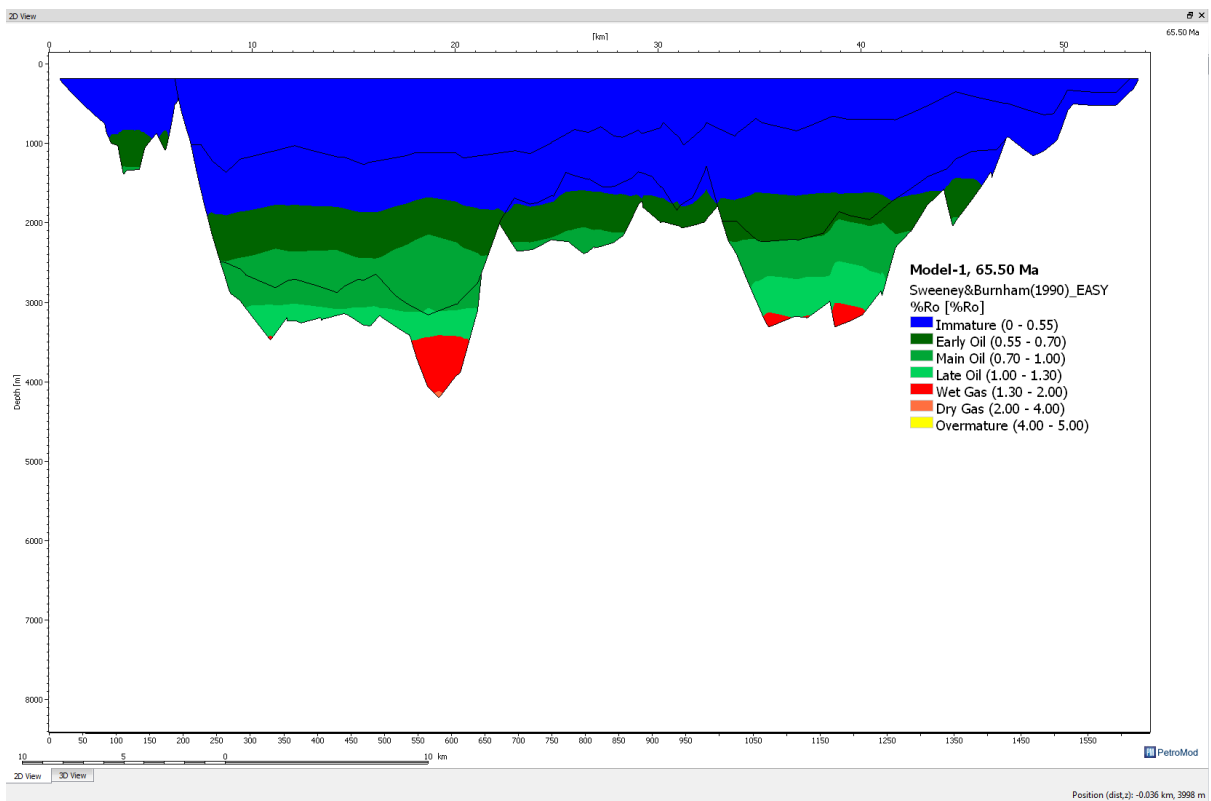


Figure 6.30: Maturity development of the Draupne FM at 65.50 Ma on the modelled line NVGTI-92-109.

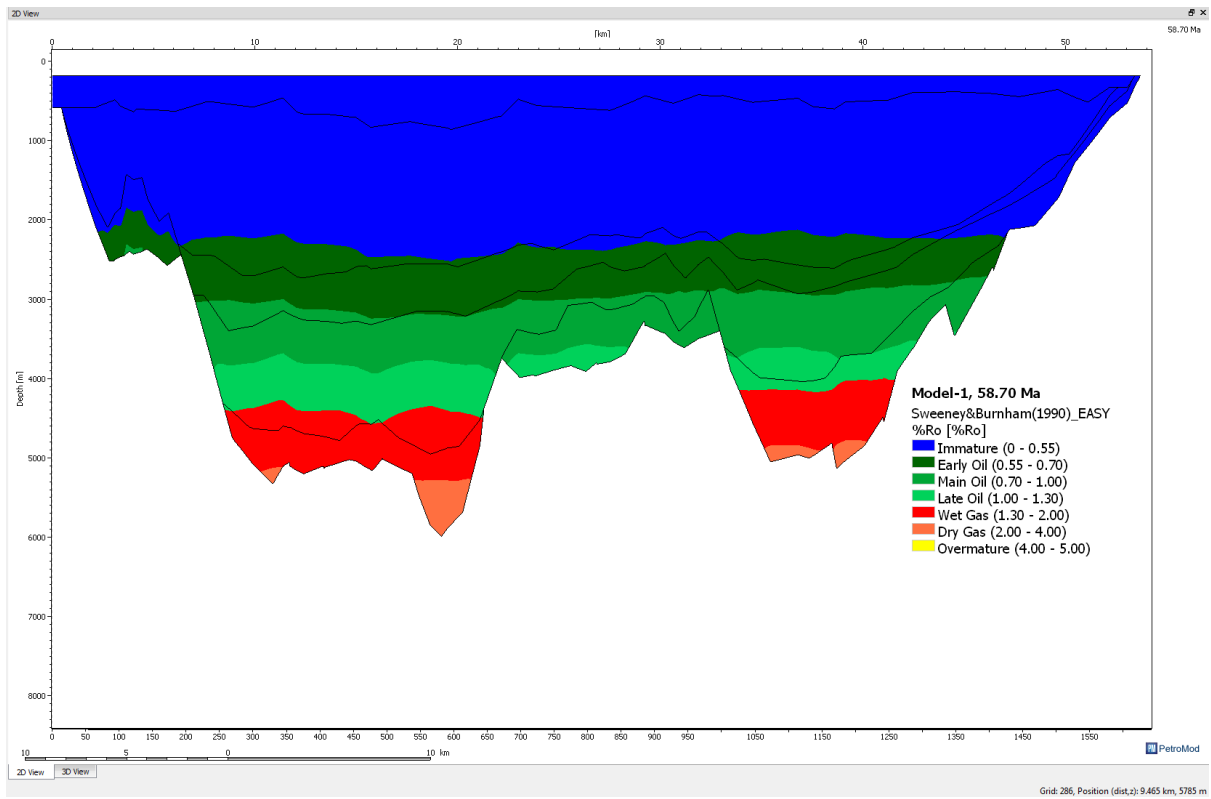


Figure 6.31: Maturity development of the Draupne FM at 58.70 Ma on the modelled line NVGTI-92-109.

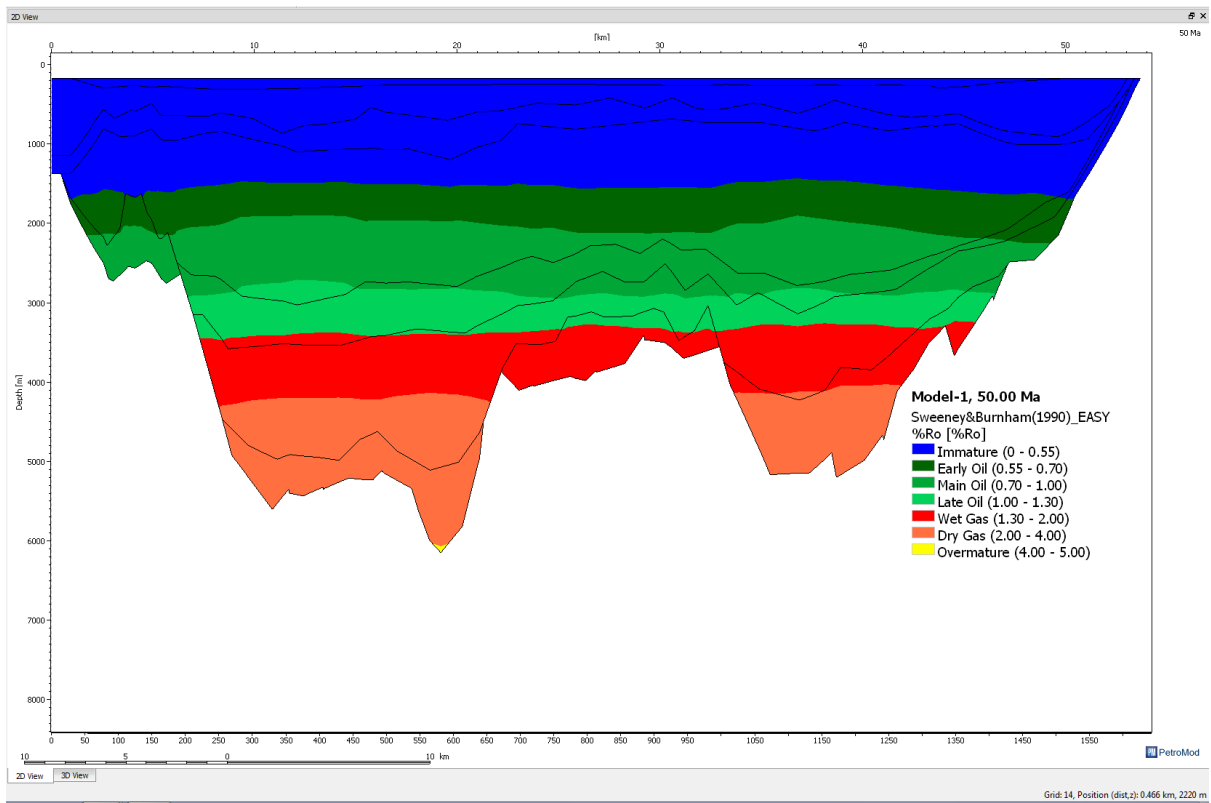


Figure 6.32: Maturity development of the Draupne FM at 50.00 Ma on the modelled line NVGTI-92-109

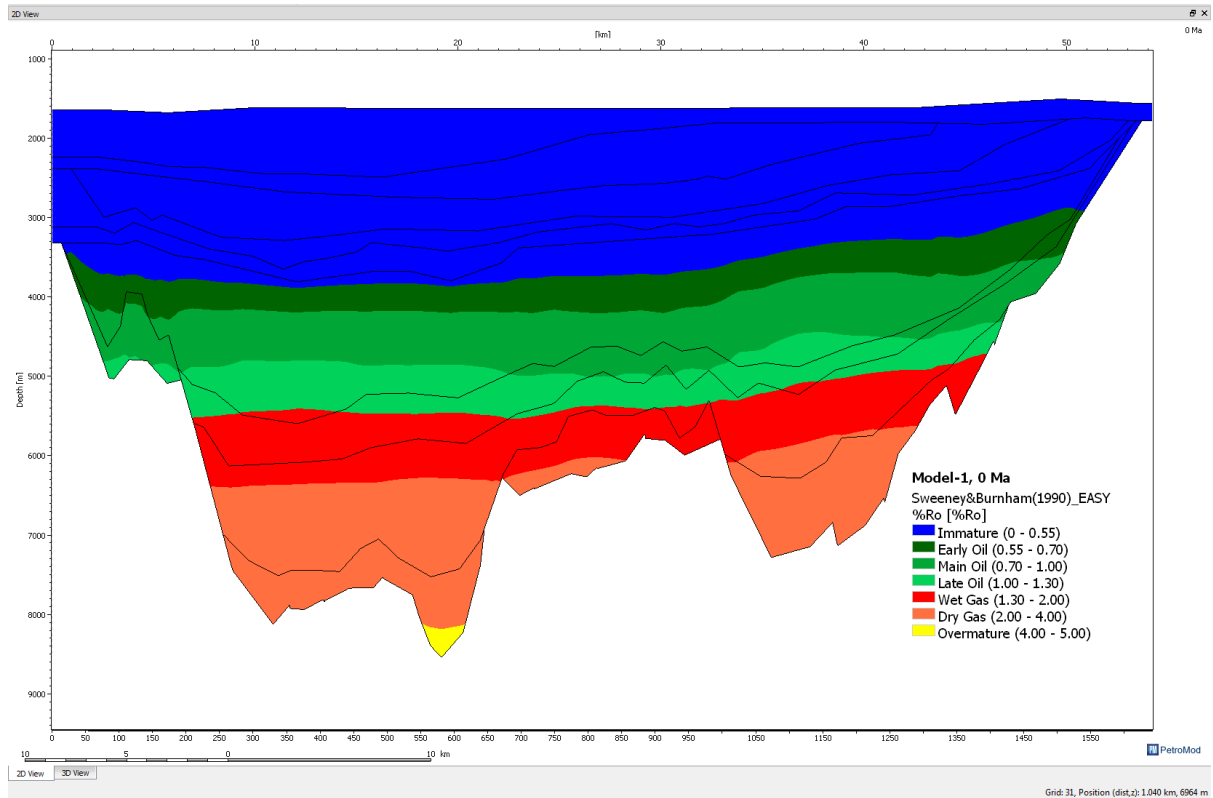


Figure 6.33: Maturity development of the Draupne FM at present time on the modelled line NVGTI-92-109.

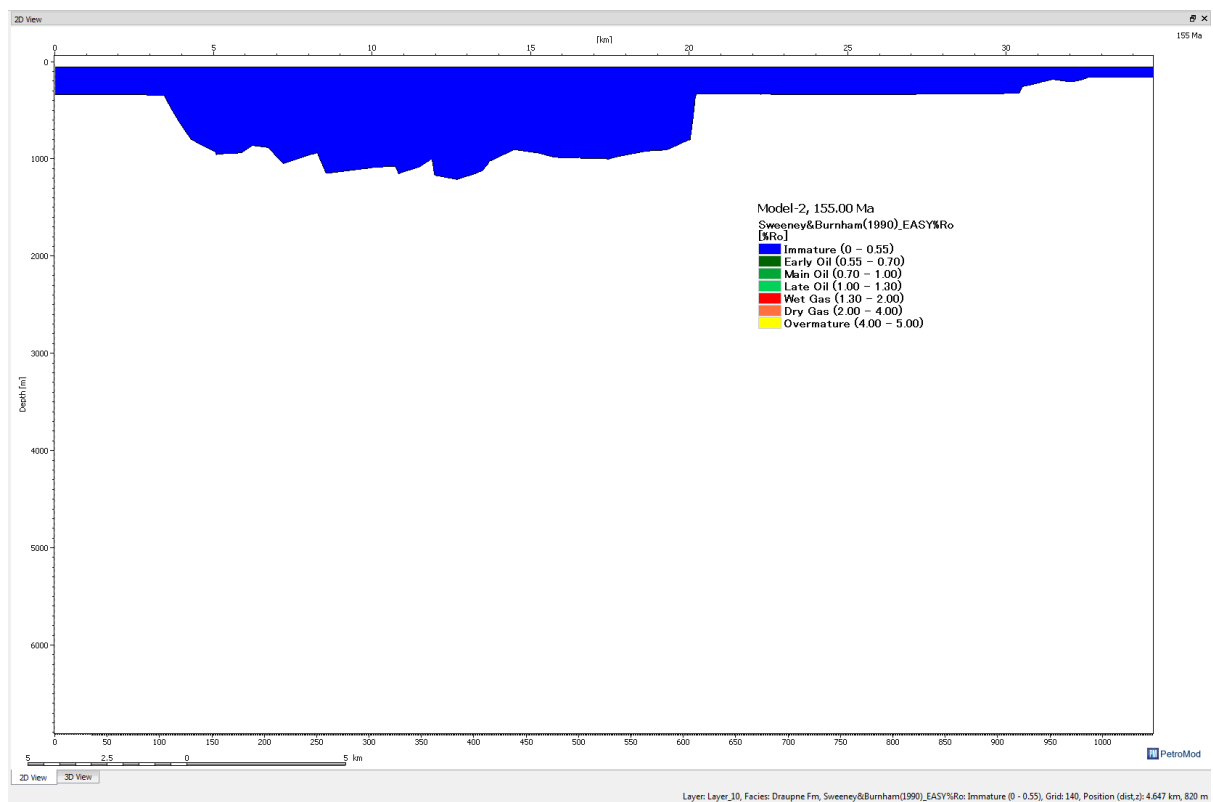


Figure 6.34: Maturity development of the Draupne FM at 155 Ma on the modelled line NVGTI-92-104.

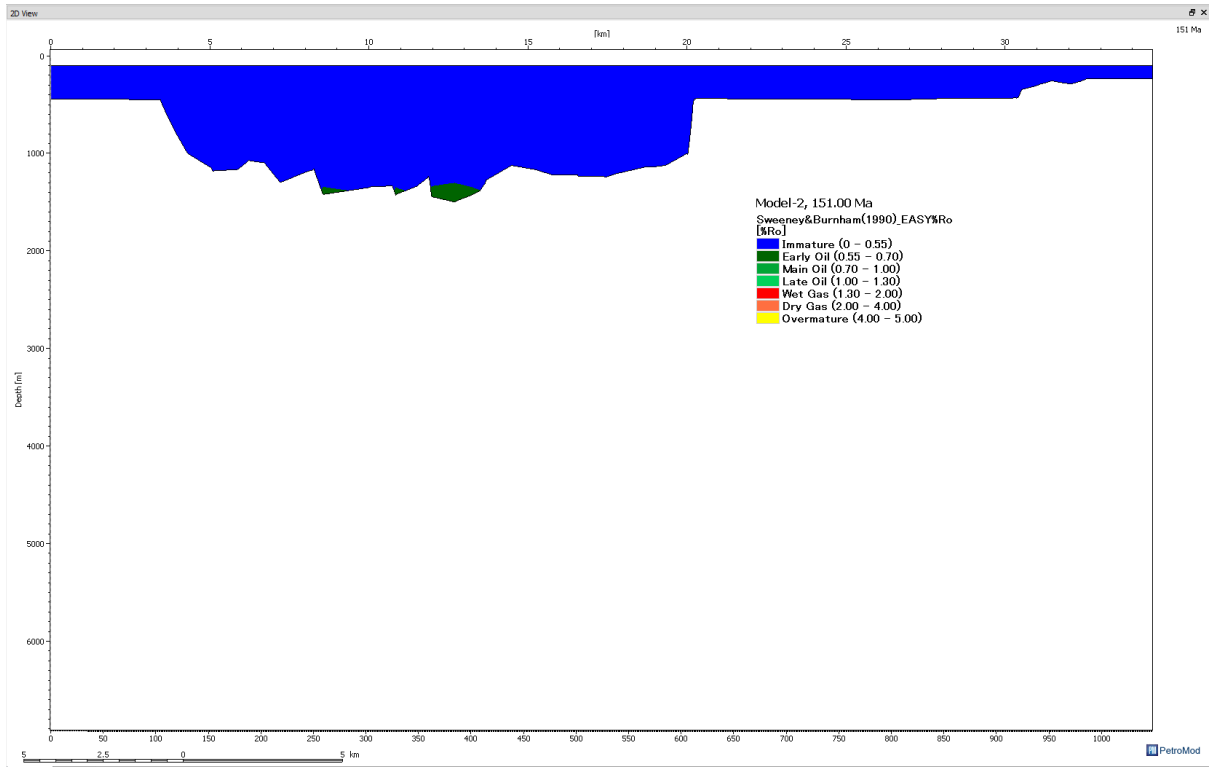


Figure 6.35: Maturity development of the Draupne FM at 151 Ma on the modelled line NVGTI-92-104.

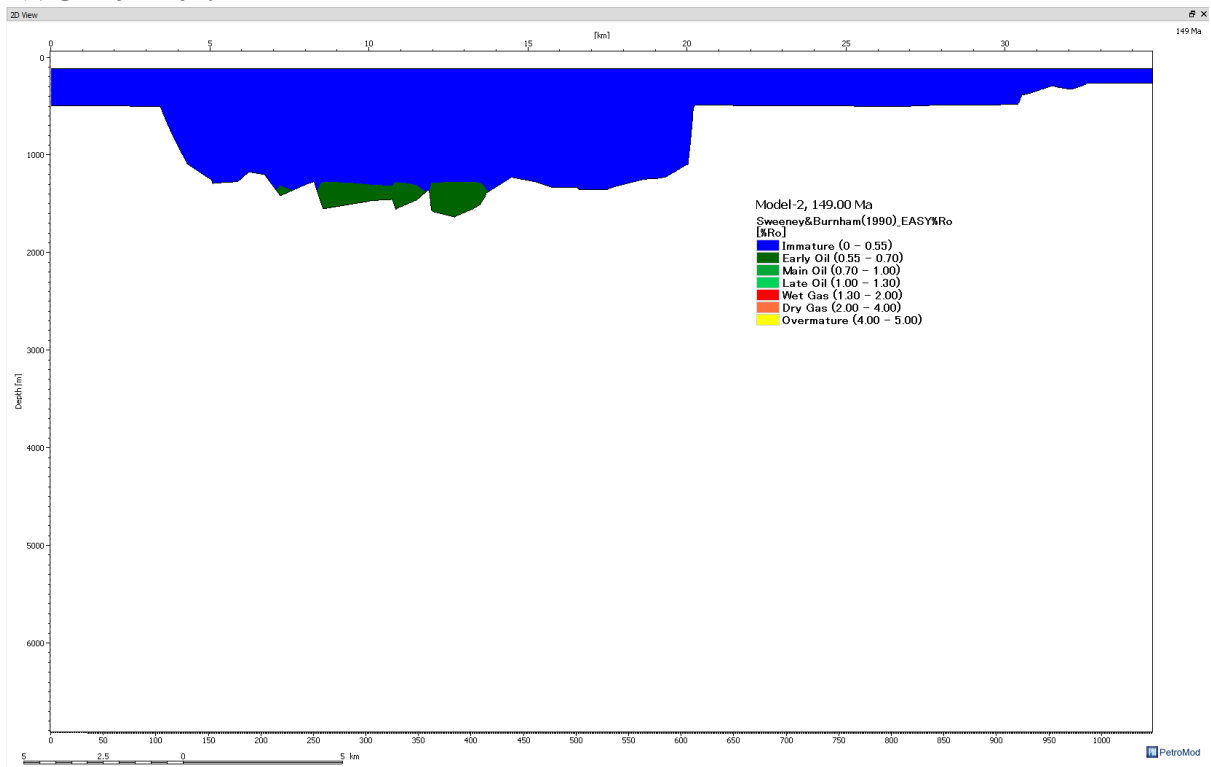


Figure 6.36: Maturity development of the Draupne FM at 149 Ma on the modelled line NVGTI-92-104.

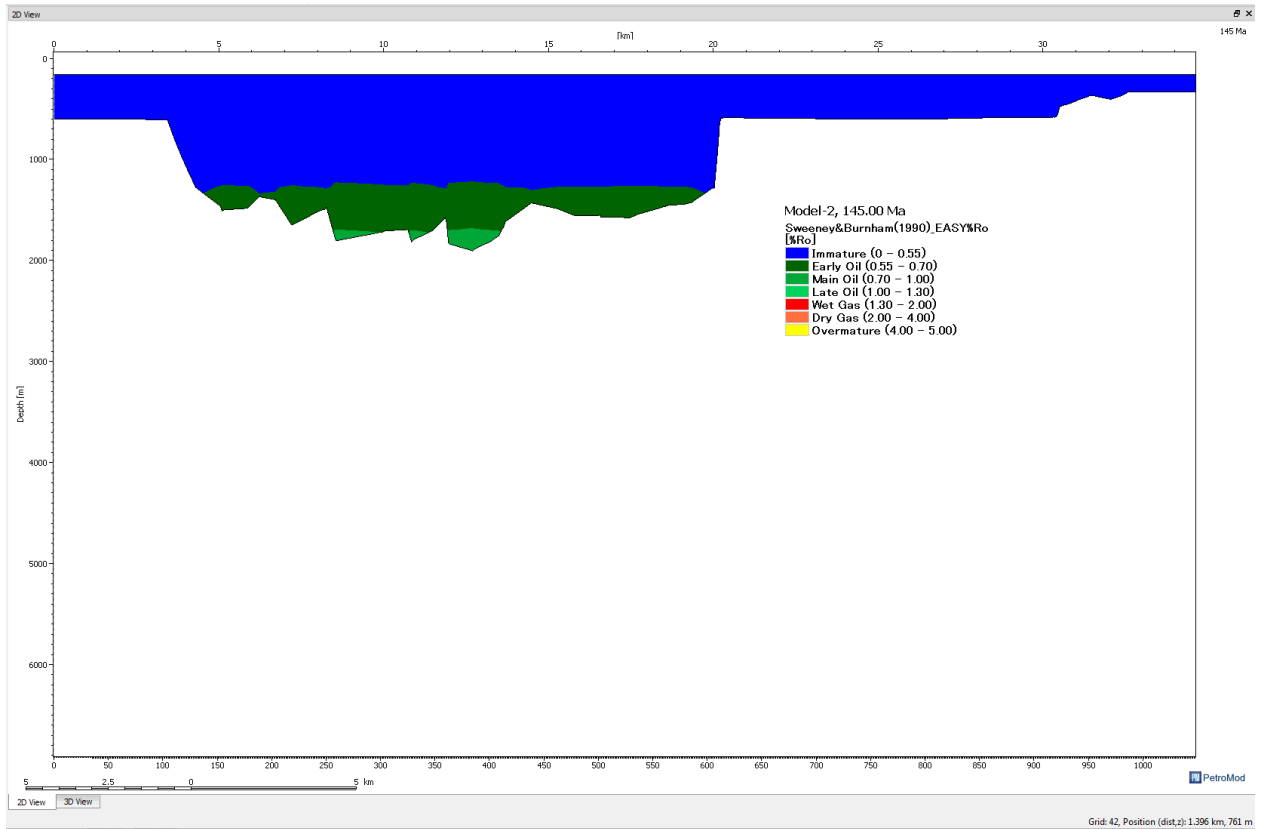


Figure 6.37: Maturity development of the Draupne FM at 145 Ma on the modelled line NVGTI-92-104.

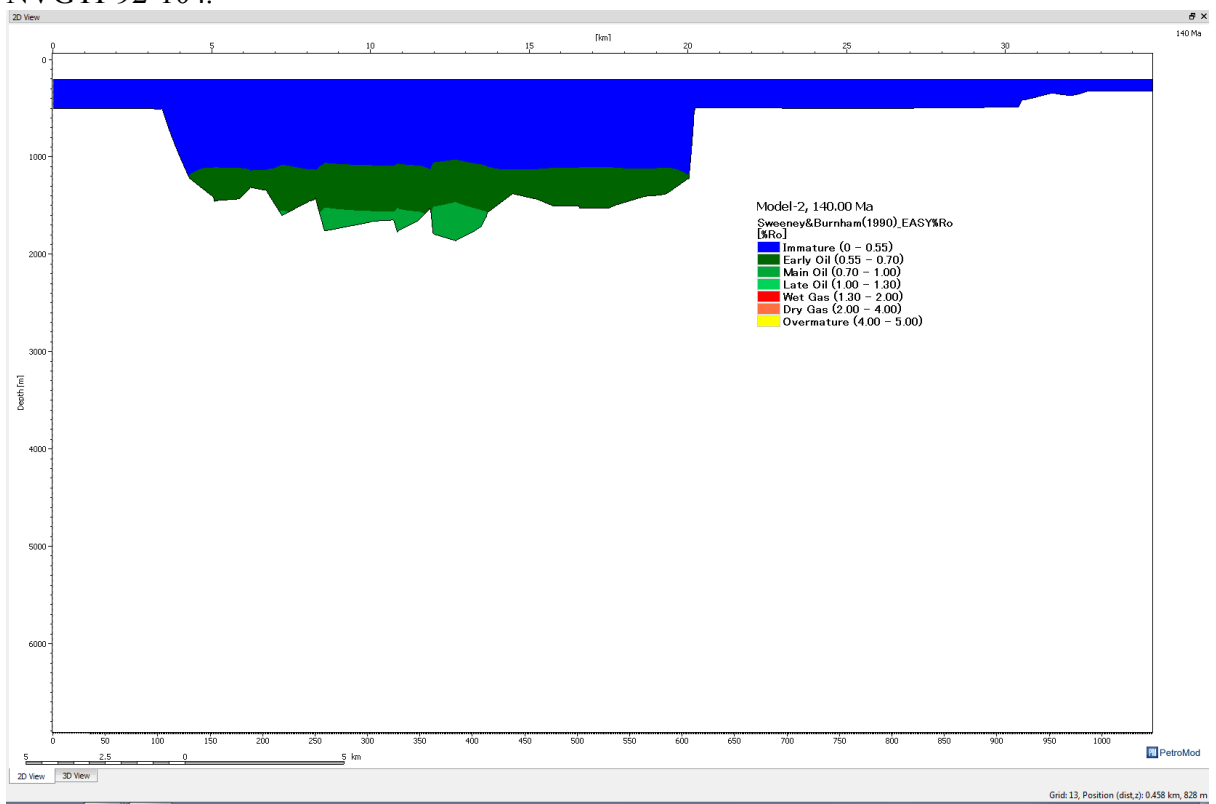


Figure 6.38: Maturity development on the Draupne FM at 140 Ma of the modelled line NVGTI-92-104



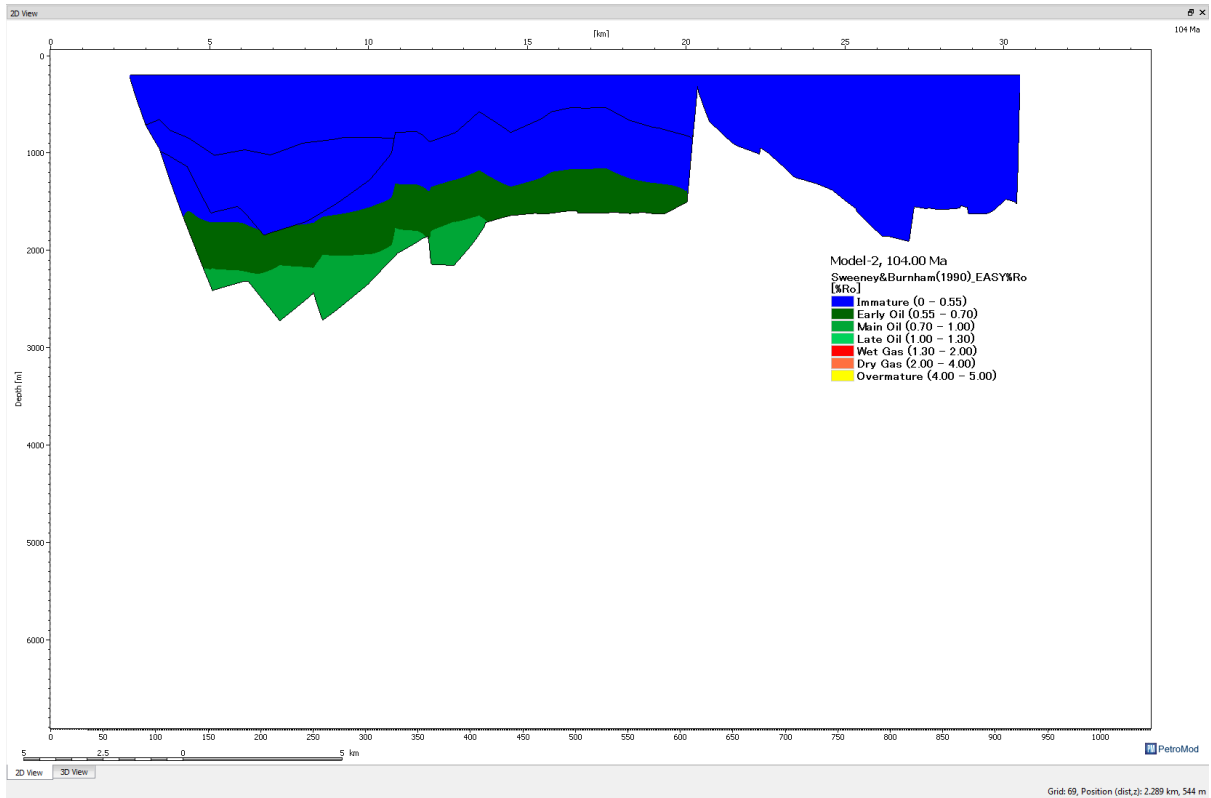


Figure 6.39: Maturity development of the Draupne FM at 104 Ma on the modelled line NVGTI-92-104.

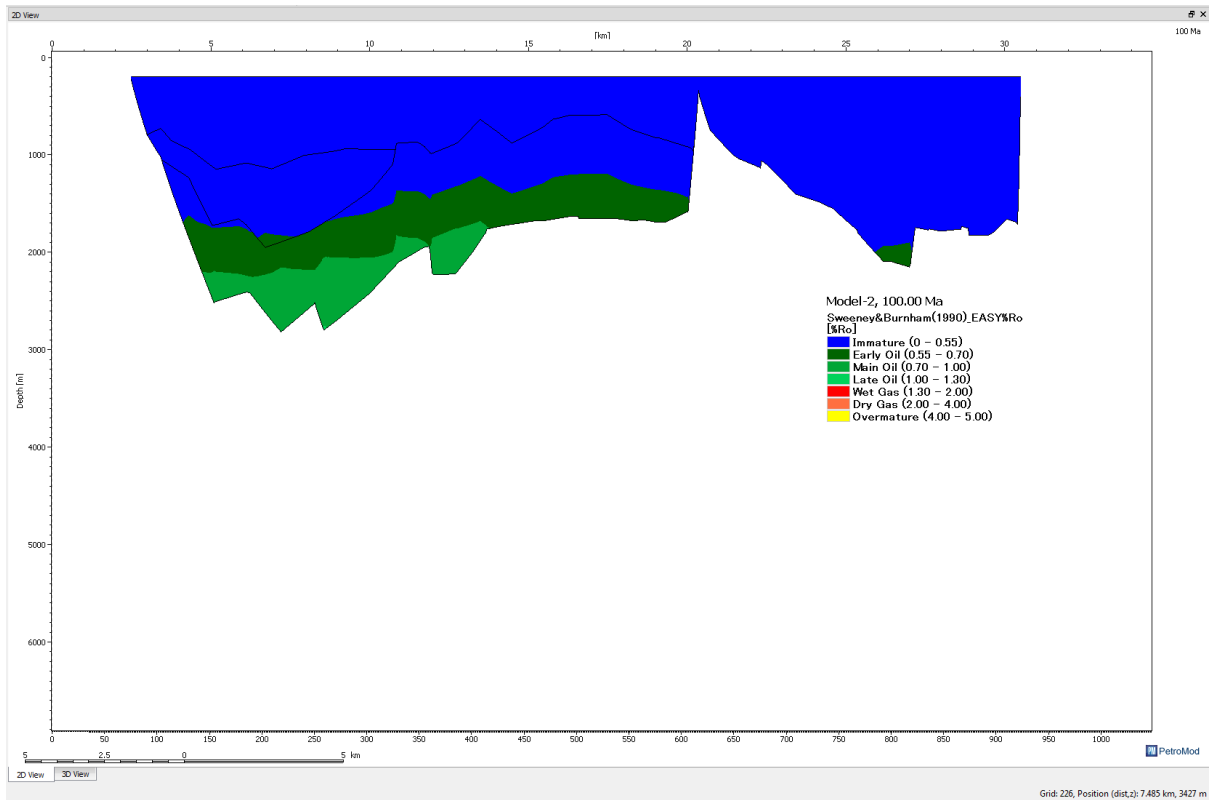


Figure 6.40: Maturity development of the Draupne FM at 100 Ma on the modelled line NVGTI-92-104.

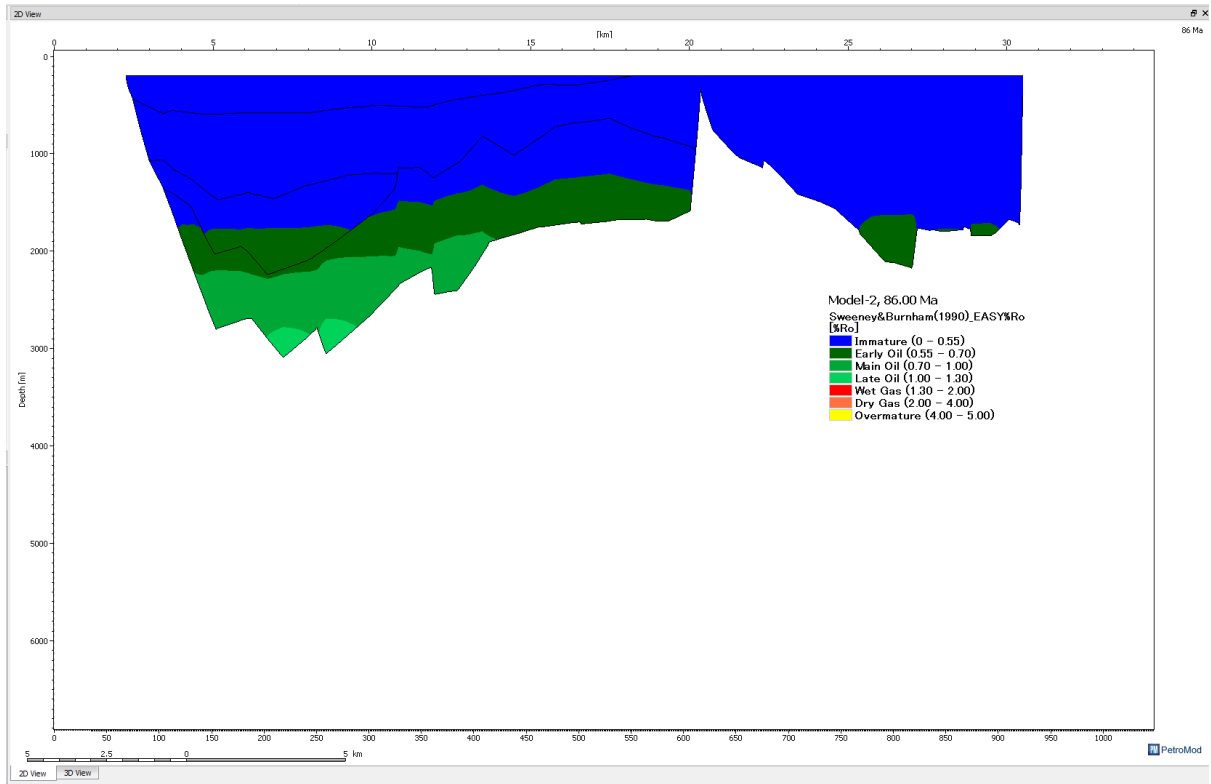


Figure 6.41: Maturity development of the Draupne FM at 86 Ma on the modelled line NVGTI-92-104.

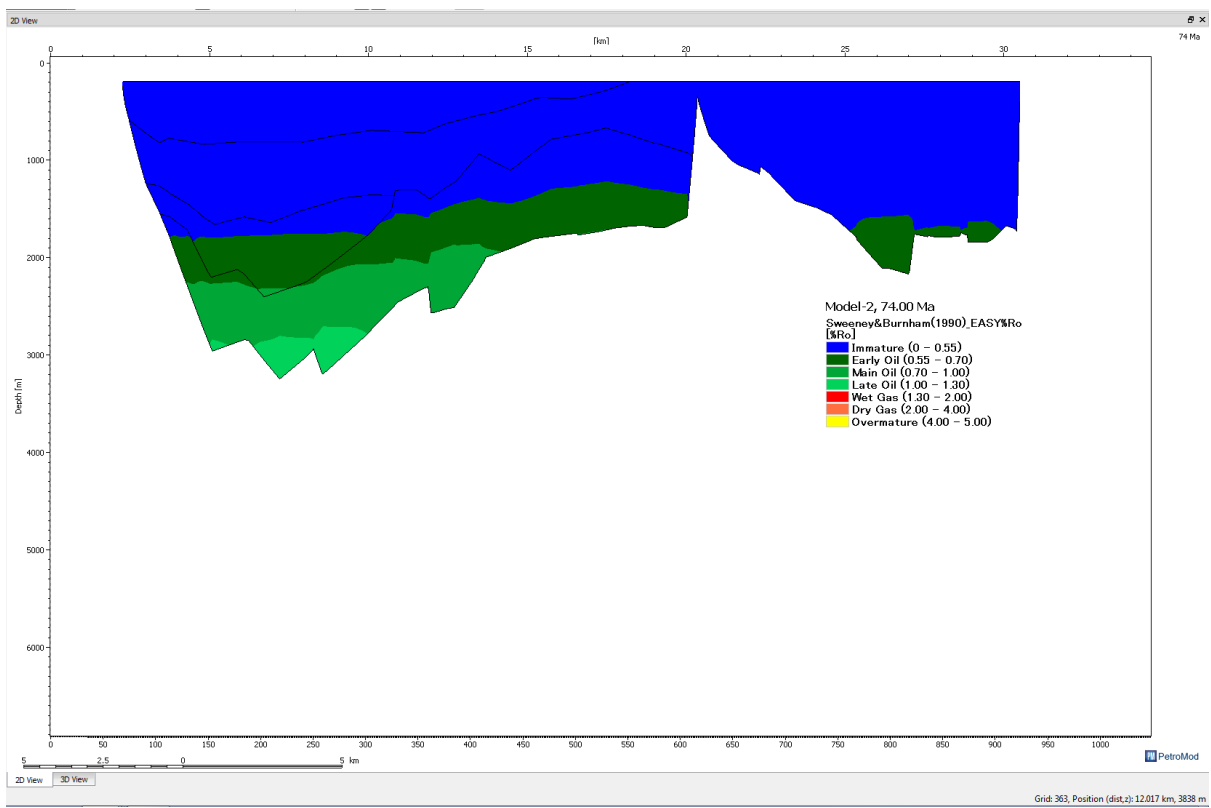


Figure 6.42: Maturity development of the Draupne FM at 74 Ma on the modelled line NVGTI-92-104.

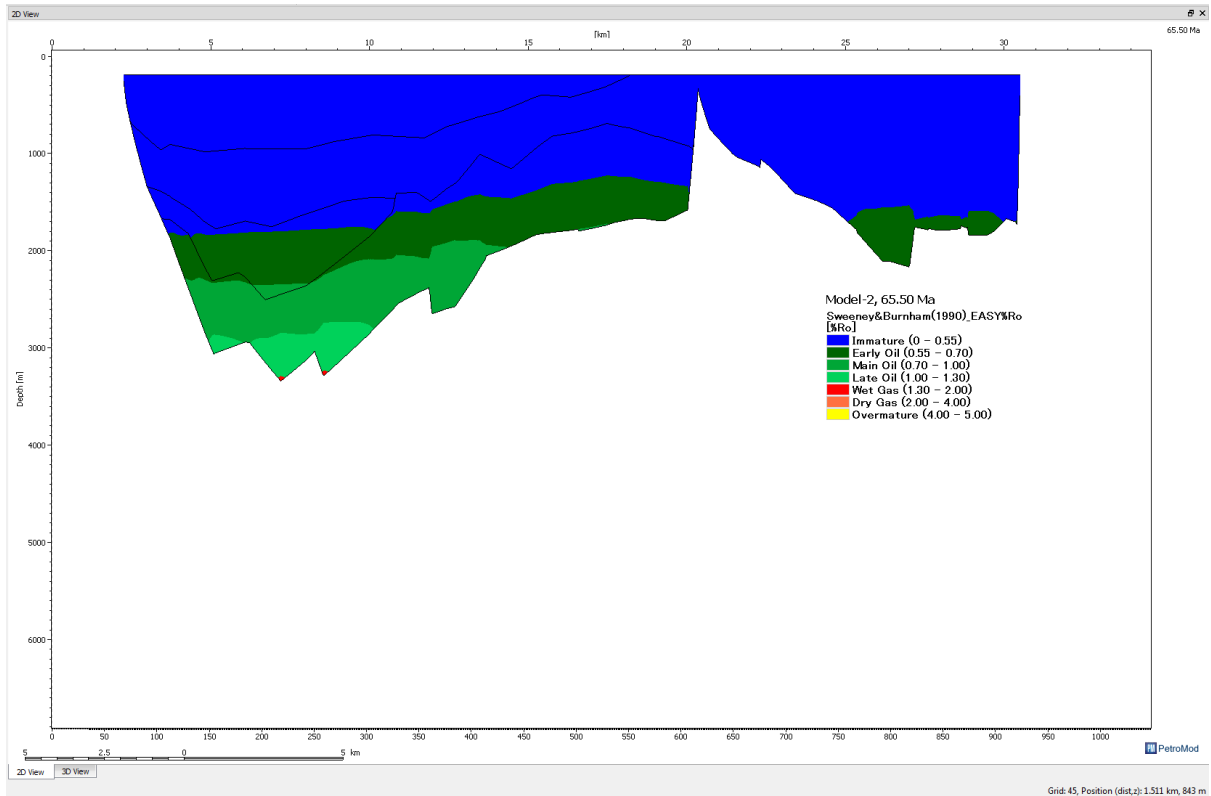


Figure 6.43: Maturity development of the Draupne FM at 65.50 Ma on the modelled line NVGTI-92-104.

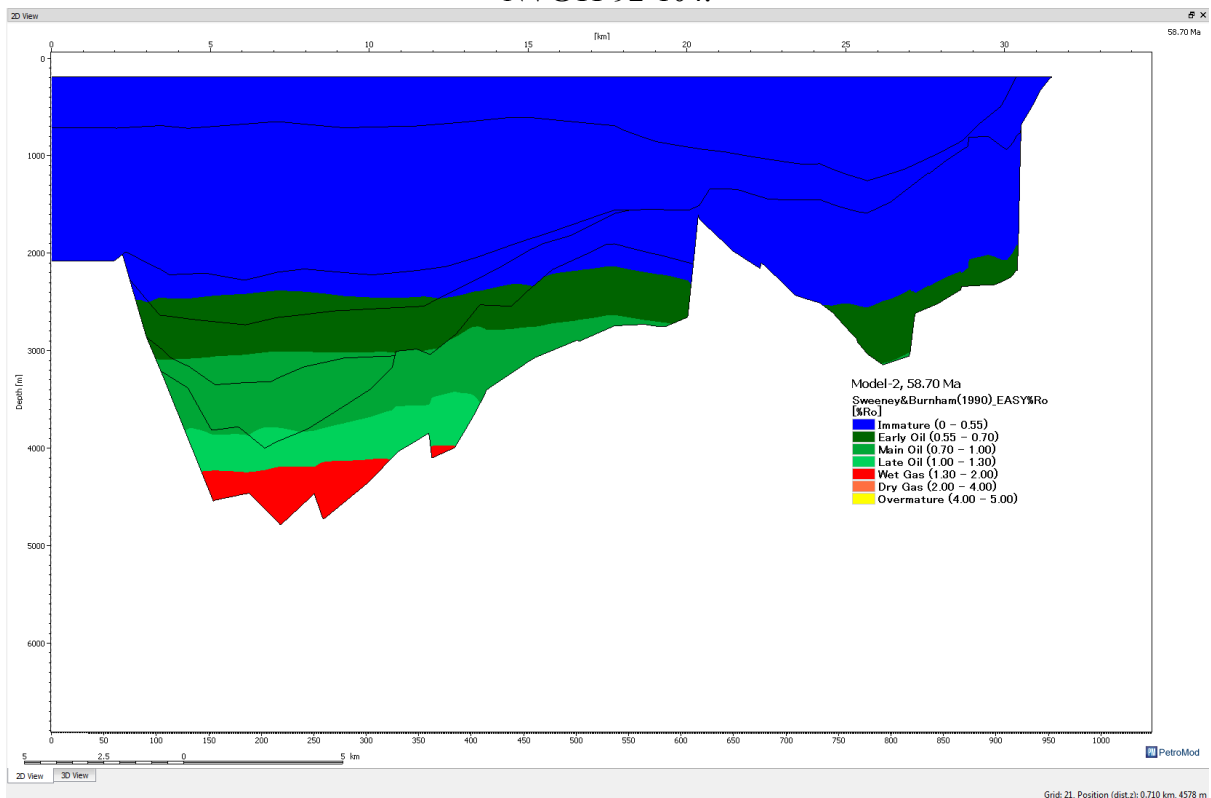


Figure 6.44: Maturity development of the Draupne FM at 58.70 Ma on the modelled line NVGTI-92-104.

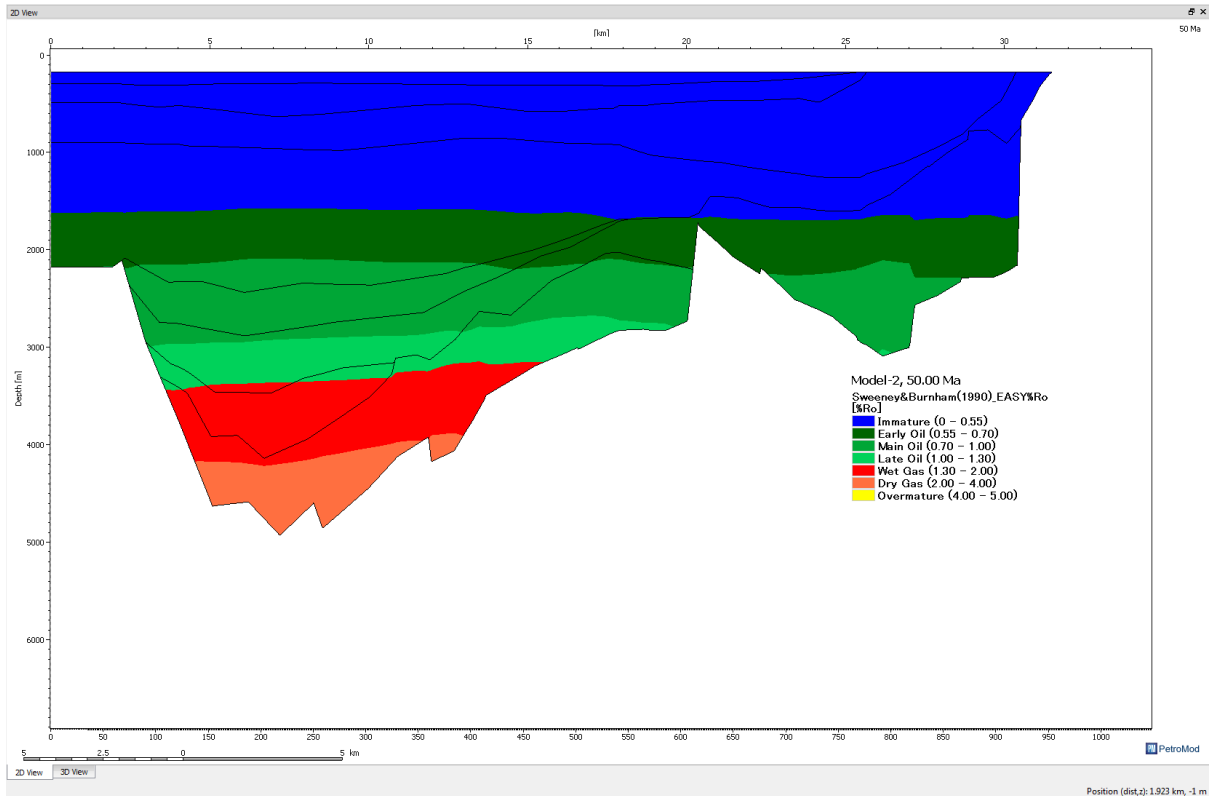


Figure 6.45: Maturity development of the Draupne FM at 50.00 Ma on the modelled line NVGTI-92-104.

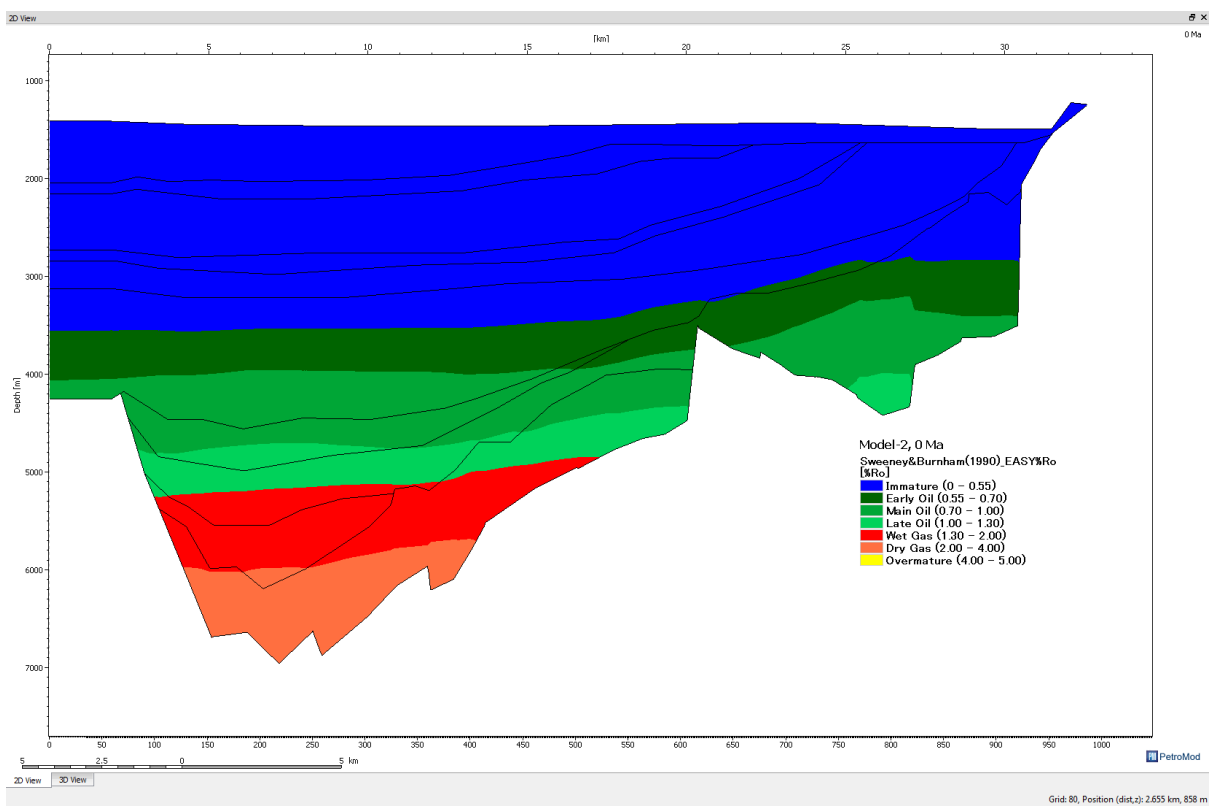


Figure 6.46: Maturity development of the Draupne FM at present time on the modelled line NVGTI-92-104.

After simulation, the results of the model showed that, the maximum temperature attained in the deeper parts of the basin is at the present day is 225°C. The late Jurassic source rock reaches a temperature of about 180°C (Fig 6.47 and 6.50). According to Sweeney and Burnham (1990), the vitrinite reflectance data shows that the source rock of the modelled basin is matured and has passed the oil window from main oil to dry gas (Fig 6.48 and 6.51). From the transformation ratio it shows that 95% to 100% of the source rock is transformed (Fig 6.49 and 6.52).

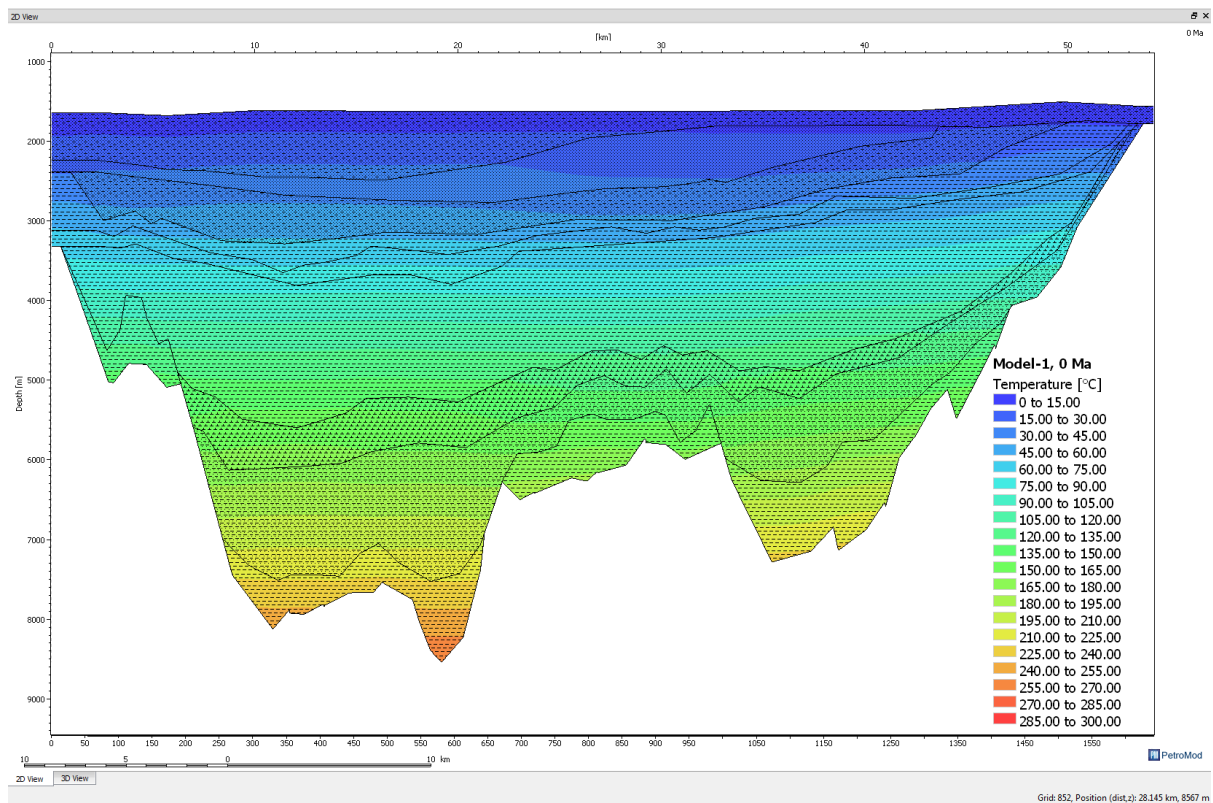


Figure 6.47: Depth converted profile showing temperature overlay of the modeled line NVGTI-92-109 at present day condition.

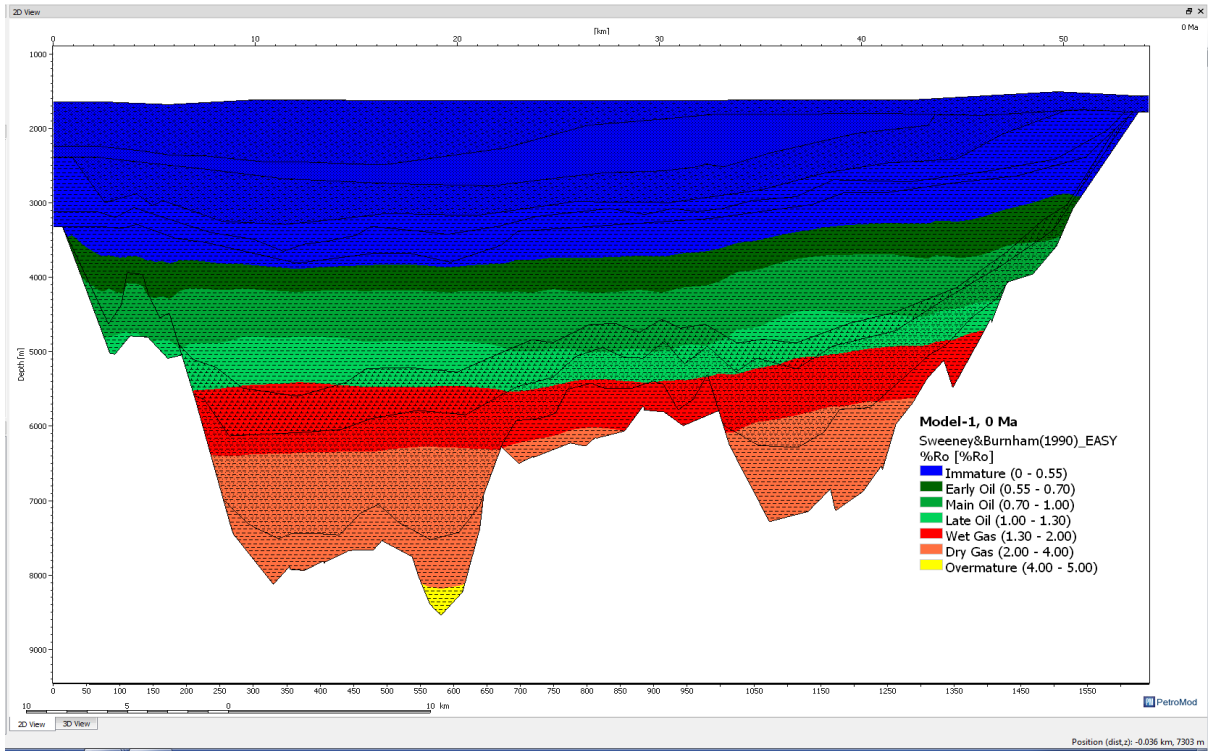


Figure 6.48: Vitrinite reflectance overlay for NVGTI-92-109 at present day condition.

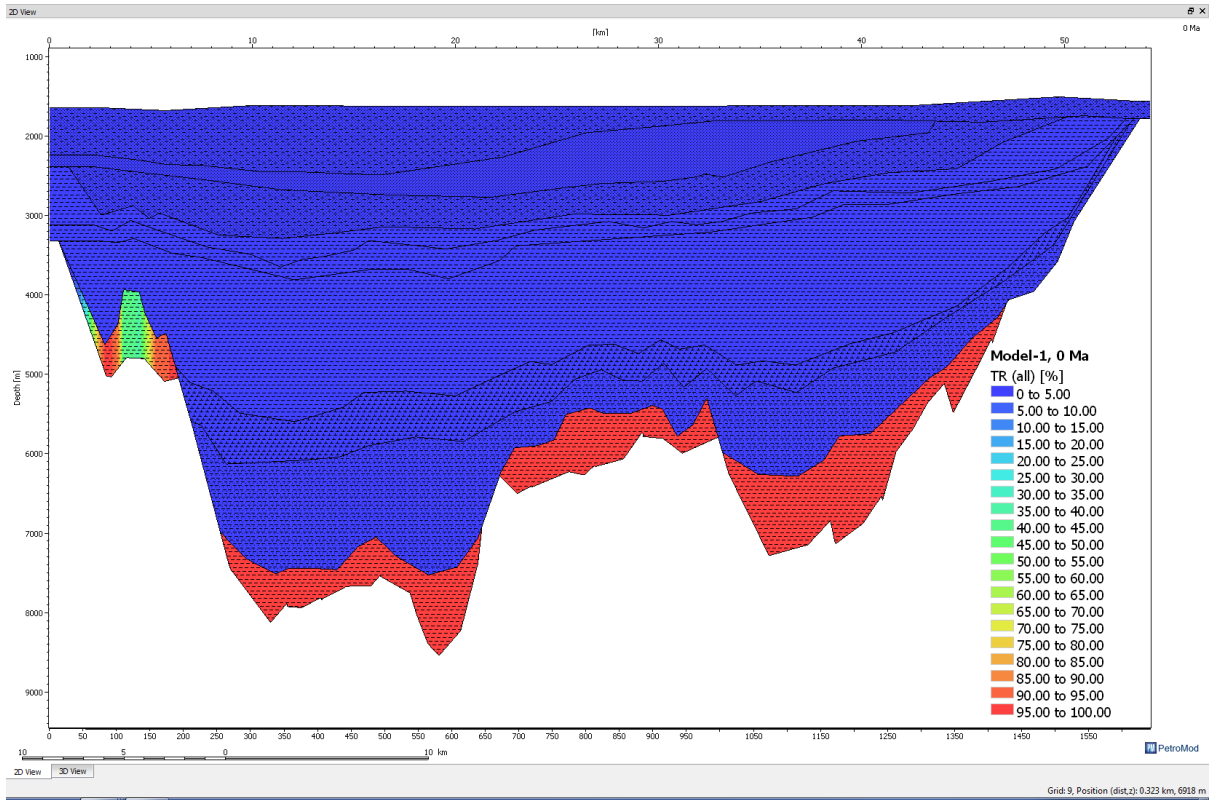


Figure 6.49: Transformation ratio overlay for NVGTI-92-109 at present day condition.

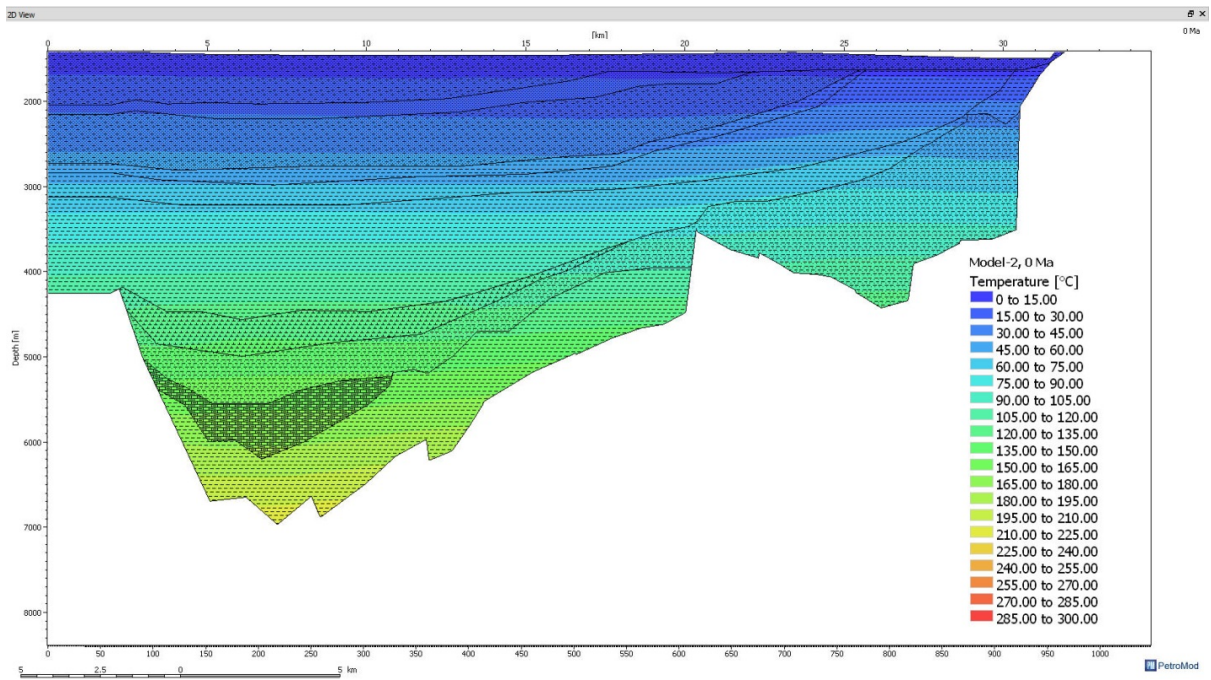


Figure 6.50: Depth converted profile showing temperature overlay of the modeled line NVGTI-92-104 at present day condition.



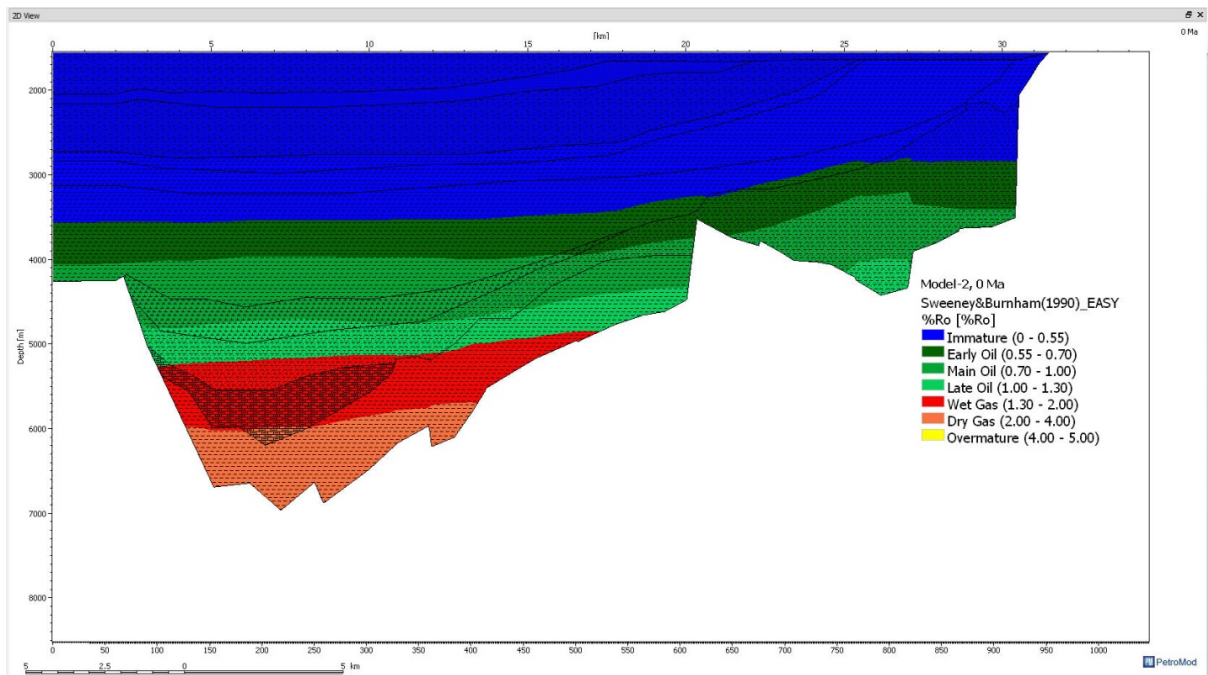


Figure 6.51: Vitrinite reflectance overlay for NVGTI-92-104 at present day condition.

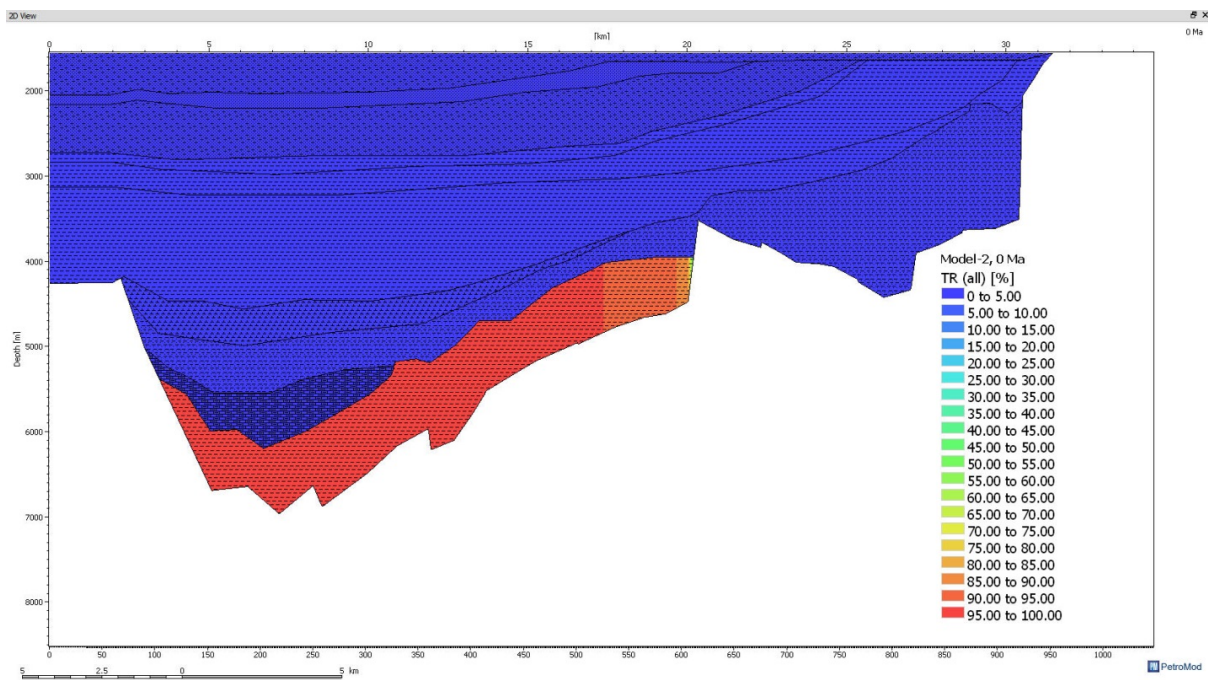


Figure 6.52: Transformation ratio overlay for NVGTI-92-104 at present day condition.

### 6.3 Migration, Saturation and accumulation

During the evolution and development of the basin, the hydrocarbons were generated, migrated and expelled from a source rock at a certain temperature and pressure depending on the burial history of the basin. By using the basin modelling software the hydrocarbon generation has been predicted by using different parameters for the source rock maturity. The



Upper Jurassic source rock has Type II kerogen, which is oil and gas prone based on the geochemical characterisation. In this work the source rock is described by reaction kinetic parameter developed by Sweeney and Burnham (1990).

The simulation model shows that the reservoir rocks are saturated with hydrocarbons to about 70% to 90% (Fig 6.53 and 6.57). The results show the capillary pressure of the source rock reached up to 70-75 MPa as shown (Fig 6.58), for the line NVGTI-92-104 and 110-120 MPa in the (Fig 6.54) for the line NVGTI-92-109. The results show that the mass of generated oil from the source rock ranges between 2.25-2.40 Mtons for NVGTI-92-104 (Fig 6.59) and 2.40-2.60 Mtons for NVGTI-92-109 (Fig 6.55), the mass of gas generated from the source rock is between 0.36-0.39Mtonsfor NVGTI-92-104 (Fig 6.62) and 0.49-0.52 Mtons for NVGTI-92-109 (Fig 6.60).

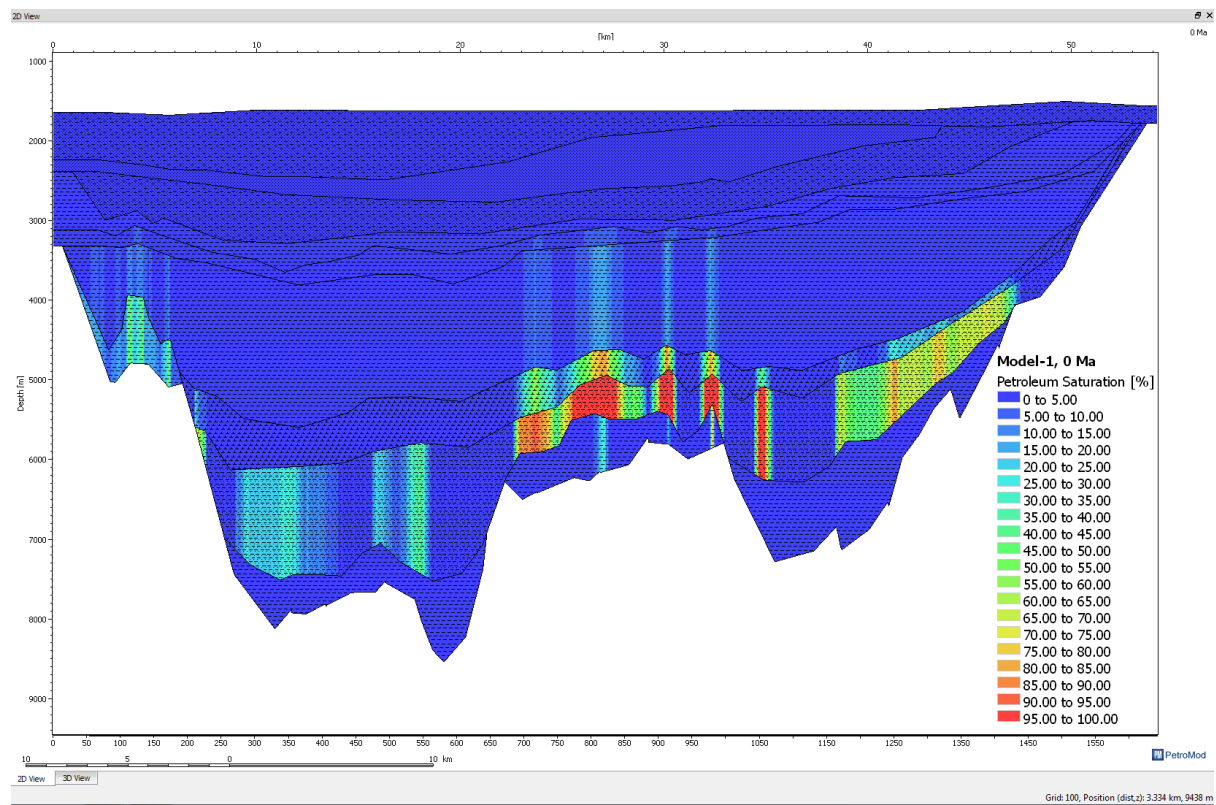


Figure 6.53: Hydrocarbon saturation overlay for NVGTI-92-109 at present day condition.

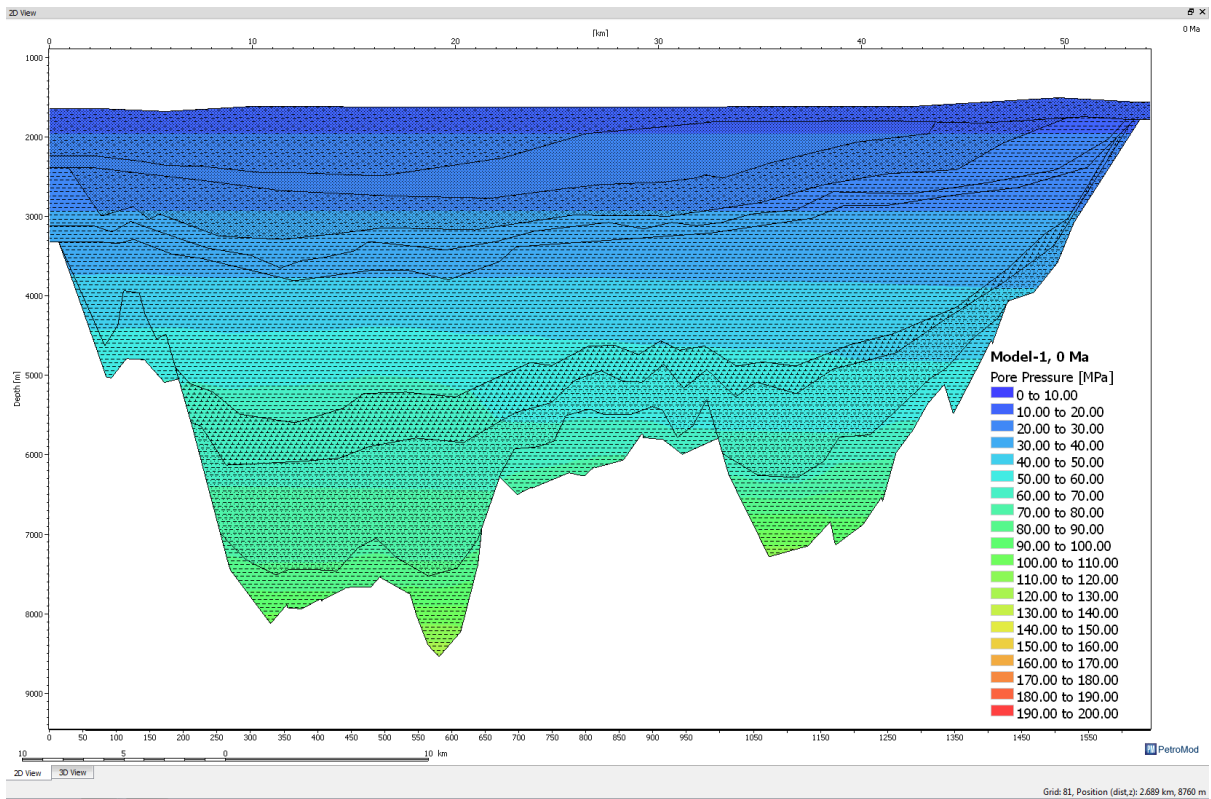


Figure 6.54: Pore pressure overlay for NVGTI-92-109 at present day condition.

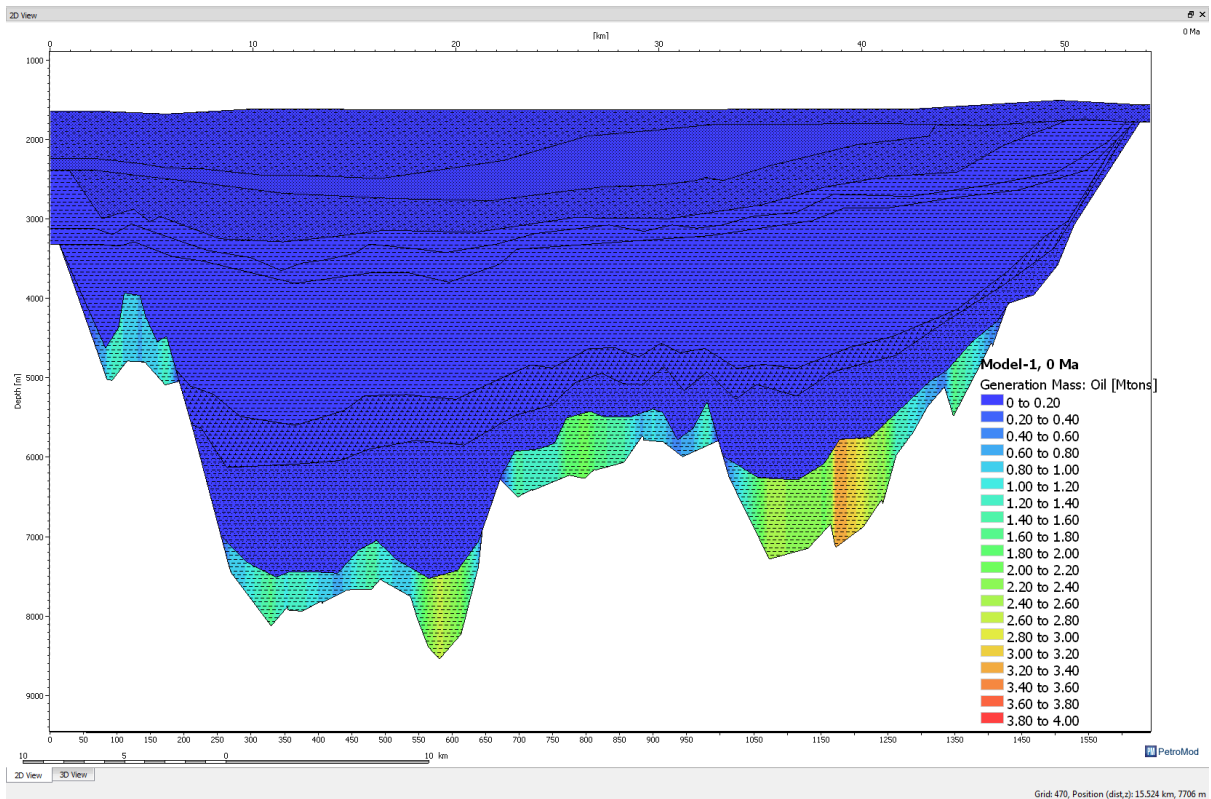


Figure 6.55: Generated mass overlay of oil for NVGTI-92-109 at present day condition.

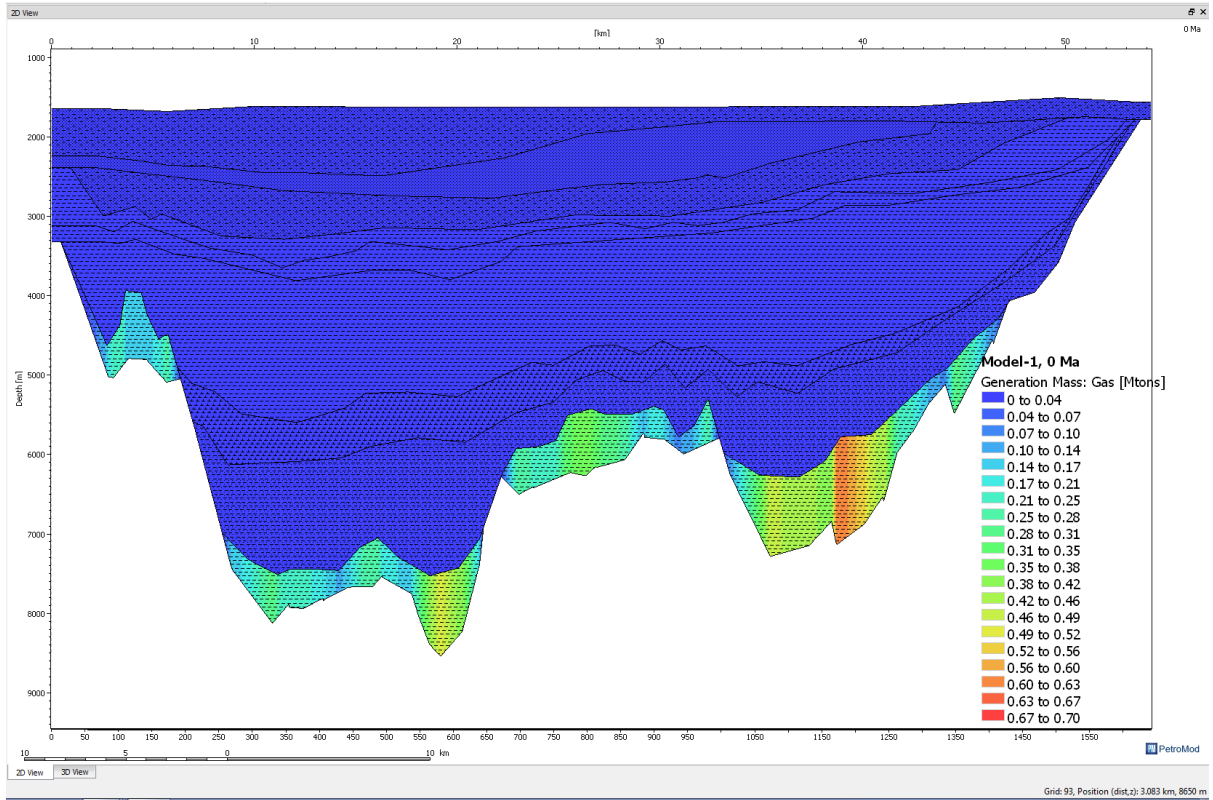


Figure 6.56: Generated mass overlay of gas for NVGTI-92-109 at present day condition.

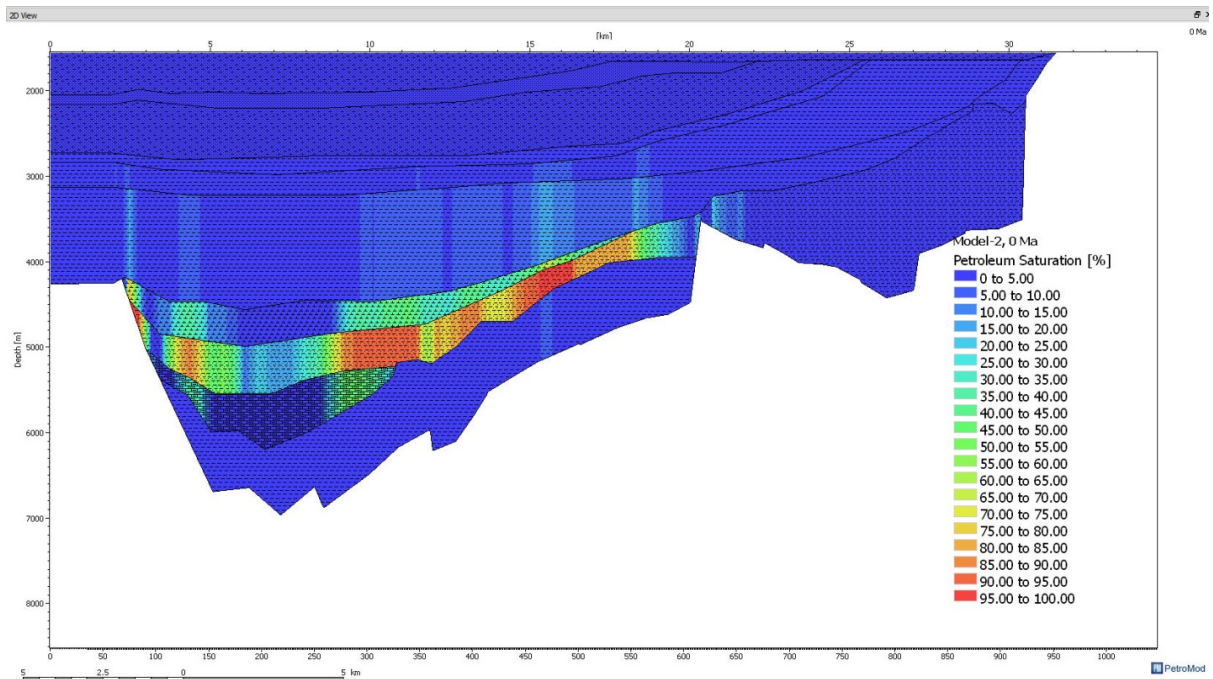


Figure 6.57: Hydrocarbon saturation overlay for NVGTI-92-104 at present day condition.



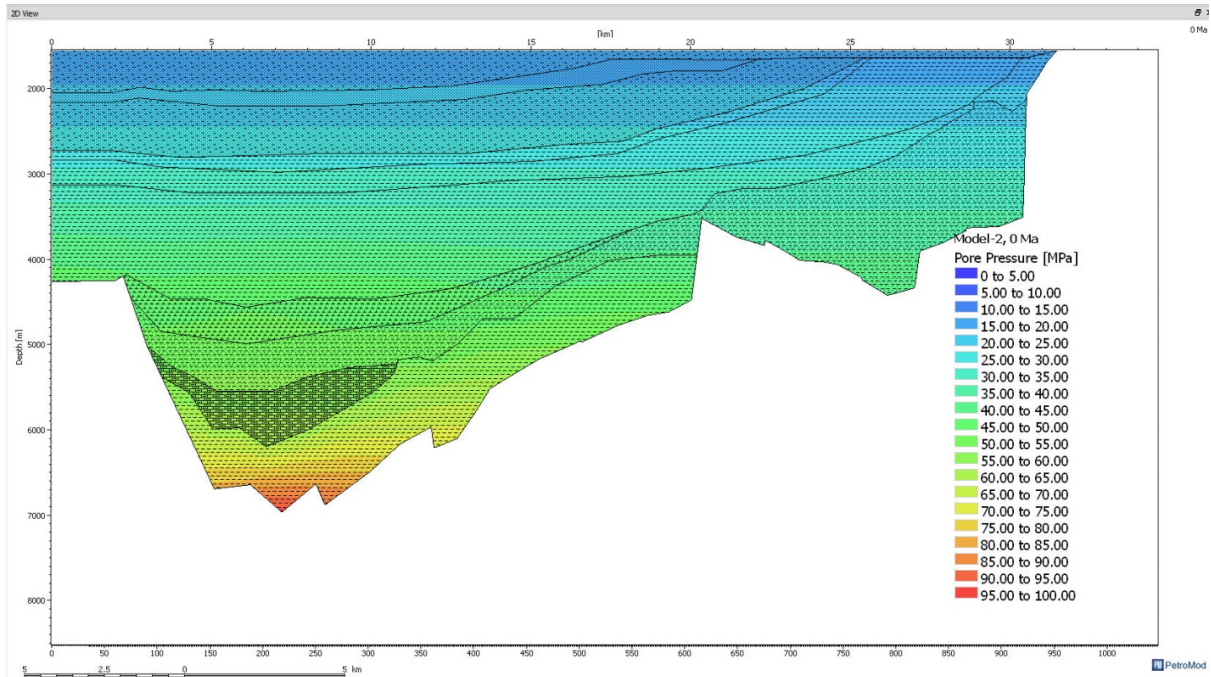


Figure 6.58: Pore pressure overlay for NVGTI-92-104 at present day condition.

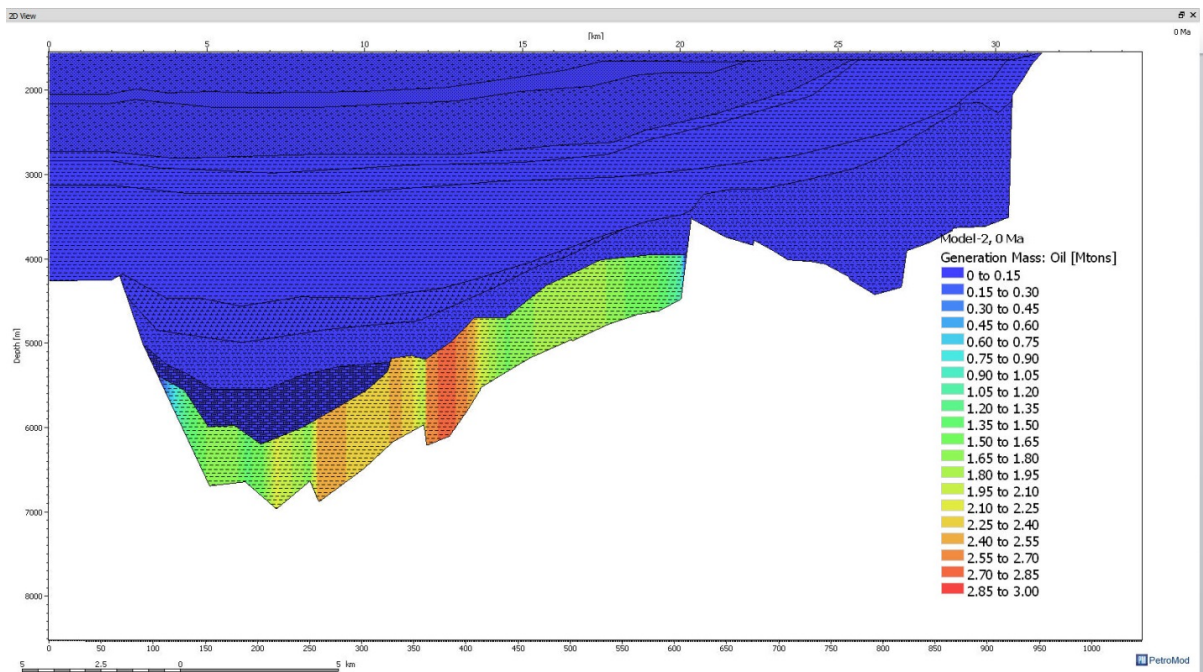


Figure 6.59: Generated mass overlay of oil for NVGTI-92-104 at present day condition.

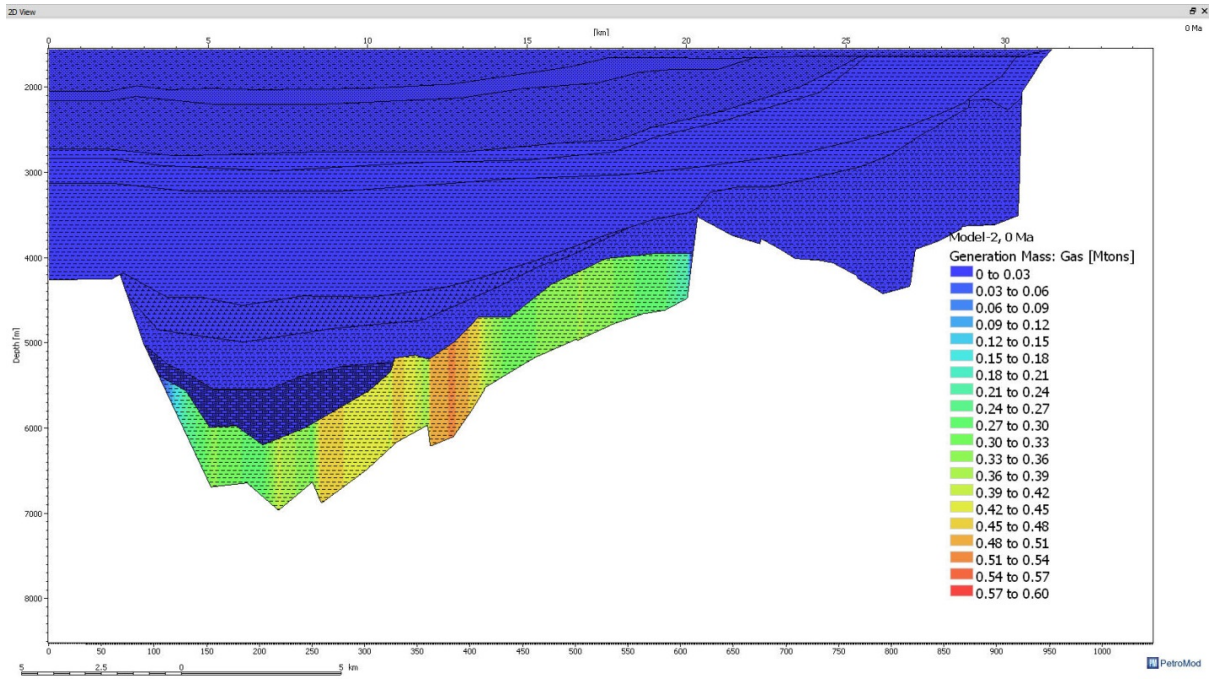


Figure 6.60: Generated mass overlay of gas for NVGTI-92-104 at present day condition.

## CHAPTER 7: DISCUSSION

Based on the results of the burial and thermal history reconstruction, in combination with the structural history of the study area, three distinct phases of basin formation are recognized, the pre-rift, syn-rift and post-rift stages. The pre-rift stage corresponds to the period from early-mid Jurassic during which the basin was tectonically stable with slow subsidence and sedimentation rates. This phase is a part of the post-rift stage to the earlier Permo-Triassic rifting event. The main rifting phase based on the modeling spanned from mid-late Jurassic to early Cretaceous. Subsidence rates were higher than previously due to the widespread active faulting across the basin, which might have been enhanced by the pre-existing structural weakness caused by the Permo-Triassic event. The post-rift phase of the basin spans from the end of rifting in the early Cretaceous to the present day. This phase from the burial curve clearly indicates the average subsidence and sedimentation rates characteristic of the thermal subsidence phase. During the evolution and development of the basin, the hydrocarbons were generated, migrated and expelled from a source rock at a certain temperature and pressure depending on the burial history of the basin. The highest heat flow reached is  $83 \text{ mW/m}^2$  which was high enough to further facilitate maturity and hydrocarbon generation. The high heat flow trend has an effect on the modelling which is earlier maturation of organic matter and onset of petroleum generation as compared to other previous studies conducted in the study area. The heat flow trend used for the modelling is considered high in comparison with other published trends for the study area.

The water depths at 23 Ma and present day are large than obtained in previous works done on the study area. This could be an error associated with the data provided and could not be corrected, it becomes unreliable to talk about the water depths. The late Jurassic source rock has Type II kerogen, which is oil and gas prone based on the geochemical characterisation. In this work the source rock is described by reaction kinetic parameter developed by Sweeney and Burnham (1990). The main source rock in the study area is the late Jurassic Draupne Formation, which is shale (organic rich, typical). In the deepest parts of the basin the source rock started to generate early oil during Upper Jurassic, main oil and late oil in the early Cretaceous, wet gas in late Cretaceous, and in Paleocene some dry gas was generated. This is much earlier oil and gas generation as compared to other studies, and this is due to an error during modeling. Since in this area most oil started to be generated in the late Cretaceous. In the deeper parts of the basin some part of the source rock overmature at the present day

condition when the burial depth of the basin is 8500 m. The simulation model shows that the reservoir rocks are saturated with hydrocarbons to about 70% to 90%, the expulsion onset of hydrocarbon in the upper Jurassic source rock is 160 Ma-170 Ma. The capillary pressure of the source rock reached up to 70-75 MPa.

## CHAPTER 8: CONCLUSIONS

A 2D approach to basin and petroleum systems modeling in combination with geological knowledge has allowed the hydrocarbon generation and migration history of the Jurassic source rocks in the northern North Sea to be studied in space and time. The study indicates that the Upper Jurassic Draupne Formation is mature in most locations in the study area. Hydrocarbon generation started in the late Jurassic to early Cretaceous and continues to present day. In the deepest parts of the basin the source rock is overmature for oil generation and expels gas in the present day. The Draupne Formation generates both oil and gas presently. The maximum temperature attained in the deepest parts of the basin is 225 °C. The late Jurassic source rock reaches a temperature of about 180°C, where 95% to 100% of the source rock is transformed. According to Sweeney and Burnham (1990), the vitrinite reflectance data shows that the source rock of the modelled basin is matured and has passed the oil window from main oil to dry gas. The reservoir rocks are saturated with hydrocarbons to about 70% to 90%, the capillary pressure of the source rock is up to 110-120 MPa. In the 2D lines the mass of generated oil from the source rock ranges between 2.25-2.40 Mtons to 2.40-2.60 Mtons, the mass of gas generated from the source rock is between 0.36-0.39 Mtons to 0.49-0.52 Mtons.



## REFERENCES

- Al-Hajeri, M. M., Al Saeed, M., Derks, J., Fuchs, T., Hantschel, T., Kauerauf, A., Neumaier, M., Schenk, O., Swientek, O., and Tessen, N., 2009, Basin and petroleum system modeling: *Oilfield Review*, v. 21, no. 2, p. 14-29.
- Barnard, P., and Bastow, M., 1991, Hydrocarbon generation, migration, alteration, entrapment and mixing in the Central and Northern North Sea: Geological Society, London, Special Publications, v. 59, no. 1, p. 167-190.
- Beach, A., 1985, Some comments on sedimentary basin development in the Northern North Sea: *Scottish Journal of Geology*, v. 21, no. 4, p. 493-512.
- Burley, S., Models of burial diagenesis for deep exploration plays in Jurassic fault traps of the Central and Northern North Sea, *in* Proceedings Geological Society, London, Petroleum Geology Conference series 1993, Volume 4, Geological Society of London, p. 1353-1375.
- Cooper, B., and Barnard, P., 1984, Source rocks and oils of the central and northern North Sea.
- Cornford, C., 1998, Source rocks and hydrocarbons of the North Sea: *Petroleum Geology of the North Sea: Basic Concepts and Recent Advances*, Fourth Edition, p. 376-462.
- Corver, M. P., Doust, H., van Wees, J.-D., and Cloetingh, S., 2011, Source-rock maturation characteristics of symmetric and asymmetric grabens inferred from integrated analogue and numerical modeling: The southern Viking Graben (North Sea): *Marine and Petroleum Geology*, v. 28, no. 4, p. 921-935.
- Coward, M., Dewey, J., Hempton, M., and Holroyd, J., 2003, Tectonic evolution: The Millennium Atlas: *Petroleum Geology of the Central and Northern North Sea*. Geological Society, London, p. 17-33.
- Curtin, D., and Ballestad, S., 1986, South Viking Graben: habitat of Mesozoic hydrocarbons: *Habitat of hydrocarbons on the Norwegian Continental Shelf: Norwegian Petroleum Society, Stavanger, Graham and Trotman*, p. 153-157.
- Dawers, N., Berge, A., Häger, K.-O., Puigdefabregas, C., and Underhill, J., Controls on Late Jurassic, subtle sand distribution in the Tampen Spur area, northern North Sea, *in* Proceedings Geological Society, London, Petroleum Geology Conference series 1999, Volume 5, Geological Society of London, p. 827-838.
- Dawers, N. H., and Underhill, J. R., 2000, The role of fault interaction and linkage in controlling synrift stratigraphic sequences: Late Jurassic, Statfjord East area, northern North Sea: *AAPG bulletin*, v. 84, no. 1, p. 45-64.
- Di Primio, R., and Skeie, J. E., 2004, Development of a compositional kinetic model for hydrocarbon generation and phase equilibria modelling: a case study from Snorre Field, Norwegian North Sea: Geological Society, London, Special Publications, v. 237, no. 1, p. 157-174.
- England, W., Mackenzie, A., Mann, D., and Quigley, T., 1987, The movement and entrapment of petroleum fluids in the subsurface: *Journal of the Geological Society*, v. 144, no. 2, p. 327-347.
- Færseth, R., 1996, Interaction of Permo-Triassic and Jurassic extensional fault-blocks during the development of the northern North Sea: *Journal of the Geological Society*, v. 153, no. 6, p. 931-944.

- Faleide, J. I., Bjørlykke, K., and Gabrielsen, R. H., 2015, *Geology of the Norwegian continental shelf*, Petroleum Geoscience, Springer, p. 603-637.
- Gabrielsen, R., Odinsen, T., and Grunnaleite, I., 1999, Structuring of the Northern Viking Graben and the Møre Basin; the influence of basement structural grain, and the particular role of the Møre-Trøndelag Fault Complex: *Marine and Petroleum Geology*, v. 16, no. 5, p. 443-465.
- Goff, J., 1983, Hydrocarbon generation and migration from Jurassic source rocks in the E Shetland Basin and Viking Graben of the northern North Sea: *Journal of the Geological Society*, v. 140, no. 3, p. 445-474.
- Goldsmith, P., Hudson, G., Van Veen, P., Triassic, D. E., Graham, C., Armour, A., and Bathurst, P., The millennium atlas: Petroleum geology of the central and northern North Sea, *in Proceedings Geological Society London 2003*, p. 105-127.
- Gregersen, U., and Johannessen, P., 2007, Distribution of the Neogene Utsira Sand and the succeeding deposits in the Viking Graben area, North Sea: *Marine and Petroleum Geology*, v. 24, no. 10, p. 591-606.
- Hantschel, T., and Kauerauf, A. I., 2009, *Fundamentals of basin and petroleum systems modeling*, Springer Science & Business Media.
- Head, M. J., Riding, J. B., Eidvin, T., and Chadwick, R. A., 2004, Palynological and foraminiferal biostratigraphy of (Upper Pliocene) Nordland Group mudstones at Sleipner, northern North Sea: *Marine and Petroleum Geology*, v. 21, no. 3, p. 277-297.
- Iliffe, J., Lerche, I., and Cao, S., 1991, Basin analysis predictions of known hydrocarbon occurrences: the North Sea Viking Graben as a test case: *Earth-Science Reviews*, v. 30, no. 1-2, p. 51-79.
- Isaksen, D., and Tonstad, K., 1989, A revised Cretaceous and Tertiary lithostratigraphic nomenclature for the Norwegian North Sea, *Bulletin 5: Norwegian Petroleum Directorate, Stavanger, Norway*.
- Johannessen, J., Hay, S., Milne, J., Jepsen, C., Gunnesdal, S., and Vayssaire, A., 2002, 3D oil migration modelling of the Jurassic petroleum system of the Statfjord area, Norwegian North Sea: *Petroleum Geoscience*, v. 8, no. 1, p. 37-50.
- Kirk, R., 1980, Statfjord field--a North Sea giant.
- Kjennerud, T., Faleide, J., Gabrielsen, R., Gillmore, G., Kyrkjebø, R., Lippard, S., and Løseth, H., 2001, Structural restoration of Cretaceous-Cenozoic (post-rift) palaeobathymetry in the northern North Sea: *Norwegian Petroleum Society Special Publications*, v. 10, p. 347-364.
- Knott, S., Burchell, M., Jolley, E., and Fraser, A., Mesozoic to Cenozoic plate reconstructions of the North Atlantic and hydrocarbon plays of the Atlantic margins, *in Proceedings Geological Society, London, Petroleum Geology Conference series 1993, Volume 4, Geological Society of London*, p. 953-974.
- Knott, S. D., 1993, Fault seal analysis in the North Sea: *AAPG Bulletin*, v. 77, no. 5, p. 778-792.
- Kubala, M., Bastow, M., Thompson, S., Scotchman, I., and Oygard, K., 2003, Geothermal regime, petroleum generation and migration: *The Millennium Atlas: Petroleum Geology of the Central and Northern North Sea*. Geological Society, London, p. 289-315.
- Magoon, L. B., and Dow, W. G., 1994, *The Petroleum System: Chapter 1: Part I. Introduction*.
- Martinelli, G., 2010, Basin and petroleum system modeling: online] <http://www.math.ntnu.no/~gabriele/PetroModPres.pdf> (accessed 12.05.2012).

- McAuliffe, C. D., 1979, Oil and gas migration--chemical and physical constraints: AAPG Bulletin, v. 63, no. 5, p. 761-781.
- McLeod, A. E., and Underhill, J., 2000, The propagation and linkage of normal faults: insights from the Strathspey–Brent–Statfjord fault array, northern North Sea: Basin Research, v. 12, no. 3 - 4, p. 263-284.
- Miles, J. A., 1990, Secondary Migration Routes in the Brent Sandstones of the Viking Graben and East Shetland Basin: Evidence from Oil Residues and Subsurface Pressure Data (1): AAPG Bulletin, v. 74, no. 11, p. 1718-1735.
- Momper, J. A., 1978, Oil migration limitations suggested by geological and geochemical considerations.
- Morad, S., Bergan, M., Knarud, R., and Nystuen, J. P., 1990, Albitization of detrital plagioclase in Triassic reservoir sandstones from the Snorre Field, Norwegian North Sea: Journal of Sedimentary Research, v. 60, no. 3.
- Moretti, I., and Deacon, K., 1995, Subsidence, maturation and migration history of the Tampen Spur area: Marine and petroleum geology, v. 12, no. 4, p. 345-375.
- Morton, A. C., 1982, Lower Tertiary sand development in Viking Graben, North Sea: AAPG Bulletin, v. 66, no. 10, p. 1542-1559.
- Mudge, D., and Bliss, G., 1983, Stratigraphy and sedimentation of the Palaeocene sands in the Northern North Sea: Geological Society, London, Special Publications, v. 12, no. 1, p. 95-111.
- Nystuen, J. P., and Fält, L.-M., 1995, Upper Triassic-Lower Jurassic reservoir rocks in the Tampen Spur area, Norwegian North Sea: Norwegian Petroleum Society Special Publications, v. 4, p. 135-179.
- Odinsen, T., Reemst, P., Van Der Beek, P., Faleide, J. I., and Gabrielsen, R. H., 2000, Permo-Triassic and Jurassic extension in the northern North Sea: results from tectonostratigraphic forward modelling: Geological Society, London, Special Publications, v. 167, no. 1, p. 83-103.
- Pegrum, R., and Spencer, A., 1990, Hydrocarbon plays in the northern North Sea: Geological Society, London, Special Publications, v. 50, no. 1, p. 441-470.
- Piñero, E., Rottke, W., Fuchs, T., Hensen, C., Haeckel, M., and Wallmann, K., 2011, 3-D numerical modeling of methane hydrate deposits.
- Rathey, R., and Hayward, A., Sequence stratigraphy of a failed rift system: the Middle Jurassic to Early Cretaceous basin evolution of the Central and Northern North Sea, *in* Proceedings Geological Society, London, Petroleum Geology Conference series1993, Volume 4, Geological Society of London, p. 215-249.
- Ravnås, R., Nøttvedt, A., Steel, R., and Windelstad, J., 2000, Syn-rift sedimentary architectures in the Northern North Sea: Geological Society, London, Special Publications, v. 167, no. 1, p. 133-177.
- Riis, F., 1996, Quantification of Cenozoic vertical movements of Scandinavia by correlation of morphological surfaces with offshore data: Global and Planetary Change, v. 12, no. 1, p. 331-357.
- Roberts, A., Yielding, G., and Badley, M., 1990, A kinematic model for the orthogonal opening of the Late Jurassic North Sea rift system, Denmark-Mid Norway: Tectonic evolution of the North Sea Rifts, p. 180-199.
- Roberts, A., Yielding, G., Kuszniir, N., Walker, I., and Dorn-Lopez, D., Mesozoic extension in the North Sea: constraints from flexural backstripping, forward modelling and fault populations, *in* Proceedings Geological Society, London, Petroleum Geology Conference series1993, Volume 4, Geological Society of London, p. 1123-1136.

- Schroeder, W., and Sylta, Ø., Modelling the hydrocarbon system of the North Viking Graben: a case study, *in* Proceedings Basin modelling: advances and applications: proceedings of the Norwegian Petroleum Society conference, 13-15 March 1991, Stavanger, Norway/edited by AG Doré et al. Dokumentet er del av serien Special publication (Norsk petroleumforening 1993, Volume 3, p. 469-484.
- Sneider, J. S., de Clarens, P., and Vail, P. R., 1995, Sequence stratigraphy of the Middle to Upper Jurassic, Viking Graben, North Sea: Norwegian Petroleum Society Special Publications, v. 5, p. 167-197.
- Telnaes, N., Cooper, B., and Jones, B., 1991, Kerogen facies, biomarkers, trace metal contents, and spectral logs as indicators of oxicity and salinity, Upper Jurassic, North Sea, Organic Geochemistry, Advances and Applications in Energy and the Natural Environment, Manchester University Press Manchester, p. 391-393.
- Thomas, D., and Coward, M., 1995, Late Jurassic-early Cretaceous inversion of the northern east Shetland basin, northern North Sea: Oceanographic Literature Review, v. 11, no. 42, p. 982.
- , 1996, Mesozoic regional tectonics and South Viking Graben formation: evidence for localized thin-skinned detachments during rift development and inversion: Marine and Petroleum Geology, v. 13, no. 2, p. 149-177.
- Thomson, K., and Underhill, J., Controls on the development and evolution of structural styles in the Inner Moray Firth Basin, *in* Proceedings Geological Society, London, Petroleum Geology Conference series 1993, Volume 4, Geological Society of London, p. 1167-1178.
- Vollset, J., and Doré, A. G., 1984, A revised Triassic and Jurassic lithostratigraphic nomenclature for the Norwegian North Sea, Oljedirektoratet.
- Walderhaug, O., and Bjørkum, P. A., 1992, Effect of meteoric water flow on calcite cementation in the Middle Jurassic Oseberg Formation, well 30/3-2, Veslefrikk Field, Norwegian North Sea: Marine and petroleum geology, v. 9, no. 3, p. 308-318.
- Welte, D., and Yalcin, M., 1988, Basin modelling—a new comprehensive method in petroleum geology: Organic Geochemistry, v. 13, no. 1-3, p. 141-151.
- Welte, D. H., Horsfield, B., and Baker, D. R., 2012, Petroleum and basin evolution: insights from petroleum geochemistry, geology and basin modeling, Springer Science & Business Media.

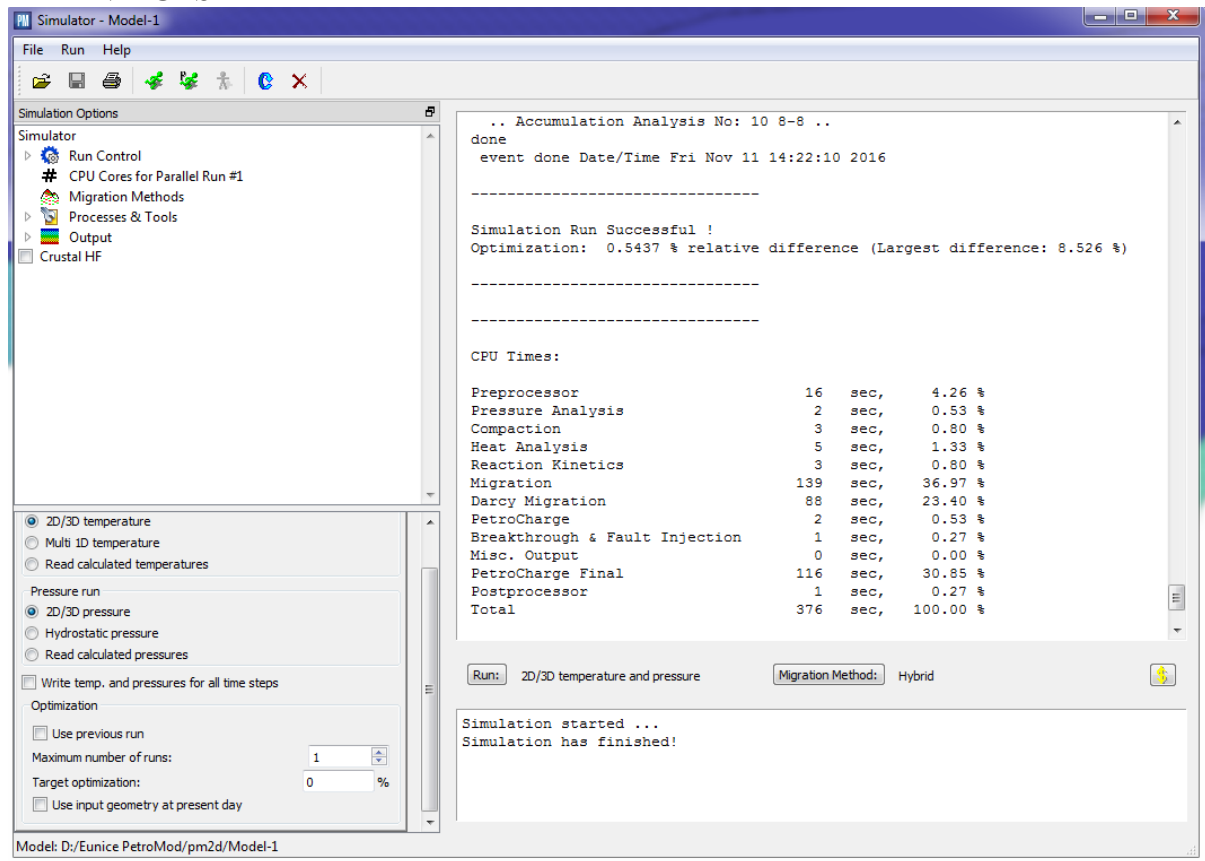
#### Other resources

Schlumberger Petromod tutorials, 2009

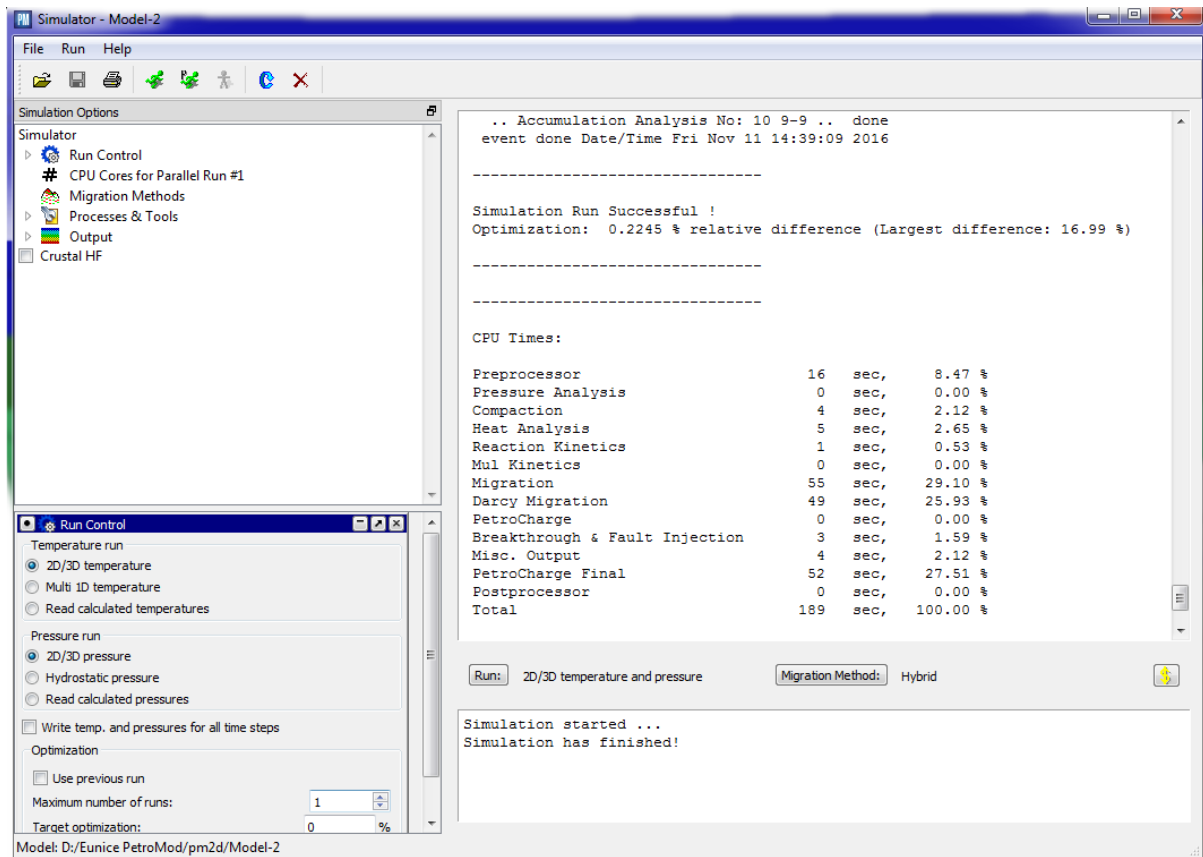
The Geological Society of America, 2009 Geological time Scale

[www.npd.no](http://www.npd.no)

## APPENDICES



AppendixA1: Simulation runs for the model-1 for NVGTI-92-109



AppendixA2.Simulation runs for the model-2 for NVGTI-92-104